Optimisation of heat exchanger network maintenance scheduling problems

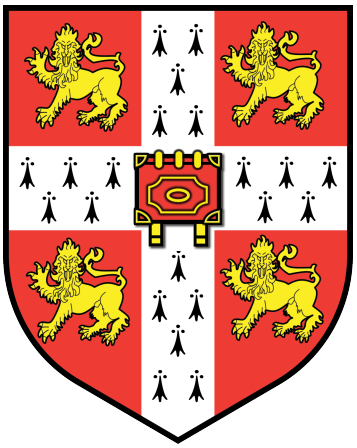

Riham Al Ismaili

Department of Chemical Engineering and Biotechnology

University of Cambridge

This dissertation is submitted for the degree of

Doctor of Philosophy

Clare Hall 2018

Summary

Optimisation of heat exchanger network maintenance scheduling problems

Riham Al Ismaili

This thesis focuses on the challenges that arise from the scheduling of heat exchanger network maintenance problems which undergo fouling and run continuously over time. The original contributions of the current research consist of the development of novel optimisation methodologies for the scheduling of cleaning actions in heat exchanger network problems, the application of the novel solution methodology developed to other general maintenance scheduling problems, the development of a stochastic programming formulation using this optimisation technique and its application to these scheduling problems with parametric uncertainty.

The work presented in this thesis can be divided into three areas. To efficiently solve this non-convex heat exchanger network maintenance scheduling problem, new optimisation strategies are developed. The resulting contributions are outlined below.

In the first area, a novel methodology is developed for the solution of the heat exchanger network maintenance scheduling problems, which is attributed towards a key discovery in which it is observed that these problems exhibit bang-bang behaviour. This indicates that when integrality on the binary decision variables is relaxed, the solution will tend to either the lower or the upper bound specified, obviating the need for integer programming solution techniques. Therefore, these problems are in actuality optimal control problems. To suitably solve these problems, a feasible path sequential mixed integer optimal control approach is proposed. This methodology is coupled with a simple heuristic approach and applied to a range of heat exchanger network case studies from crude oil refinery preheat trains. The demonstrated methodology is shown to be robust, reliable and efficient.

In the second area of this thesis, the aforementioned novel technique is applied to the scheduling of the regeneration of membranes in reverse osmosis networks which undergo fouling and are located in desalination plants. The results show that the developed solution methodology can be generalised to other maintenance scheduling problems with decaying performance characteristics.

In the third and final area of this thesis, a stochastic programming version of the feasible path mixed integer optimal control problem technique is established. This is based upon a multiple scenario approach and is applied to two heat exchanger network case studies of varying size and complexity. Results show that this methodology runs automatically with ease without any failures in convergence. More importantly due to the significant impact on economics, it is vital that uncertainty in data is taken into account in the heat exchanger network maintenance scheduling problem, as well as other general maintenance scheduling problems when there is a level of uncertainty in parameter values.

List of peer reviewed publications

(i) **Al Ismaili, R.**, Lee, M. W., Wilson, D. I., Vassiliadis, V. S., 2018. Heat exchanger network cleaning scheduling: From optimal control to mixed-integer decision making. Computers and Chemical Engineering 111, 1-15.

(ii) Adloor, S. D., **Al Ismaili, R.**, Vassiliadis, V. S., 2018. Errata: Heat exchanger network cleaning scheduling: From optimal control to mixed-integer decision making. Computers and Chemical Engineering 115, 243-245.

I would like to dedicate this thesis to my parents and my son.

Preface

This dissertation is the result of my own work and includes nothing which is the outcome of work done in collaboration, except as declared specifically in the text.

I confirm that it is not substantially the same as any that I have submitted, or, is being concurrently submitted for a degree or diploma or other qualification at the University of Cambridge or any other University or similar institution except as declared in the Preface and specified in the text. I further state that no substantial part of my dissertation has already been submitted, or, is being concurrently submitted for any such degree, diploma or other qualification at the University of Cambridge or any other University of similar institution except as declared in the Preface and specified in the text.

This dissertation does not exceed 65,000 words or 150 figures, including bibliography, tables and equations.

Riham Al Ismaili

January, 2018

Acknowledgements

I would like to begin by expressing my immense thanks to my supervisor Dr. Vassilios S. Vassiliadis for his continuous support and advice over many discussions ranging from optimisation to deteriorating performance processes throughout my graduate studies at the University of Cambridge. It has been a great pleasure to work with him. I would also like to thank my advisor, Prof. D. Ian Wilson for his guidance in the topic of fouling and parametric uncertainty. A special thanks to Dr. Min Woo Lee for his constructive support, collaboration and input in multiple areas. I consider myself fortunate to have known you all.

Thanks to all members of the Process Systems Engineering group for creating such an excellent and inviting research environment, especially Antonio del Río Chanona, Dongda Zhang and Fabio Fiorelli who provided help in all areas. I would also like to thank Walter Kähm for his support.

To my friends in the Chemical Engineering and Biotechnology department without whom my PhD journey would not have been the same. Thanks to Geertje van Rees, David Cox, Noha Al-Otaibi, Aazraa Oumayyah, Arely Gonzales and Hassan Alderazi.

To the Clare Hall rowing team for all those early morning rowing training sessions and many enjoyable races without which my experience in Cambridge would not have been the same. Special thanks to Helena Pérez-Vallevas, Laura Brooks, Jennifer Daffron, Vasiliki Mavroeidi, Shen Gao, Anna Huefner, Lukas Vermach, Sara Russo and Konstantinos Ziovas.

To my friends back home, Dania Al Mahruqy, Mariam Hosny and Aisha Al Maamary as well as my cousins Sariya Al Ismaili, Hanan Al Kindi and Nada Al Hasani for always being there for me.

I would also like to acknowledge financial support from my employer Petroleum Development Oman (PDO) and the Ministry of Higher Education in the Sultanate of Oman for awarding me this scholarship.

I am grateful to my parents for their relentless support and encouragement. I would also like to thank my siblings for their belief in me. A special thanks to my son for always being able to put a smile on my face no matter what the situation.

Contents

List of Figures

List of Tables

Nomenclature

Roman symbols

$\bar{a}$	mean of stochastic linear fouling rate [ft^2°F/Btu]
A	area of exchanger [m^2]
a	linear fouling rate [m^{2}K/J]
$\bar{C}_E$	mean of stochastic fuel cost [£/J]
C	specific heat capacity of fluid [J/kg K]
C_{cl}	cost of cleaning action [£]
C_{EL}	electrical power cost [USD/kW h]
C_E	cost of fuel [£/kJ]
C_{FC}	membrane regeneration fixed cost, per cleaning action [USD]
C_M	maintenance cost [£]
C_{VC}	membrane regeneration variable cost, per module [USD]
C_X	downtime cost [£]
Co	concentration of stream [ppm]
Co^{ave}	average concentration across high pressure side of membrane [ppm]
Dm	solute transport parameter [kg/m^{2}s]
F	mass flowrate of stream [kg/s]

f	function
F_b	booster pump flowrate [kg/s]
F_t	turbine flowrate [kg/s]
H	Hamiltonian
J	junction condition
Km	permeability of membrane [kg/sN]
KW_b	electrical duty of booster pump [kW]
KW_t	electrical duty of turbine [kW]
L	Lagrangian
l_f	membrane fibre length [m]
l_s	membrane fibre seal length [m]
m	vector dimension
MOC	membrane regeneration cost [USD]
N_C	total number of cleaning actions
NE	number of exchangers
Nm	number of RO modules
NP	number of periods
NU	number of membrane units
Obj	objective [£]
OC	operating cost to be minimised [USD]
P	ratio of capacity flow-rates
p	vector of parameters
POC	booster pump operation cost [USD]

Pr	pressure of stream [N/m^2]
Pr^{drop}	pressure drop across membrane module [N/m^2]
Pr_b	booster pump pressure [N/m^2]
Pr_t	turbine pressure [N/m^2]
Q	duty of exchanger [W]
Q_F	extra furnace power requirement [W]
$\bar{R}_f^{\infty}$	mean of stochastic asymptotic fouling resistance [hft^2°F/Btu]
$\dot{R}_f$	fouling rate [m^{2}K/J]
$\dot{R}_n$	instantaneous net fouling rate [m^{2}K/J]
r_i	inner radius of membrane fibre [m]
r_o	outer radius of membrane fibre [m]
R_f	fouling resistance [m^{2}K/W]
R_f^{∞}	asymptotic fouling resistance [m^{2}K/W]
S	number of scenarios
Sm	membrane surface area [m^2]
T	temperature of stream [K]
t	time [s]
t'	elapsed time since the last cleaning action [s]
TOC	turbine energy saving cost [USD]
U	overall heat transfer coefficient [W/m^{2}K]
u	control variable
U_c	overall heat transfer coefficient in clean condition [W/m^{2}K]
v	vector of continuous variables

x	differential state variable
y	binary variable
z	algebraic state variable

Greek symbols

α	effectiveness term
β	MINLP objective to be minimised
γ	membrane correction factor
ΔPr	pressure difference between bulk and permeate streams [N/m^2]
$\Delta\pi$	osmotic pressure difference between wall and permeate streams [N/m^2]
δ_c	thickness of coke layer [m]
δ_g	thickness of gel layer [m]
ΔT_{lm}	logarithmic mean temperature difference [K]
Δt	duration of time [s]
η	membrane specific coefficient
η_c	the fraction of the clean value to which the overall heat transfer coefficient is restored after cleaning
η_{eff}	efficiency of booster pump or turbine
η_f	furnace efficiency
λ	Euler-Lagrange multiplier
μ	Euler-Lagrange multiplier
μ_v	dynamic viscosity of water [kg/ms]
π	osmotic pressure [N/m^2]
π_o	osmotic pressure constant [N/m^{2}ppm]

ρ	density of water [kg/m^3]
ρ^{water}	density of pure water [kg/m^3]
ρ_b	density of seawater at booster pump [kg/m^3]
ρ_t	density of brine at turbine [kg/m^3]
$\bar{\tau}$	mean of stochastic decay constant [s]
τ	decay constant [s]
ϕ	terminal cost [£]
φ_d	deposition rate [m^{2}K/J]
φ_r	removal rate [m^{2}K/J]
ψ	weight coefficient

Abbreviations

$\mathscr{NP}$	nondeterministic polynomial time
AMPL	a mathematical programming language
B&B	branch and bound
BONMIN	basic open source nonlinear mixed integer
BTA	backtracking threshold accepting
CIT	crude inlet temperature
CPU	central processing unit
DAE	differential algebraic equation
DICOPT	discrete and continuous optimiser
FWHM	full width at half maximum
GA	genetic algorithm

GAMS	general algebraic modeling system
GB	gigabyte
GBD	general Benders decomposition
GCC	Gulf Cooperation Council
GHz	gigahertz
GMS	generator maintenance scheduling
GNP	gross national product
HEN	heat exchanger network
HEX	heat exchanger
IPM	interior point method
IPOPT	interior point optimiser
KSA	Kimura-Sourirajan analysis
MILP	mixed-integer linear programming
MINLP	mixed-integer nonlinear programming
MIOCP	mixed-integer optimal control problem
MIP	mixed-integer programming
MM	million
MP	mathematical programming
NLP	nonlinear programming
NPC	net present value of operating costs [£]
NTU	number of transfer units
OA	outer approximation
OA/ER	outer approximation/equality relaxation

OCP	optimal control problem
OS X	unix-based operating system
PHT	preheat train
ppm	parts per million
RAM	random access memory
RO	reverse osmosis
RON	reverse osmosis network
RSD	relative standard deviation [%]
SA	sensitivity analysis
SD	standard deviation
TA	threshold accepting
UROPM	unified RO performance model
USD	United States dollars

Subscripts & superscripts

0	initial condition
b	bulk solution
bcp	beginning of cleaning subperiod
bop	beginning of operating subperiod
c	cold fluid
CL	cleaning subperiod
clean	clean condition
ecp	end of cleaning subperiod
eop	end of operating subperiod

F	final
f	feed stream
h	hot fluid
in	inlet stream
j	j-th cleaning action
max	maximum
min	minimum
n	exchanger no. or membrane unit no.
OP	operating subperiod
out	outlet stream
p	period no.
perm	permeate stream
r	reject stream
S	scenario no.
v	vector of continuous variables
w	membrane wall
X	beginning or end of cleaning or operating subperiod
y	vector of binary variables

Chapter 1

Introduction and literature survey

Fouling of heat transfer surfaces is a long established major industry-wide problem. Due to the reduction in heat transfer caused by fouling, this leads to the loss of efficiency in heat exchangers. This in turn results in a decline in production due to frequent shutdown periods for cleaning and additional maintenance actions. Fouling has been described by [133] as the major unresolved problem in heat transfer. Moreover, it is one of the most significant issues affecting heat exchanger operation and thus has been depicted by [142] as a nearly universal problem in heat exchanger equipment and design. Furthermore, [128] stated that this problem is of great significance in large networks of heat exchangers, particularly those situated in crude oil refinery distillation unit preheat trains (PHTs), which are required to operate continuously over several years between shutdowns.

Fouling is offset through process turndown or increased utility consumption with the associated surge in greenhouse gas emissions. This is necessary in order to meet operation requirements such as temperature and pump-around targets. However, in cases where fouling-related pressure drop changes reduce throughput, plant shutdown is often required. The reduction of production rates and increased energy consumption lead to significant economic losses. In studies from the 1980s to the early 1990s, the cost of heat exchanger fouling due to cleaning, fluid treatment, additional hardware and loss of production has been estimated at 0.25% of the gross domestic product (GDP) of industrialised countries [95]. The estimated total cost of heat exchanger fouling based on 1995 figures in the UK and USA are of the order of 2.5 billion United States Dollars (USD) and 14 billion USD, respectively [28]. Allowing for inflation, the

corresponding figures for 2018 would be approximately 4.1 billion USD and 23 billion USD, respectively. Economic losses are more significant in larger heat exchanger networks (HENs) which are associated with long continuous operational times, specifically in crude distillation unit PHTs situated in oil refineries. Based on 1995 figures, the cost associated specifically with crude oil fouling in PHTs worldwide were estimated to be of the order of 4.5 billion USD [111]. Accounting for inflation, the corresponding figure for 2018 would be around 7.4 billion USD.

Fouling mitigation techniques include addition of antifoulant chemicals, using more robust heat transfer equipment, and regular cleaning of fouled units. Cleaning of heat exchangers has a negative impact on operating costs due to the unit being taken offline. However, with the development of optimisation strategies such as those proposed by [18, 45, 46, 64, 77, 127], among others, these costs can be minimised resulting in overall gains due to improved heat transfer of the network over time.

Current solution methods still present limitations. Some approaches suffer from failure in convergence [45, 128], while others are computationally expensive [77] and result from unsuitable approximated models [45]. Furthermore, some methods are incapable of handling problems involving many variables of similar effect [41] and current methods used by industry are not guaranteed to be optimal [128].

To address the aforementioned challenges, research presented in this thesis focuses on the development of novel, robust and reliable strategies to minimise the cost of fouling in networks of heat exchangers primarily situated in crude oil refinery distillation unit PHTs. The problems considered in this thesis involve offline cleaning strategies and are constrained mixed-integer nonlinear programming (MINLP) problems. The detailed thesis structure will be presented in Section 1.4 after a comprehensive literature survey.

1.1 The physicochemical processes leading to fouling

In this section, the nature of the HEN maintenance scheduling problem is presented in terms of the physicochemical processes leading to the fouling phenomenon, the remediation steps involved and types of fouling.

Fouling is the accumulation, *i.e.* deposition, of unwanted solid material on a surface. Building an understanding of the physicochemical processes leading to fouling through modelling is imperative to mitigating its impacts. One such example is [84] who proposed a 2-D dynamical model to predict the milk deposit patterns on the surfaces of plate heat exchangers. Their model is based on chemical reaction and mass transfer, among other factors. From their results, fouling is shown to be highly dependent on process operating conditions. [84] concluded that the parameters affecting the fouling phenomenon, more specifically the flow and mass deposit, depended mainly on the milk temperature and processing time.

The physicochemical process leading to fouling have been categorised by [36] into 5 main categories:

(i) Crystallisation which can be subdivided into precipitation (also known as scaling) and solidification. Precipitation consists of the deposition of dissolved salts which at process conditions become supersaturated at the heat transfer surface, whereas solidification fouling is due to cooling below the solidification temperature of a dissolved component, such as in the case of the formation of wax on crude oil heat transfer surfaces.

(ii) Particulate which is concerned with the deposition of suspended particles such as clay and iron oxide on heat transfer surfaces.

(iii) Chemical reaction which involves the deposition of material on the heat transfer surface due to chemical reaction in which the heat transfer surface is not involved.

(iv) Corrosion which is a consequence of exposure to other ions such as flowing oxygenated water in heat exchangers handling natural waters and cooling systems of water-cooled internal combustion engines.

(v) Biofouling which occurs when live matter is in contact with wetted surfaces.

[19] summarised that the biofoulant development is the net result of several physical, chemical and microbial processes which includes:

(i) The transportation of dissolved and particulate matter from the bulk fluid to the surface.

(ii) Firm microbial cell attachment to the surface.

(iii) Microbial transformations, such as growth and reproduction within the biofilm resulting in production of organic matter.

(iv) Partial detachment of the biofilm due primarily to fluid shear stress.

A 5×5 matrix was proposed by [36] which summarises the mechanistic steps for fouling into:

(i) Initiation which is also known as the delay period and is the period in which the new or clean exchanger is taken into operation. The high heat transfer coefficient may remain unchanged for a short duration during which initial deposition occurs such as nutrient deposition for biological growth. For certain fouling categories, specifically crystallisation and chemical reaction, the duration of the initiation period is affected by surface temperature.

(ii) Transport where mass transport of at least one primary element from the bulk fluid to the heat transfer surface is required.

(iii) Attachment where the foulant must latch on to the surface.

(iv) Removal.

(v) Ageing which may increase the strength of the deposit material by polymerisation, recrystallisation, dehydration, *etc.* In addition, with the exception of waxing problems, the mechanistic step ageing is promoted further by the increasing temperature of the deposit as well as operating time. [107] outlined that ageing converts the initial gel deposit into a harder, more conductive form, called coke.

[107] further categorised fouling formation into 3 different groups:

(i) Single layer depositions which are due to chemical reactions, such as coke formation, polymerisation, protein denaturation in food industries and so forth.

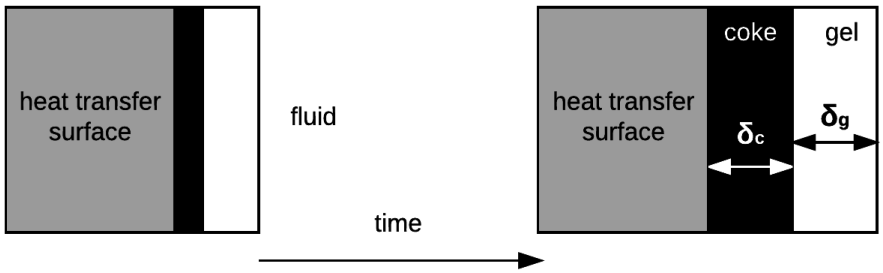

Figure 1.1.1: Schematic of a double layer fouling deposition. The coke layer is represented in black while the gel layer is in white. Thicknesses of the coke and gel layers are represented by δ_c and δ_g, respectively. Adapted from [61].

(ii) Double layer depositions which consist of a soft exterior deposit (gel) due to ageing and a harder interior layer (coke), which forms as a result of transformation of the initial soft deposit due to ageing. Removal of the gel layer is achieved using a cleaning-in-place method based on treatment with a solvent. This chemical process is not effective for the coke layer, which requires offline mechanical cleaning. Figure 1.1.1 demonstrates this double layer mechanism.

(iii) Biofouling.

1.2 Introduction to the heat exchanger network maintenance scheduling problem

This section will introduce the general concepts of the HEN maintenance scheduling problem, along with the mathematical modelling of this optimisation problem, which are essential for the understanding of this thesis.

The HEN cleaning scheduling problem is a discrete decision making problem where a decision must be made as to when cleaning should be performed, which unit is to be cleaned and in some cases which method of cleaning is to be used, *e.g.* chemical or mechanical cleaning. It consists of nonlinear equations which contain binary decision variables as well as continuous variables and hence it is combinatorial in nature. This results in a MINLP model which is non-convex, *i.e.* has multiple local minima and it

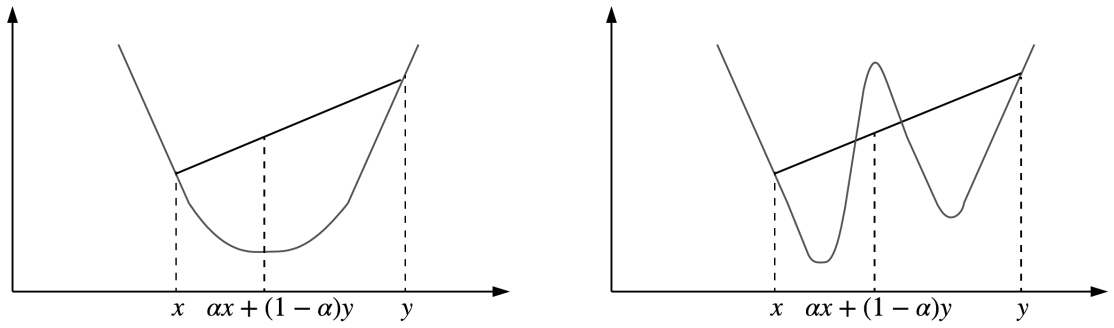

(a) **(b)**

Figure 1.2.2: (a) Convex function and (b) Non-convex function

is therefore difficult to find the global minimum. Figure 1.2.2 schematically represents a convex and non-convex function where f is defined to be a convex function if its domain $S \in \mathbb{R}^n$ is a convex set, and if for any two points x and y in this domain, the graph of f lies below the straight line connecting $(x, f(x))$ to $(y, f(y))$ in the space $\mathbb{R}^{n+1}$. In other words, the following property is satisfied [97]:

$$f(\alpha x + (1-\alpha)y) \leq \alpha f(x) + (1-\alpha) f(y) \qquad \forall \alpha \in [0,1] \tag{1.1}$$

The effect of fouling on heat transfer performance is quantified in lumped parameter models of process heat transfer via the fouling resistance. The impact of fouling resistance is more severe for heat exchangers with a high overall heat transfer coefficient.

$$\frac{1}{U} = \frac{1}{U_c} + R_f \tag{1.2}$$

Equation (1.2) expresses the overall heat transfer coefficient, U, in relation to the fouling resistance, R_f. U_c denotes the overall heat transfer coefficient in the clean condition. The instantaneous net fouling rate, $\dot{R}_n$, is related to the fouling resistance, R_f, by:

$$\dot{R}_n \triangleq \frac{dR_f}{dt} \triangleq \varphi_d - \varphi_r \tag{1.3}$$

where φ_d and φ_r are the deposition and removal rates, respectively, with t representing time. Depending on the relative extents of deposition and removal rates, the fouling resistance-time curve can exhibit linear, falling or asymptotic behaviour as outlined in Figure 1.2.3. [16] reported negative fouling resistances occurring due to surface roughness. This process continues until the additional heat transfer resistance overcomes the advantage of increased turbulence. The time period from the beginning of the fouling process until the fouling resistance again becomes zero is called the roughness delay time [5].

Linear fouling is indicative of a constant deposition rate with a negligible removal rate, *i.e.* $\varphi_r \approx 0$. In this model, the relationship between deposited mass and time is in the form of Equation (1.4).

$$R_f = at \tag{1.4}$$

where a is the slope of the line, *i.e.* the linear fouling rate for a particular heat exchanger. An asymptotic rate fouling curve is indicative of a constant deposition rate and of the removal rate being directly proportional to the deposit thickness until $\varphi_r = \varphi_d$ at the asymptote. In this model, the rate of fouling gradually falls with time, so that eventually a steady-state is reached where there is no net increase of deposition on the surface and there is a possibility of continued operation of the equipment without additional fouling. The relationship between deposit mass and time is in the following form:

$$R_f = R_f^{\infty}\left(1 - \exp(-t'/\tau)\right) \tag{1.5}$$

where R_f^{∞} is the asymptotic fouling resistance, τ is the decay constant and t' is the elapsed operating time since the last cleaning action. A falling rate fouling curve also results from a falling deposition rate, where the mass of deposit increases nonlinearly with time, but does not reach the steady-state value of the asymptotic case.

Assuming an exchanger is perfectly insulated and the flow regime is laminar, the heat duty, Q, is linearly related to the inlet and outlet temperatures through the energy

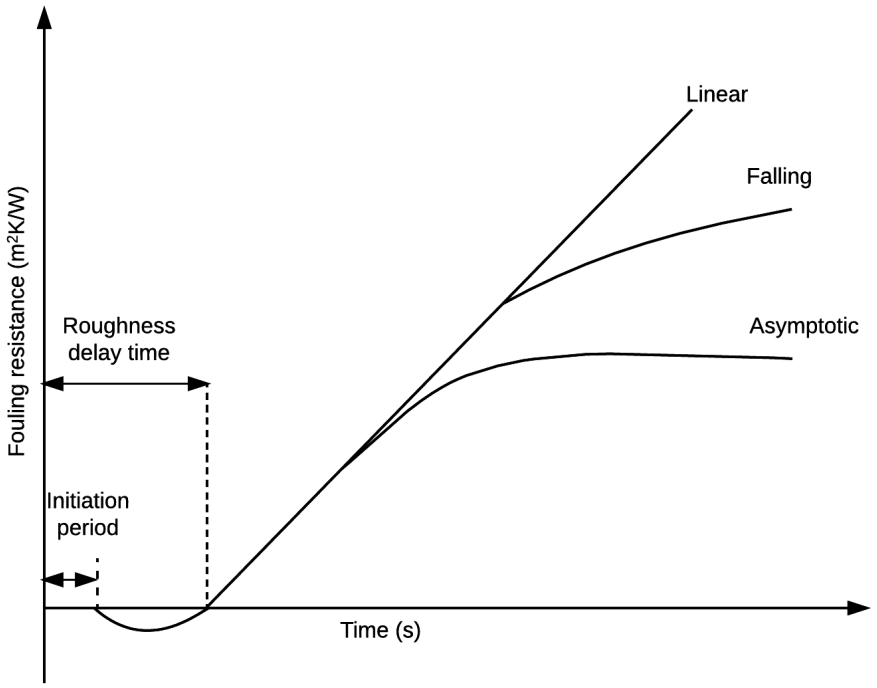

Figure 1.2.3: Fouling rate versus time curves. Adapted from [69].

balances outlined in Equations (1.6) and (1.7).

$$Q = F_{\mathrm{c}} C_{\mathrm{c}} (T_{\mathrm{c}}^{\mathrm{out}} - T_{\mathrm{c}}^{\mathrm{in}}) \tag{1.6}$$

$$Q = F_{\mathrm{h}} C_{\mathrm{h}} (T_{\mathrm{h}}^{\mathrm{in}} - T_{\mathrm{h}}^{\mathrm{out}}) \tag{1.7}$$

where F is the mass flow rate of the stream, C is the specific heat capacity of the fluid, T is the temperature of the fluid. Subscripts c and h denote the cold and hot streams, respectively, whereas superscripts in and out denote the inlet and outlet streams, respectively. The duty of a single-pass shell and tube heat exchanger operating in counter-current mode is given by Equation (1.8), which is based on the logarithmic mean temperature difference method.

$$Q = UA\Delta T_{lm} \tag{1.8}$$

where A is the area of the exchanger and ΔT_{lm} is the logarithmic temperature difference, which is defined as:

$$\Delta T_{lm} = \frac{\left(T_{\mathrm{h}}^{\mathrm{out}} - T_{\mathrm{c}}^{\mathrm{in}}\right) - \left(T_{\mathrm{h}}^{\mathrm{in}} - T_{\mathrm{c}}^{\mathrm{out}}\right)}{\ln\left[\left(T_{\mathrm{h}}^{\mathrm{out}} - T_{\mathrm{c}}^{\mathrm{in}}\right) / \left(T_{\mathrm{h}}^{\mathrm{in}} - T_{\mathrm{c}}^{\mathrm{out}}\right)\right]} \tag{1.9}$$

For the HEN cleaning scheduling problem, the objective is to minimise the operating and cleaning costs due to fouling over a specified horizon of time, t_{F}, and is given by Equation (1.10). The form of this objective is generally common to all approaches. Local considerations may give slightly different mathematical expressions. However, the differences lie in the solution approach.

$$Obj = \int_0^{t_{\mathrm{F}}} \left(\frac{C_E Q_F(t)}{\eta_f} + C_M(t) + C_X(t) \right) dt + \sum_j^{N_C} C_{cl,j} \tag{1.10}$$

The extra furnace energy consumption is described by the term $Q_F(t)$ which is determined based on the temperature of the crude oil entering the furnace, *i.e.* the crude inlet temperature (CIT). C_E and η_f represent the cost of fuel and the furnace efficiency, respectively. C_M and C_X refer to the extra cost associated with maintenance and downtime (production losses) incurred due to fouling, respectively. $C_{cl,j}$ is the cost of the j-th cleaning action. The total number of cleaning actions in the time horizon, t_{F}, is described by N_C.

The dynamic nature of the model is represented by Equation (1.3). Hence, an integration strategy is required to obtain numerical solutions for the differential equations and to integrate the energy, maintenance and downtime costs over a particular time horizon, t_{F}. The approach of [86] to the MINLP formulation results in a highly non-convex problem as they do not discretise time into fixed period durations, which by being considered as continuous decision variables results in considerable computational effort. Hence, for the formulation of the MINLP problem, the total time horizon is convenient to be discretised into a finite number of periods, NP, of fixed duration, Δt, in which cleaning actions are to be performed within these periods. The time required to clean an exchanger is integrated into the problem by further dividing each period into fixed sub-periods. A graphical representation is shown in Figure 1.2.4. Superscripts CL and OP denote cleaning and operating sub-periods, respectively.

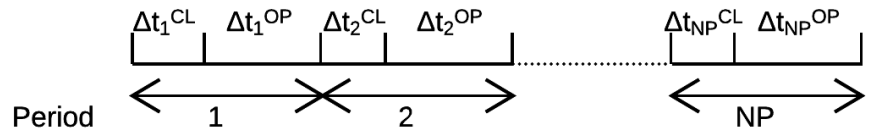

Figure 1.2.4: Time discretisation in MINLP formulation. Adapted from [128].

Binary variables, $y_{n,p}$, are used to describe the cleaning status of each exchanger in each cleaning sub-period, where

$$y_{n,p} = \left\{ \begin{array}{cc} 0 & \text{if the } n\text{-th heat exchanger is cleaned in period } p \\ 1 & \text{otherwise} \end{array} \right\} \forall n, p \tag{1.11}$$

Within an operating sub-period, this binary variable is fixed to 1 for all n, *i.e.* all units are online. Considering the case where $C_M = C_X = 0$ and the above, the objective function in Equation (1.10) becomes:

$$Obj = \int_0^{t_F} \frac{C_E Q_F(t)}{\eta_f} dt + \sum_{p=1}^{NP} \sum_{n=1}^{NE} C_{cl}(1 - y_{n,p}) \tag{1.12}$$

where NE is the number of exchangers considered for cleaning and NP is the number of periods. For the purpose of attaining results that can be compared to published ones from case studies in literature, C_{cl}, is taken to be independent of the exchanger size and duty. In industrial practice this is not the case, as larger exchangers take more effort to clean and will thus have a higher value of C_{cl} and vice versa. The amount of time taken to clean depends on the installation: if the exchanger must be isolated, removed and relocated for cleaning, these operations can determine the cleaning time. Furthermore, different cleaning methods will have different durations, but this is not considered in this work, although if necessary the optimisation models can include this with great ease.

1.3 Solution procedures for the HEN maintenance scheduling problem

This section will present the HEN cleaning scheduling optimisation problem formulation and review the different approaches used to solve this problem.

The non-convex MINLP cleaning scheduling problem has the general form:

$$\min_{y} \beta = f(v,y) \tag{1.13a}$$

subject to

$$g(v) = 0 \tag{1.13b}$$

$$h(v,p) = 0 \tag{1.13c}$$

$$s(v) \geq 0 \tag{1.13d}$$

$$v \in V \subseteq \mathbb{R}^{m_v} \tag{1.13e}$$

$$y \in Y \subseteq \{0,1\}^{m_y} \tag{1.13f}$$

where $f(v,y)$ is a function which defines the criterion to be optimised, *i.e.* minimising cost due to fouling, $g(v) = 0$ and $h(v,p) = 0$ are equality constraints that must be satisfied, *e.g.* mass and energy balances, and $s(v) \geq 0$ are inequality constraints that also must be satisfied, *e.g.* safety measurements or quality constraints. v is the vector of continuous variables, y is the vector of binary variables, m_{v} and m_{y} are the dimensions of vectors v and y, respectively. Due to the non-convex nature of the HEN cleaning scheduling problem, a reasonable aim is to obtain a good local optimum. Hence,

solution methods used to solve convex MINLP problems coupled with multiple starting points can be applied to these problems. This is the approach followed in this work.

The MINLP models can be solved using mathematical programming (MP) techniques based on MINLP through a number of ways: (i) the outer approximation (OA); (ii) outer approximation/equality relaxation (OA/ER); or (iii) generalised Benders decomposition (GBD) method, and also MP techniques based on MILP through reformulation. In addition, stochastic search approaches, such as the standard threshold accepting (TA) algorithm or variations of it, can be used as well as greedy heuristics which are currently used in industrial practice. These approaches are explained in detail in the following subsections.

1.3.1 Mathematical programming (MP) approaches based on mixed-integer nonlinear programming (MINLP)

The OA, OA/ER and GBD algorithms utilise a decomposition strategy where the MINLP problem is decomposed to a nonlinear programming (NLP) problem, in which the binary variables are fixed, and a mixed-integer programming (MIP) problem. The NLP problem is the primal problem whereas the MIP problem is the master problem. The upper bound to the MINLP problem is provided by the primal problem which supplies the set of continuous variables to be used by the master problem. Meanwhile, the master problem provides a lower bound to the MINLP problem and the set of binary variables to be used by the primal problem.

For a convex MINLP problem, after a few iterations the upper bound will be equal to the lower bound and the algorithm will terminate. In this case, the solution produced is the global optimum.

For a non-convex MINLP problem, the lower bound is not always valid as there is a possibility of cutting off sections of the feasible region. Therefore, the global solution may be left out of the search at some iteration. In this case, the lower bound will exceed the upper bound at some iteration, which will lead to termination of the algorithm.

The OA method was developed by [34]. The method is based on outer approximation and relaxation principles coupled with decomposition. The algorithm effectively exploits the structure of MINLP problems and consists of solving an alternating finite sequence of NLP subproblems and relaxed versions of a MIP linear master problem.

The master problem is derived using primal information, which consists of the solution of the continuous variables of the primal problem, and is based on an OA, *i.e.* linearisation of the nonlinear objective and constraints around the primal solution. The solution of the master problem and lower bound provides the next set of fixed binary variables to be used in the next primal problem. As iterations go on, two sequences of updating upper and lower bounds are generated which are non-increasing and non-decreasing, respectively, and converge after a number of iterations.

The OA algorithm is developed for problems which exclude nonlinear equality constraints. Hence this method assumes that nonlinear equalities can be eliminated algebraically or numerically.

This method was used by [127] for the case of a raw juice preheat train in a sugar refinery network consisting of 11 exchangers. The objective in this problem was the maximisation of the target temperature over a 120 day campaign. [128] extended the problem to a larger network over a longer campaign where they considered 2 case studies: (i) a 14 HEN over a 3 year horizon and (ii) an operating plant consisting of 27 units of exchangers for a 2 year horizon which they solved using a multi-start procedure.

For the purpose of handling explicitly nonlinear equality constraints, [74] developed the OA/ER algorithm for the solution of MINLP problems. The principle of this method is the relaxation of the nonlinear equality constraints into inequalities followed by application of the OA algorithm. Relaxation of the nonlinear equality constraints is based on the sign of the associated Lagrange multipliers when the primal problem is solved with the fixed binary variables. [105] highlighted the drawbacks of the OA/ER methods stating that the formulation of the master problem at each iteration involves the linearisation of the objective function and the nonlinear constraints around the primal solution. Linear approximations for non-convex functions are often invalid. Furthermore, [105] also stated that a large number of constraints are added to the master problem at each iteration. Hence, the computational effort for solving the corresponding MIP master problem dramatically increases after only a few iterations.

[106] considered the impact of ageing on fouling and cleaning dynamics in which an extra decision variable was added to the scheduling model, capturing the choice of cleaning method. They solved a small network of 4 heat exchangers using the optimiser DICOPT® [73] which is based on the OA/ER algorithm. The OA/ER algorithm was

able to obtain a cleaning schedule for the case where the deposit and ageing rates were fixed to a certain value, but failed to generate a solution when these rates were temperature-dependent due to the fact that the model becomes very nonlinear.

Due to the large computational effort required to produce a local solution and the possibility of failure in convergence, [104] used an alternative MINLP algorithm, the GBD method [11, 44]. The key feature of GBD is that only one constraint is added to the master problem at each iteration resulting in a small sized MIP master problem which remains such even after numerous iterations. [50] highlighted the weakness of this method: the lower bounds of the OA method are greater or equal to the ones of the GBD method, thus GBD commonly requires a significantly large number of iterations. However, the MINLP cleaning scheduling problem is non-convex thus with more iterations the possibility of cutting off sections of the feasible region decreases. The distinct feature of the GBD method in comparison to the OA/ER algorithm is that the master problem is derived from nonlinear duality theory making use of the Lagrange multipliers produced in the primal problem. In every iteration, the primal solution provides certain information, expressed as a Benders cut, on the assignment of master problem variables. A Benders cut eliminates some assignments that are not acceptable and is added to the master problem narrowing down its search space, thus leading to optimality [22].

1.3.2 Mathematical programming (MP) approaches based on mixed-integer linear programming (MILP)

Alternatively, this problem can be solved by reformulating certain differential algebraic equations (DAEs) from an MINLP model to a MILP model as in the work of [77], who applied a rigorous MILP model to a crude oil preheat train. They avoided introducing linear approximations through the use of standard transformations to obtain linear expressions. This was based on the idea of parameterising the heat transfer coefficient of the units with the aid of the binary variables of the formulation. In their model, nonlinearity occurred only through products of continuous variables with binary variables and products of binary variables to each other. [104] highlighted the drawbacks of their method by recognising that in order to maintain the linear characteristics, extra variables and constraints must be added. The number of extra constraints grows exponentially with the number of time intervals, thus making the solution of large

problems of realistic size computationally impractical. To overcome this drawback, a decomposition method was proposed by [77]. This was based on the assumption that the cleaning schedule of an individual unit is not affected by the cleaning decisions of the rest of the units. Using this decomposition technique, the computational effort for acquiring a solution was reduced immensely. However, [104] stated that this assumption is invalid and will not work for strongly coupled networks arising from hot streams passing through units in series.

1.3.3 Stochastic search approaches

As an alternative to MP techniques, stochastic search techniques can be used. Stochastic search approaches involve a random choice being made in the search direction as the algorithm iterates towards a solution [131].

[106] used a simple stochastic search method to solve the cleaning schedule for a small network of 4 units over one year time horizon with dual fouling layers in which the deposition and ageing rates are a function of temperature. [106] reported that solutions using MP techniques for this case failed as the problem becomes very nonlinear. Furthermore, [130] explored the use of stochastic optimisation techniques to solve the HEN cleaning scheduling problem. They developed a method derived from the standard TA algorithm termed the backtracking threshold accepting (BTA) algorithm. TA is a local search method proposed by [33, 93]. The algorithm starts with a random feasible solution and searches the neighbouring solution space by making random moves. Unlike a classical local search, TA allows the escape from local minima by allowing uphill movements in which deteriorations in the objective value are accepted, given they are not worse than a particular threshold. The main modification of this method in comparison with the classical TA algorithm is the addition of a backtracking step in case a given number of new configurations do not gain acceptance. [130] compared the BTA with the OA algorithm in 2 large case studies based on crude oil refinery PHTs, showing that the CPU time taken to solve the problems is significantly smaller. However, the drawback of using stochastic optimisation algorithms is that global optimality cannot be guaranteed.

With regards to the last observation, nonetheless, it should also be noted that direct use of an MINLP approach on the HEN scheduling problem only leads to a local

feasible solution. This is due to the fact that the underlying dynamic model has no guarantees of convexity and hence only local solutions can be obtained. It is further noted that the nonlinearity of the model is such that often MINLP algorithms, such as the OA method and its variants, may fail frequently due to inconsistent linearisation of the constraints during NLP solution iterations.

1.3.4 Greedy heuristics

Greedy heuristics, which is the methodology currently used by industry, is a simple and intuitive algorithm in which the solution is constructed in stages. At each stage, the value of a scheduling action is assigned by making a decision based on heuristics, such as the current best savings or lowest cost. There is frequently no look-ahead to the impact of a local decision to long-term economics of the operation of the HEN. The greedy algorithm chooses the locally most attractive option with no concern for its effect on global optimality. Therefore, solutions found through greedy algorithms are not guaranteed to be optimal.

Greedy algorithms are useful when the time available to solve a problem is extensively limited. In the spectrum of solution approaches to combinatorial optimisation problems, greedy schemes can be seen as lying at one end of the spectrum with MP techniques lying at the other extreme. In the middle are stochastic search approaches such as simulated annealing and genetic algorithms (GA).

The GA is named from the process of drawing an analogy between the components of a configuration vector x and the genetic structure of a chromosome with the goal of maximising a function $f(x)$ of the vector $x = (x_1, x_2, x_N)$ [123], while simulated annealing is a stochastic local search technique that operates iteratively by choosing an element y from a neighbourhood $N(x)$ of the present configuration x: the candidate y is either accepted as the new configuration or rejected [72]. The solution quality is best when using MP techniques, while it is worst when using greedy heuristics. However, the former technique is associated with an increase in solution time [139].

For the HEN maintenance scheduling problem, such simple strategies consider cleaning actions only in the current period. [128] compared their produced MINLP results using the OA method with that of a simple greedy algorithm, showing that the former approach is more efficient when it converged, as it considered all the options over

the complete horizon. However, due to the non-convexity of the problem, neither the MINLP OA algorithm nor the greedy heuristic can guarantee global optimality.

1.4 Thesis structure

This thesis can be subdivided into the following parts:

(i) The development of novel approaches for optimisation of HEN maintenance scheduling problems (Chapter 3 and Chapter 4);

(ii) Generalisation of the methodology to multiperiod maintenance scheduling problems (Chapter 5) ; and

(iii) HEN maintenance scheduling problems with parametric uncertainty (Chapter 6).

The current chapter (Chapter 1) gives a general outline to vital concepts needed for the core material of this thesis.

Chapter 2 reviews the detailed aims and objectives achieved by the work presented in this thesis.

Chapter 3 commences with the presentation of the general HEN maintenance scheduling problem formulation. In the core of the chapter, novel approaches based on MINLP to solve this problem are presented. A set of HEN case studies of different sizes, configuration and fouling models from the open literature demonstrate that these methods are able to optimally produce schedules with the best reported computational time.

In Chapter 4, the first section presents the formulation of the HEN cleaning scheduling problem as an optimal control problem (OCP). This is followed by a theoretical demonstration of bang-bang OCP property. In the next section, a novel methodology for the solution of the HEN cleaning scheduling problem based on a feasible path optimal control approach, *i.e.* sequential approach, is presented. A number of HEN cleaning scheduling case studies from the open literature demonstrate that this approach is robust, reliable, and efficient.

In Chapter 5, the novel approach presented in Chapter 4 is generalised to other maintenance scheduling problems through application to the scheduling of membrane regeneration actions in reverse osmosis (RO) membrane networks. In the first section, the RO membrane network scheduling problem is introduced along with motivations for this problem. In the following sections, the problem formulation is presented and similarities with HEN maintenance scheduling problems are discussed in terms of decaying performance processes. The next sections presents an RO case study description from the open literature and the problem solution methodology, respectively. Results for the case study are presented and discussed in the final sections of this chapter demonstrating that the feasible path optimal control approach can be deployed to address generalised maintenance scheduling problems.

Chapter 6 presents a novel approach for optimisation of HEN maintenance schedules with parametric uncertainty. This chapter initially gives a general introduction to parametric uncertainty in decision making followed by a literature survey of methodologies used for solving optimisation problems with uncertainty. In the core of the chapter, the problem formulation is presented followed by implementation details and modifications of case studies from the open literature. In the final two sections, results are presented for these case studies along with a thorough discussion and report of observations, showing that this methodology is stable and is efficient.

Chapter 7 presents the overall conclusions of the current thesis and proposes future research directions.

Chapter 2

Aim and objectives

2.1 Research aim

Due to the limitation of current solution methods for the multiperiod optimisation of cleaning schedules of HENs as aforementioned in Chapter 1, there is a great need to develop efficient, reliable and robust solution methods for this problem and other discrete decision making based maintenance scheduling problems arising in chemical engineering processes. Therefore, the general aim of this thesis is to make novel contributions to the solution of HEN maintenance scheduling problems.

2.2 Research objectives

Objective I: Develop novel techniques for the multiperiod optimisation of scheduling HEN cleaning problems (Chapter 3 and Chapter 4)

HEN cleaning scheduling problems present a great challenge due to their complex combinatorial nature. Three novel methods are proposed based on solving the relaxed MINLP HEN cleaning scheduling problem:

(i) Using an infeasible path MINLP based approach coupled with rounding

An important observation missed by previous authors is the near bang-bang nature of the HEN cleaning scheduling problem. If the decision variable is relaxed, *i.e.* $y_{n,p}$ is allowed to vary between 0 and 1, and the solution occurs when the decision variable is at either extreme bound of the feasible region, this is termed a bang-bang solution. By recognition of this characteristic, the relaxed NLP of the MINLP can be solved by any standard, large-scale constrained nonlinear optimisation solver, such as an interior point method (IPM). This obviates the need for combinatorial optimisation methods. The technique is followed by a simple rounding process, when required if the solution is not totally bang-bang, to obtain a solution to this problem with very little computational effort.

(ii) Using an infeasible path MINLP based approach coupled with a direct branch and bound (B&B) method

In the case where many singular arcs exist, *i.e.* $y_{n,p}$ is fractional and rounding does not give a good solution, it is alternatively proposed to apply a direct B&B technique to solve this problem. A direct B&B method is an attractive option as it searches the solution space of a given problem for the best one. The B&B method uses bounds for the function to be optimised combined with the value of the current best solution enabling the algorithm to search parts of the solution space only implicitly.

(iii) Using a feasible path optimal control approach coupled with rounding

The HEN cleaning scheduling problem can be categorised as a mixed-integer optimal control problem (MIOCP) where discrete (binary) control decisions are made over a known time horizon with the objective of minimising cost. MIOCPs are concerned with the optimisation of dynamic systems and have been largely explored with mathematical techniques. As such, a multistage sequential optimal control approach for the solution of the HEN maintenance scheduling problem is most suitable. The technique is followed by a simple rounding strategy.

Objective II: Demonstrate that the techniques developed can be generalised to multiperiod maintenance scheduling problems in chemical engineering processes (Chapter 5)

The proposed research approach is not limited to the HEN scheduling cleaning problem. The novel techniques developed can be applied to other important multiperiod maintenance scheduling problems which are based on discrete decision making. For

instance, in the water treatment industry, maintenance scheduling examples include RO membranes which are subject to biofouling. RO is an important membrane separation process widely used in desalination applications. Biofouling decreases production capacity, water quality and increases operational costs. The regeneration of membranes through cleaning is necessary to remove such foulants and restore membrane performance.

Objective III: Improve solution robustness through stochastic programming techniques (Chapter 6)

Heat exchangers are typically over-designed in terms of their heat exchange area. This is chosen with fouling in mind as well as the numerous uncertainties in data and prediction. Accounting for uncertainty is vital as it influences the cleaning schedule optimisation. Uncertainties in parameters which need to be addressed include heat transfer coefficients, kinetics for fouling layer formation, temperature effect, process economics, *etc.*

The final aim is to make use of stochastic programming techniques to deal with uncertainties in the HEN cleaning scheduling model through computational experiments. As such, a suitable multi-scenario approach is proposed.

Chapter 3

MINLP approaches for HEN cleaning scheduling problems

This chapter presents two methodologies based on an infeasible path MINLP approach for the solution of the HEN cleaning scheduling problem. In these cases, time is discretised into periods and further discretised into cleaning and operating sub-periods, where the beginning and end of the cleaning period is denoted by superscripts bcp and ecp. Similarly, superscripts bop and eop denote the beginning and end of the operating sub-periods. The first approach uses an IPM coupled with a simple rounding scheme to take care of any fractional binary variables, $y_{n,p}$, that arise. In the case where many binary variables are fractional, this simple rounding scheme may not result in good solutions, therefore the second approach uses an IPM coupled with a direct B&B technique. Results show both of these methods achieve good solutions with minimal computational time. This is due to the very few fractional binary variables that result which is attributed towards the bang-bang nature of these problems. This is discussed further in Section 3.5.

3.1 Problem formulation as a MINLP problem

Cleaning decisions are made at the beginning of each period. Using the time discretisation outlined in Figure 1.2.4 and binary variable $y_{n,p}$ shown in Equation (1.11), the overall heat transfer coefficient shown in Equation (1.2) can be rewritten for each

of the sub-period points in time: bcp, ecp, bop, and eop. The overall heat transfer coefficient for unit n at the beginning of the first cleaning sub-period, $U_{n,p}^{\text{bcp}}$, can be written as Equation (3.1).

$$U_{n,p}^{\text{bcp}} = U_{0,n} \qquad \forall n, p = 1 \tag{3.1}$$

where $U_{0,n}$ represents the initial value of the overall heat transfer coefficient and is equivalent to $U_{c,\text{n}}$ if the unit is in a clean condition at the start of the operating horizon. The overall heat transfer coefficient at the end of each cleaning sub-period is defined in relation to that at the beginning of the cleaning sub-period:

$$U_{n,p}^{\text{ecp}} = y_{n,p} \frac{U_{n,p}^{\text{bcp}}}{1 + U_{n,p}^{\text{bcp}} \dot{R}_{f,n} \Delta t^{\text{CL}}} + \eta_c U_{c,n} (1 - y_{n,p}) \qquad \forall n, p \tag{3.2}$$

Equation (3.2) resets the overall heat transfer coefficient to the clean condition, $\eta_c U_{c,n}$, if exchanger n is cleaned in period p, *i.e.* $y_{n,p} = 0$. η_c denotes the fraction of the clean value to which the overall heat transfer coefficient is restored after cleaning, while $\dot{R}_{f,n}$ is the fouling rate. For exchanger n undergoing linear fouling this is defined as a constant parameter based on plant data reconciliation, as shown in Equation (3.3).

$$\dot{R}_{f,n} = a \qquad \forall n \tag{3.3}$$

For the purpose of attaining results that can be compared to published ones from case studies in the open literature, the duration of the cleaning sub-period, Δt^{CL}, is taken to be independent of the exchanger size and duty. In industrial practice this is not the case, as the cleaning time from one exchanger to another will vary depending on its size and duty. Larger exchangers will take longer to clean and vice versa. Furthermore, different cleaning methods will have different durations, but this is not considered in this work. Such variations in cleaning time can be readily accommodated within all mathematical programming models proposed in this research.

The overall heat transfer coefficient at the beginning of each operating sub-period is

related to that in the previous cleaning sub-period by:

$$U_{n,p}^{\text{bop}} = U_{n,p}^{\text{ecp}} \qquad \forall n,p \tag{3.4}$$

and that at the end of each operating sub-period can be expressed as:

$$U_{n,p}^{\text{eop}} = \frac{U_{n,p}^{\text{bop}}}{1 + U_{n,p}^{\text{bop}} \dot{R}_{f,n} \Delta t^{\text{OP}}} \qquad \forall n,p \tag{3.5}$$

The overall heat transfer coefficient at the beginning of each consecutive cleaning sub-period can be calculated from Equation (3.6).

$$U_{n,p}^{\text{bcp}} = U_{n,p-1}^{\text{eop}} \qquad \forall n, p = 2,\ldots,NP \tag{3.6}$$

For the case of asymptotic fouling, Equation (3.2) is replaced with Equation (3.7), where the overall heat transfer coefficient at the end of the cleaning sub-period is represented in relation to that of the initial value, $U_{0,n}$, at the start of the operating horizon.

$$U_{n,p}^{\text{ecp}} = y_{n,p} \frac{U_{0,n}}{1 + U_{0,n} R_{f,n,p}^{\text{ecp}}} + \eta_c U_{c,n} (1 - y_{n,p}) \qquad \forall n,p \tag{3.7}$$

where the asymptotic fouling resistance at the end of the cleaning sub-period is calculated via Equation (3.8).

$$R_{f,n,p}^{\text{ecp}} = R_{f,n}^{\infty} \left(1 - \exp\left[\frac{-{t'_{n,p}}^{\text{CL}}}{\tau_n} \right] \right) \qquad \forall n,p \tag{3.8}$$

where ${t'_{n,p}}^{\text{CL}}$ is the elapsed time since the last cleaning action in the cleaning sub-period for exchanger n in period p and can be defined for the first period through Equation (3.9).

$${t'_{n,p}}^{\text{CL}} = \Delta t^{\text{CL}} \qquad \forall n, p = 1 \tag{3.9}$$

For consecutive cleaning sub-periods, this is calculated through:

$$t'_{n,p}{}^{\mathrm{CL}} = y_{n,p}(t'_{n,p-1}{}^{\mathrm{OP}} + \Delta t^{\mathrm{CL}}) \qquad \forall n, p = 2, \ldots, NP \tag{3.10}$$

where $t'_{n,p-1}{}^{\mathrm{OP}}$ is the elapsed time since the last cleaning action for exchanger n in the previous operating sub-period and is expressed in Equation (3.11).

$$t'_{n,p}{}^{\mathrm{OP}} = t'_{n,p}{}^{\mathrm{CL}} + \Delta t^{\mathrm{OP}} \qquad \forall n, p \tag{3.11}$$

Similarly, for the case of asymptotic fouling, to calculate the overall heat transfer coefficient at the end of the operating sub-period Equation (3.5) is replaced with Equation (3.12).

$$U^{\mathrm{eop}}_{n,p} = \frac{U_{0,n}}{1 + U_{0,n} R^{\mathrm{eop}}_{f,n,p}} \qquad \forall n, p \tag{3.12}$$

where the asymptotic fouling resistance at the end of the operating sub-period is calculated through:

$$R^{\mathrm{eop}}_{f,n,p} = R^{\infty}_{f,n} \left(1 - \exp\left[\frac{-t'_{n,p}{}^{\mathrm{OP}}}{\tau_n} \right] \right) \qquad \forall n, p \tag{3.13}$$

Calculation of the performance of an existing network is a requirement for the scheduling problem, in which the network is simulated based on rating calculation. Hence, the number of transfer units (NTU) effectiveness method [56] is used to assess the performance of each heat exchanger instead of direct usage of Equations (1.8) and (1.9). This is achieved by rearranging Equations (1.8) and (1.9) in terms of a rating calculation. The units are modelled as simple countercurrent exchangers. The effectiveness term, denoted by α, and the ratio of capacity flow rates, denoted by P, defined in Equations (3.14) and (3.15), respectively, are reproduced from [128]:

$$\alpha_{n,p} = \frac{U_{n,p} A_n}{F_{\mathrm{h},n} C_{\mathrm{h},n}} \qquad \forall n, p \tag{3.14}$$

$$P_n = \frac{F_{\mathrm{h},n} C_{\mathrm{h},n}}{F_{\mathrm{c},n} C_{\mathrm{c},n}} \qquad \forall n \tag{3.15}$$

Equation (3.14) can be rewritten for each of the sub-period points in time: bcp, ecp, bop and eop, as shown in Equation (3.16).

$$\alpha^{\mathrm{X}}_{n,p} = \frac{U^{\mathrm{X}} A_n}{F_{\mathrm{h},n} C_{\mathrm{h},n}} \qquad \forall n,p \tag{3.16}$$

where superscript X denotes bcp, ecp,bop and eop. Given that all exchangers are online during the operating sub-period and by combination and rearrangement of Equations (1.6) to (1.9), the temperature of the hot and cold streams leaving each exchanger can be calculated. The temperatures of the hot and cold streams leaving an exchanger are determined by:

$$T^{\mathrm{out}}_{\mathrm{h},n,p} = T^{\mathrm{in}}_{\mathrm{h},n,p} - \frac{1}{P_n}\left(T^{\mathrm{out}}_{\mathrm{c},n,p} - T^{\mathrm{in}}_{\mathrm{c},n,p}\right) \qquad \forall n,p \tag{3.17}$$

$$T^{\mathrm{out}}_{\mathrm{c},n,p} = \left[\frac{P_n(\exp(-\alpha_{n,p}(P_n-1))-1)}{\exp(-\alpha_{n,p}(P_n-1))-P_n}\right] T^{\mathrm{in}}_{\mathrm{h},n,p} + \left[\frac{(1-P_n)\exp(-\alpha_{n,p}(P_n-1))}{\exp(-\alpha_{n,p}(P_n-1))-P_n}\right] T^{\mathrm{in}}_{\mathrm{c},n,p} \qquad \forall n,p \tag{3.18}$$

Equations (3.17) and (3.18) are applicable to most preheat configurations which feature $P_n < 1$. If the alternative case arises where $P_n > 1$, these equations must be amended. By incorporating the different sub-period points in time: bcp, ecp,bop and eop, Equation (3.17) can be rewritten as:

$$T^{\mathrm{out,X}}_{\mathrm{h},n,p} = T^{\mathrm{in,X}}_{\mathrm{h},n,p} - \frac{1}{P_n}\left(T^{\mathrm{out,X}}_{\mathrm{c},n,p} - T^{\mathrm{in,X}}_{\mathrm{c},n,p}\right) \qquad \forall n,p \tag{3.19}$$

The temperature of the cold stream leaving an exchanger at the beginning of the operating sub-period is defined by:

$$
\begin{aligned}
T^{\text{out,bop}}_{\text{c},n,p} &= \left[\frac{P_n(\exp(-\alpha^{\text{bop}}_{n,p}(P_n-1))-1)}{\exp(-\alpha^{\text{bop}}_{n,p}(P_n-1))-P_n}\right] T^{\text{in,bop}}_{\text{h},n,p} \\
&+ \left[\frac{(1-P_n)\exp(-\alpha^{\text{bop}}_{n,p}(P_n-1))}{\exp(-\alpha^{\text{bop}}_{n,p}(P_n-1))-P_n}\right] T^{\text{in,bop}}_{\text{c},n,p} \qquad \forall n,p
\end{aligned} \tag{3.20}
$$

The same expression is generated for the cold stream temperature leaving an exchanger at the end of the operating sub-period. For the beginning of the cleaning sub-period using the time discretisation and binary variable $y_{n,p}$, the temperature of the cold outlet stream is given by:

$$
\begin{aligned}
T^{\text{out,bcp}}_{\text{c},n,p} &= \left[\frac{P_n(\exp(-\alpha^{\text{bcp}}_{n,p}(P_n-1))-1)}{\exp(-\alpha^{\text{bcp}}_{n,p}(P_n-1))-P_n}\right] y_{n,p} T^{\text{in,bcp}}_{\text{h},n,p} \\
&+ \left(1-y_{n,p}+y_{n,p}\left[\frac{(1-P_n)\exp(-\alpha^{\text{bcp}}_{n,p}(P_n-1))}{\exp(-\alpha^{\text{bcp}}_{n,p}(P_n-1))-P_n}\right]\right) T^{\text{in,bcp}}_{\text{c},n,p} \qquad \forall n,p
\end{aligned} \tag{3.21}
$$

Again, the same expression is generated for the cold stream temperature leaving an exchanger at the end of the cleaning sub-period.

The cold inlet temperature of the first exchanger in the network is fixed and is based on an external stream. For the case of crude oil refinery PHTs this is the crude feed temperature. Subsequent exchangers' cold inlet temperatures are determined based on the cold outlet temperature of the immediate upstream exchanger. The same is applicable for the hot inlet stream temperature. If an exchanger is being cleaned, the inlet cold stream bypasses the exchanger and the corresponding hot stream is diverted to the next exchanger.

The objective to be minimised is the expected net present value of the operating costs (NPC) arising from the tradeoff between furnace extra fuel costs due to fouling and

heat exchanger cleaning costs which includes manpower, chemicals and maintenance. This is shown in Equation (3.22).

$$\min_{y_{n,p}} NPC = \sum_{p=1}^{NP} C_E \frac{(Q_F^{\text{clean}} - Q_{F,p})}{\eta_f} + \sum_{p=1}^{NP}\sum_{n=1}^{NE} C_{cl}(1 - y_{n,p}) \qquad \forall n, p \qquad (3.22)$$

where Q_F^{clean} is the furnace's energy consumption for the clean condition and $Q_{F,p}$ is the total actual energy consumption in period p. As the cleaning sub-period, Δt^{CL} can vary for each exchanger, the total actual energy consumption is approximated using the following expression:

$$Q_{F,p} = \frac{Q_{F,p}^{\text{bcp}} + Q_{F,p}^{\text{ecp}}}{2} \overline{\Delta t}^{\text{CL}} + \frac{Q_{F,p}^{\text{bop}} + Q_{F,p}^{\text{eop}}}{2} \Delta t^{\text{OP}} \qquad \forall p \qquad (3.23)$$

where

$$\overline{\Delta t}^{\text{CL}} = \frac{\sum_{n=1}^{NE} \Delta t_n^{\text{CL}}}{NE} \qquad \forall n \qquad (3.24)$$

This expression approximates the energy consumption in each sub-period using a linear approximation.

Selection constraints are imposed on the binary variables such as processing considerations, performance targets, *i.e.* temperature bounds on the performance of exchangers and plant protocol. These constraints impose a restriction on the combination of cleaning actions allowed thus reducing solution space and simulations to be performed, resulting in faster convergence. Logical selection constraints are also imposed preventing a unit from being cleaned in the direct period after it is last cleaned:

$$y_{n,p} + y_{n,p-1} \geq 1 \qquad \forall n, p = 2, \ldots, NP \qquad (3.25)$$

In addition, all units are constrained to be online during the first period, where:

$$y_{n,p} = 1 \qquad \forall n, p = 1 \qquad (3.26)$$

3.2 Problem solution methodology and implementation

In this section, we introduce the IPM and rounding scheme used throughout this chapter, as well as the direct B&B technique which is suitable for cases where many non-integer $y_{n,p}$ result and rounding does not yield a good solution.

3.2.1 Interior Point Method (IPM) with rounding scheme

The IPM is a polynomial-time algorithm which was first proposed by [67] to solve linear programs. The method is based on approaching the optimal solution from the strict interior of the feasible region rather than the boundaries as in the simplex method published by [25] in 1947. The simplex method, as shown in Figure 3.2.1, involves traveling along the constraints going from one vertex or corner point to another until an optimal value for the objective is found at a vertex. The drawback of this method is that its worst complexity is exponential.

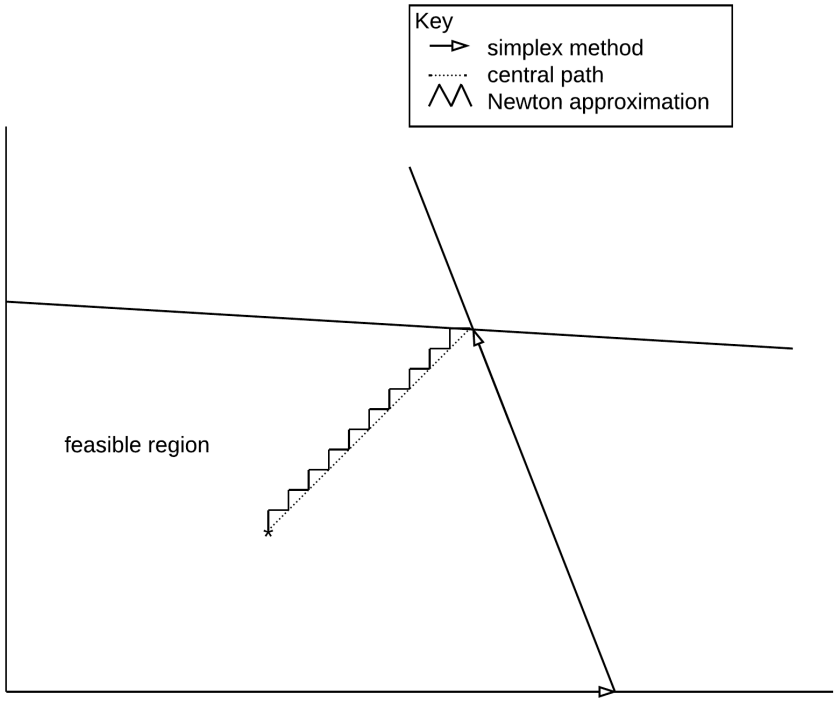

Figure 3.2.1: Interior point and simplex method illustrations

Another way of approaching nonlinear programming problems is to dualise the constraints such that the constraints are integrated into the problem, resulting in an unconstrained nonlinear programming problem. To transform the problem shown in Equations (3.27a) to (3.27c) into the standard form shown in Equations (3.28a) to (3.28d), slack variables are introduced to the inequality constraints to convert them to equalities. This is done by setting $b_i - a_i(y) \equiv s_i$, where s_i are the slack variables, giving $b_i - a_i(y) - s_i = 0$ subject to $s_i \geq 0$. These equality constraints are represented by the standard form $c(y) = 0$ shown in Equation (3.28b).

$$\min_y f(y) \tag{3.27a}$$

subject to

$$a_i(y) \leq b_i \tag{3.27b}$$

$$i = 1, \ldots, m \tag{3.27c}$$

$$\min_y f(y) \tag{3.28a}$$

subject to

$$c(y) = 0 \tag{3.28b}$$

$$y \geq 0 \tag{3.28c}$$

$$y \in \mathbb{R}^m \tag{3.28d}$$

A continuous function known as a barrier function is used to dualise the constraints. The most common types of barrier functions are inverse and logarithmic barrier func-

tions. For instance, in the mathematical programming problem displayed in Equation (3.29a), taking the negative logarithm of the constraint slacks results in the barrier function approaching infinity as variable y approaches the boundaries of the feasible region.

$$\min_{y} f(y) - \psi \sum_{i=1}^{m} \log(b_i - a_i(y)) \tag{3.29a}$$

barrier function:

$$-\sum_{i=1}^{m} \log(b_i - a_i(y)) \to \infty \,\text{as}\, y \to a_i(y) \leq b_i \tag{3.29b}$$

Since the objective is to be minimised, the barrier function prevents the search point from going outside the feasible region. The value of ψ is the weight coefficient and thus controls the strength of the barrier function. A large ψ entails that the current point is far away from the boundaries giving the analytical centre of the feasible region, marked as $*$ in Figure 3.2.1. Decreasing ψ slowly and taking time to find the precise optimal point for each ψ value, traces out the central path. This is quite time consuming and a computationally intense process.

An alternative is to approximate the path by utilising Newton's method for solving NLPs. To achieve polynomial-time complexity, ψ is decreased gradually and a Newton step is used for each decrease in ψ which results in a small zig-zag pattern convergence to the optimal point. Practically, ψ can be decreased quicker to get faster convergence. In summary, Newton's method approximates the path through the interior of the feasible region and this technique is referred to as IPMs.

IPMs are theoretically advantageous due to their polynomial-time complexity and more importantly their practical advantage as a range of difficult industrial problems including nonlinear large-scale models have been solved using these methods. Applications include heating, ventilating and air conditioning systems energy consumption optimisation problems [75], simultaneous dynamic processing and production planning for a multi-product plant [12], *etc.*

As the IPM cannot handle the mixed integer decision variables $y_{n,p}$, a simple rounding scheme is proposed. Throughout this work, the rounding scheme presented in Equa-

tion (3.30) is imposed on the optimal relaxed NLP of the MINLP which is denoted by $y^*_{n,p}$. It is recognised that a simple rounding scheme will not generate good results when many singular arcs exist, *i.e.* fractional decision variables. Therefore, we alternatively propose implementing a direct B&B method to arrive at a feasible MINLP solution. This is outlined in the next subsection.

$$y_{n,p} = \left\{ \begin{array}{l} 1 \,\text{if}\, y^*_{n,p} \geq 0.5 \\ 0 \,\text{if}\, y^*_{n,p} < 0.5 \end{array} \right\} \tag{3.30}$$

3.2.2 Direct Branch and Bound (B&B) method

B&B is the most widely used tool for solving large scale $\mathscr{NP}$-hard combinatorial optimisation problems. The B&B method is based on the concept of solving the continuous relaxation of the programming problem and branching on the fractional variables [23]. Generally, B&B algorithms search the complete solution space for a given problem for the best solution. The number of potential solutions increases exponentially with the number of variables, hence explicit enumeration is usually impossible. Thus, B&B algorithms make use of bounds for the function to be optimised in combination with the value of the current best solution enabling the algorithm to search parts of the solution space only implicitly. The solution status is described by a pool of unexplored subsets and the best solution found so far. A search tree is dynamically generated where the unexplored subspaces are represented as nodes which are processed through each iteration by a B&B algorithm.

There are three major elements taking place with every iteration: (i) selection of the node to process; (ii) calculation of bounds and (iii) branching of the node. Branching refers to the subdivision of the node solution space into two or more subspaces that are examined in a succeeding iteration. This is achieved by addition of a new constraint on each node that is branched. During each iteration, a check is made to establish whether there is a single solution contained in the subspace or otherwise. If the former holds, the generated solution is compared with the current best one and the better of the two is kept. Else, the subspace bounding function is calculated and compared to the current best solution. The subspace is then either discarded or stored with its bound depending on whether the subspace contains an optimal solution. Once the search terminates, the overall best solution found is declared as the optimal solution.

Termination of the search is signalled by completing the examination of all parts of the solution space. Usually though, to avoid complete evaluation of the entire B&B tree, a tolerance is specified for the difference between the current lower bound and upper bound (the best feasible and fully integer solution available) so as to declare earlier termination, good enough for practical purposes. It is worth noting that for MINLP problems, the upper bound for the first node is calculated by solving the NLP model without integer constraints, *i.e.* relaxation of these constraints. Therefore, if the problem is non-convex, the lower bound calculated, which is based on the upper bound, is not the true one and may be much lower. Furthermore, premature fathoming, *i.e.* early termination of the node, may occur if only one local NLP solution is generated at each node.

3.2.3 Implementation

Python is a high performance object-oriented programming language that is easy to learn and is user-friendly compared to other traditional languages such as Fortran, C and C++, which require considerable training and extensive time in terms of program development, compiling and debugging. A Python environment has been selected for implementation due to two main advantages: Python's ability to prototype rapidly and the availability of a large set of libraries to perform specific computing tasks.

Furthermore, this environment contains a Python optimisation modelling objects package (Pyomo), which is an open source tool for modelling optimisation applications in Python. Pyomo can be used to define symbolic problems, create concrete problem instances and solve these instances with standard solvers. Pyomo provides a capability that is commonly associated with algebraic modelling languages such as AMPL [43] and GAMS [115], but Pyomo's modelling objects are embedded within a full-featured high-level programming language with a rich set of supporting libraries [53].

In this work we use the solver IPOPT, which is an IPM using logarithmic barriers and implements several advancements [68]. IPOPT is used as a library in Pyomo and is an open source software package for large-scale nonlinear systems optimisation. [140] demonstrate the performance of IPOPT code with a detailed numerical study based on hundreds of problems indicating increased robustness, thus making it the most reliable large-scale NLP solver available to date.

For the implementation of the direct B&B method, we use the solver BONMIN [15], which uses a simple B&B algorithm based on solving a continuous nonlinear program at each node of the search tree and branching on variables. BONMIN is a basic open source nonlinear mixed integer programming software package and uses IPOPT as the NLP solver.

Due to the non-convex nature of the scheduling problem, 50 starting points are used and the best objective value is reported. Starting points are generated by randomly selecting the status of each heat exchanger, *i.e.* operating or cleaning, in every period. This is done through a random choice of 0 or 1 for all the decision variables' starting points and is implemented via the random.choice function in Python. Results are obtained on an Intel Core i5, 4 GB RAM and 1.4 GHz MacBook Air running on OS X (2014 model).

3.3 Case studies descriptions

In this section, the case studies for the scheduling of cleaning actions for HENs are introduced along with their associated data. Both linear and asymptotic fouling behaviour are considered.

3.3.1 Case study A

A single heat exchanger from [77] is considered as shown in Figure 3.3.2. Both linear and asymptotic fouling are modelled. Based on [77]'s model, constant flows and properties throughout the horizon are assumed. In addition, [77] assume that the temperatures are constant throughout the sub-period. These assumptions are also applicable to case studies B to D and are made for the purpose of achieving results that can be compared to published ones from case studies in the open literature. Two different cleaning costs are used: £0 and £4000. There is no mention of the furnace fuel cost C_E in the work of [77]; however, a cost of £2.93/MM Btu is used in our work, which is based on the cost reported by [130]. This also applies to case studies B and C. The work of [130] is the source of data for [77]'s models where they compare their solution for their MILP approach with those obtained by [130] who use the OA/ER

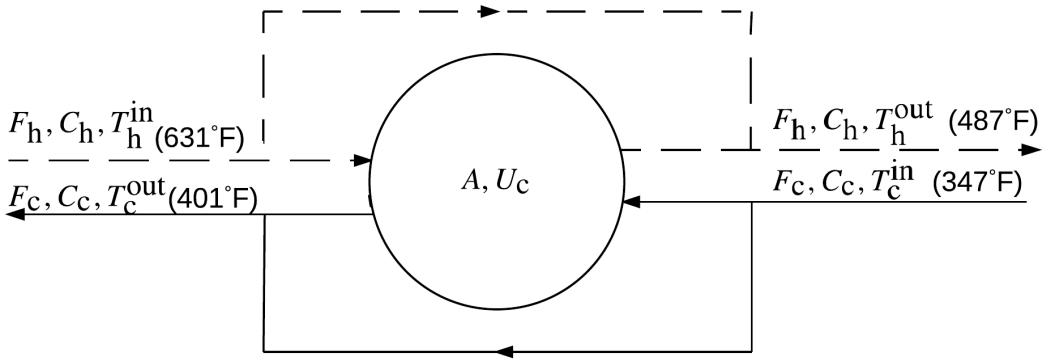

Figure 3.3.2: Single heat exchanger case. Temperature values are given for initial, clean condition. Adapted from [77].

algorithm. Although [77] state that they take into account the decay of the heat transfer coefficient in each sub-period η_c, there is no mention of this value in their work. Hence, we considered the value of parameter η_c to be 1 in this case study as well as in case studies B to D. The single heat exchanger is modelled over a 24 month operating horizon. Data for this case study is presented in Table 3.3.1. The single unit is constrained to be online in the first period and logical constraints are imposed (Equation (3.25)). These constraints are also applicable to case studies B and C.

3.3.2 Case study B

Four heat exchangers in series for a crude distillation unit PHT, where heat is recovered from distillation column products and pump-around streams, are considered. This is displayed in Figure 3.3.3. Only linear fouling is considered in this case with a cleaning cost of £4000. The four heat exchanger case is modelled over two operating horizons: 12 months and 18 months. Data for this case study is presented in Table 3.3.2.

3.3.3 Case study C

A 10 unit HEN located in crude oil distillation unit PHTs undergoing linear and asymptotic fouling is considered as shown in Figure 3.3.4. The number of periods considered is $NP = 18$ for this network and both £0 and £4000 cleaning costs are used.

Table 3.3.1: Data for single heat exchanger case. Adapted from [77].

Parameter	Value
F_{h} [lb/h]	208000
F_{c} [lb/h]	649000
C_{h} [Btu/lb°F]	0.67
C_{c} [Btu/lb°F]	0.57
U_{c} [Btu/hft^2°F]	88.1
U_0 [Btu/hft^2°F]	88.1
A [ft^2]	1257
a (linear fouling) [ft^2°F/Btu]	3.88×10^{-7}
R_f^{∞}(asymptotic fouling) [hft^2°F/Btu]	6.73×10^{-3}
τ (decay constant)[month]	4
Δt^{CL} [month]	0.20
Δt^{OP} [month]	0.80
η_f	0.75

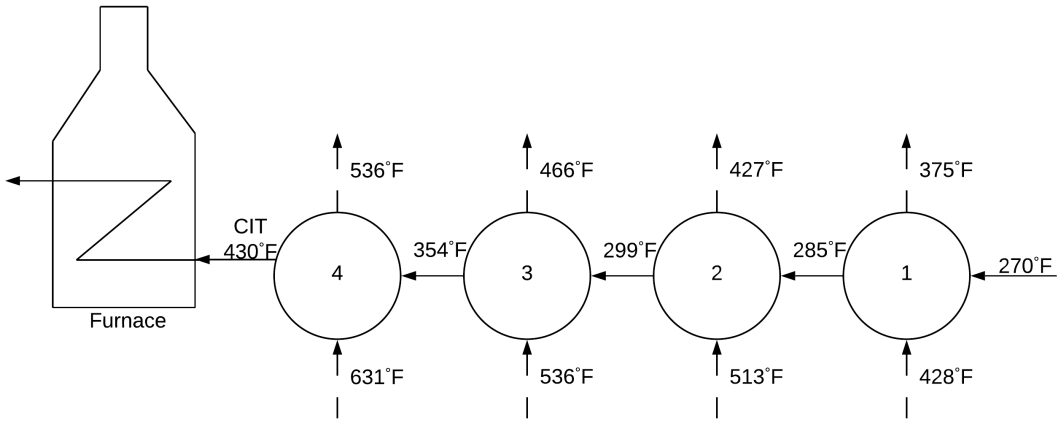

Figure 3.3.3: Four heat exchanger case. Temperature values are given for initial, clean condition. Adapted from [77].

Table 3.3.2: Data for four heat exchanger case. Adapted from [77].

Parameter	Heat Exchanger			
	1	2	3	4
F_h [lb/h]	141000	73800	423000	429000
C_h [Btu/lb°F]	0.67	0.70	0.62	0.62
A [ft^2]	465	287	1192	1488
a (linear fouling, $\times 10^7$) [ft^2°F/Btu]	3.07	3.27	3.68	3.88
F_c [lb/h]	721000			
C_c [Btu/lb°F]	0.46			
U_c [Btu/hft^2°F]	88.1			
U_0 [Btu/hft^2°F]	88.1			
Δt^{CL} [month]	0.20			
Δt^{OP} [month]	0.80			

Data for this case study is presented in Table 3.3.3. In addition to the logical constraints, selection and operational constraints are also imposed through consideration of performance targets or acceptable operating practice, as presented in Table 3.3.4. These constraints are based only on exchanger cleaning actions. However, in practice, temperature bounds on the performance of exchangers are required to be applied, for example in the case of desalter temperature control considered by [60]. For the purpose of achieving results that can be compared to published ones from case studies in the open literature, only the constraints shown in Table 3.3.4 are imposed on this case study.

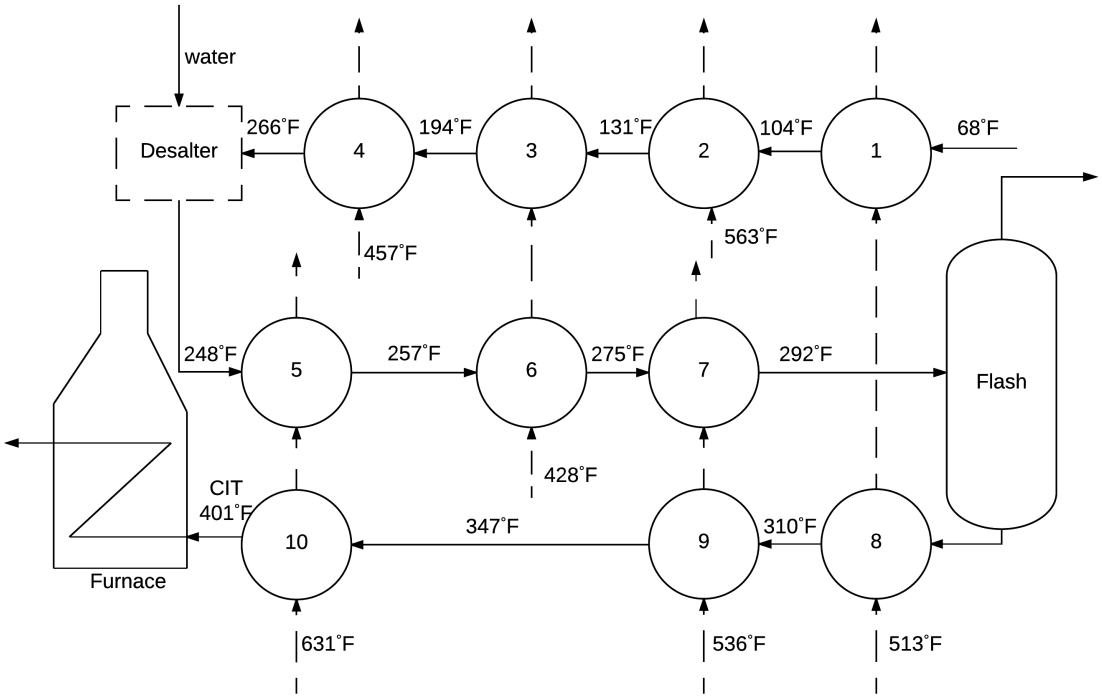

Figure 3.3.4: 10 unit HEN case. Temperature values are given for initial, clean condition. Adapted from [77].

3.3.4 Case study D

A 25 unit HEN for a crude oil refinery preheat train from [129] is modelled as shown in Figure 3.3.5. The second cold stream located between the desalter and flash is evenly split into two branches while the third cold stream is evenly split into four branches. Longer durations of operation, where the number of periods are $NP = \{24, 36\}$, are considered in this network and the cleaning cost incurred for cleaning operations, C_{cl}, is £5000 per cleaning action. For this case, the duration of the cleaning and operating sub-periods are equal with $\triangle t^{\mathrm{cl}} = \triangle t^{\mathrm{op}} = 15$ days. If the cleaning time did depend on the size of the exchanger, these durations would have to be unit dependent. Data for this case study is presented in Table 3.3.5. The furnace fuel cost C_E is £0.34/kW day. Similarly to the previous case study, in addition to the logical constraints, selection and operational constraints are also imposed as shown in Table 3.3.6. Again, these constraints are based only on cleaning actions, $y_{n,p}$. Only these constraints are imposed

Table 3.3.3: Data for 10 unit HEN case. Adapted from [77].

Parameter	Heat Exchanger									
	1	2	3	4	5	6	7	8	9	10
F_{h} [lb/h]	141000	738000	423000	429000	208000	423000	210000	141000	283000	208000
F_{c} [lb/h]	721000	721000	721000	721000	721000	721000	721000	649000	649000	649000
C_{h} [Btu/lb°F]	0.67	0.70	0.62	0.62	0.67	0.62	0.69	0.67	0.69	0.67
C_{c} [Btu/lb°F]	0.46	0.46	0.46	0.46	0.55	0.55	0.55	0.57	0.57	0.57
A [ft^2]	465	287	1192	1488	183	546	492	437	885	1257
a (linear fouling, $\times 10^7$) [ft^2°F/Btu]	1.23	1.84	1.23	1.64	3.07	2.25	3.07	3.27	3.68	3.88
R_f^{∞}(asymptotic fouling, $\times 10^3$) [hft^2°F/Btu]	1.61	2.41	1.61	2.14	4.02	2.95	4.02	4.29	4.82	5.09
τ (decay constant) [month]	4									
U_{c} [Btu/hft^2°F]	88.1									
U_0 [Btu/hft^2°F]	88.1									
Δt^{CL} [month]	0.20									
Δt^{OP} [month]	0.80									
η_f	0.75									

Table 3.3.4: Operational constraints for 10 unit HEN case.

only one unit of exchangers 1-4 can be cleaned in each period	$y_{1,p}+y_{2,p}+y_{3,p}+y_{4,p} \geq 3 \; \forall p$
only one unit of exchangers 5-7 can be cleaned in each period	$y_{5,p}+y_{6,p}+y_{7,p} \geq 2 \; \forall p$
temperature drop across desalter	$T^{in,X}_{c,5,p} = T^{out,X}_{c,4,p} - 18 \; \forall p$

in order to achieve results that can be compared to published ones from case studies in the open literature.

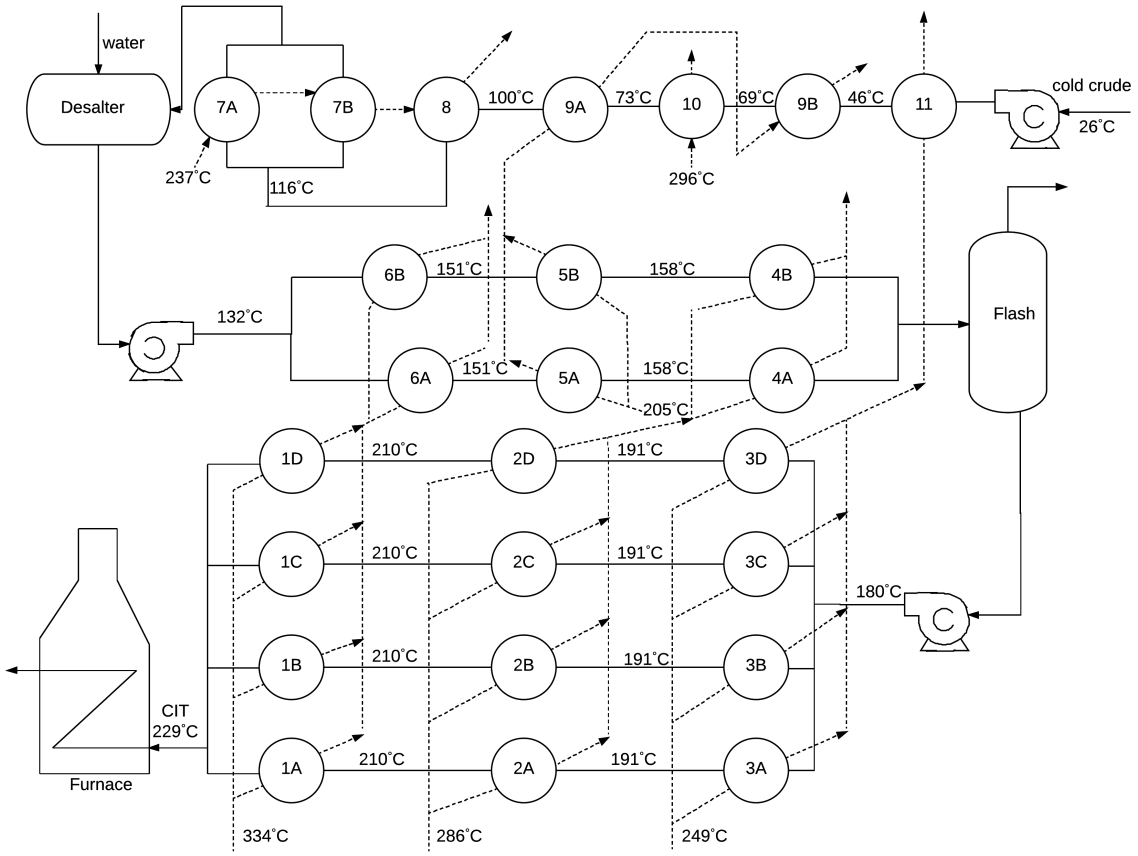

Figure 3.3.5: 25 unit HEN case. Solid lines, cold (crude) streams; dashed lines, hot streams; CIT, crude inlet temperature to furnace. Temperature values are given for initial, clean condition. Adapted from [129].

Table 3.3.5: Data for 25 unit HEN case. Adapted from [129].

HEX	F_h (kg s^{-1})	F_c (kg s^{-1})	C_h (kJ $kg^{-1}K^{-1}$)	C_c (kJ kg^{-1} K^{-1})	U_c (kW $m^{-2}K^{-1}$)	A (m^2)	$a \times 10^{11}$ (m^2KJ^{-1})
1A	8.7	23	2.8	2.4	0.5	21.3	1.9
2A	11.4	23	2.9	2.4	0.5	29.7	1.8
3A	4.8	23	2.8	2.4	0.5	31.4	1.6
1B	8.7	23	2.8	2.4	0.5	21.3	1.9
2B	11.4	23	2.9	2.4	0.5	29.7	1.8
3B	4.8	23	2.8	2.4	0.5	31.4	1.6
3C	8.7	23	2.8	2.4	0.5	21.3	1.9
2C	11.4	23	2.9	2.4	0.5	29.7	1.8
3C	4.8	23	2.8	2.4	0.5	31.4	1.6
1D	8.7	23	2.8	2.4	0.5	21.3	1.9
2D	11.4	23	2.9	2.4	0.5	29.7	1.8
3D	4.8	23	2.8	2.4	0.5	31.4	1.6
4A	23	47.4	2.8	2.3	0.5	26.7	1.5
5A	28	47.4	2.6	2.3	0.5	35.4	1.1
6A	17.4	47.4	2.9	2.3	0.5	79.1	1.5
4B	23	47.4	2.8	2.3	0.5	29.2	1.6
5B	28	47.4	2.6	2.3	0.5	35.4	1.1
6B	17.4	47.4	2.9	2.3	0.5	79.1	1.5
7A	25	47.4	2.6	1.92	0.5	60.8	0.8
7B	25	47.4	2.6	1.92	0.5	80.3	0.8
8	49.6	95	2.6	1.92	0.5	129	0.8
9A	55.8	95	2.6	1.92	0.5	110	0.9
9B	55.8	95	2.6	1.92	0.5	96.6	0.9
10	3.3	95	2.9	1.92	0.5	8.5	0.6
11	19.1	95	2.8	1.92	0.5	56.6	0.6

Table 3.3.6: Operational constraints for 25 unit HEN case.

vacuum residue rundown temperature target	$y_{1A,p} + y_{1B,p} + y_{1C,p} + y_{1D,p} + y_{6A,p} + y_{6B,p} \geq 5$
atmospheric middle pump-around target	$y_{2A,p} + y_{2B,p} + y_{2C,p} + y_{2D,p} + y_{4A,p} + y_{4B,p} \geq 5$
side-stream rundown temperature target	$y_{3A,p} + y_{3B,p} + y_{3C,p} + y_{3D,p} + y_{11,p} \geq 4$
atmospheric top pump-around target	$y_{5A,p} + y_{5B,p} + y_{9A,p} + y_{9B,p} \geq 3$
vacuum pump-around target	$y_{7A,p} + y_{7B,p} + y_{8,p} \geq 2$
one hot end exchanger is allowed to be cleaned at a time	$y_{1A,p} + y_{2A,p} + y_{3A,p} \geq 2$
	$y_{1B,p} + y_{2B,p} + y_{3B,p} \geq 2$
	$y_{1C,p} + y_{2C,p} + y_{3C,p} \geq 2$
	$y_{1D,p} + y_{2D,p} + y_{3D,p} \geq 2$
maintenance of the flash temperature	$y_{4A,p} + y_{5A,p} + y_{6A,p} \geq 2$
	$y_{4B,p} + y_{5B,p} + y_{6B,p} \geq 2$
maintenance of the desalter temperature	$y_{7A,p} + y_{7B,p} + y_{8,p} + y_{9A,p} + y_{9B,p} + y_{10,p} + y_{11,p} \geq 6$
temperature drop across desalter	$T^{\text{in}}_{\text{c},6p} = T^{\text{out}}_{\text{c},7p} - 10$

3.4 Computational results and discussion

In this section, computational results for the IPM and direct B&B techniques on each of the case studies are presented. For case studies A and B, solutions are obtained using the rounding scheme. The B&B method is demonstrated in case studies C and D in addition to the rounding scheme. For case studies A, B and C, the solutions obtained are compared in the schedules shown in Table 3.4.7, Tables 3.4.10 to 3.4.11 and Tables 3.4.14 to 3.4.17 with the schedules obtained by [77] using the MILP formulation. For case study D, the solutions are compared in the schedules shown in Tables 3.4.20 and 3.4.21 with the schedules obtained by [129] using the OA method and BTA algorithm. In the economic comparison, we fixed the solutions obtained by [77] and [129], and evaluated them using our model. This is done because the discretised ODE nonlinear model is used here, and hence, the constraints of this model are satisfied. These are shown in Tables 3.4.8, 3.4.12, 3.4.18 and 3.4.22, where the best obtained solution is reported for each of the cases. Solution metrics which include the worst cost out of 50 runs of different starting points, mean cost and relative standard deviation (RSD) about the mean value for each case is reported in Tables 3.4.9, 3.4.13, 3.4.19 and 3.4.23. Additionally, the total computational time for the multiple runs is also reported in these tables.

3.4.1 Case study A

Fouling rates have a great impact on the performance of the heat exchanger models. The asymptotic fouling case has larger initial fouling rates causing a rapid decay in the crude inlet temperatures, resulting in a much larger objective value for the uncleaned case (*e.g.* £313k *vs.* £203k in Table 3.4.8). Generally, more cleaning actions are performed in the asymptotic fouling scenarios than in the corresponding linear ones, as shown in Table 3.4.7, with the cleaning actions increasing from 3 to 5 in the £4k cleaning cost scenario of this work's solution. This is primarily attributed towards the early loss of exchanger efficiencies.

For the reported schedules with a cleaning cost of £4k, there is an absence of cleaning actions near the start and end of the operating horizon, as there is little incentive to clean a relatively clean unit, and there is little time for the cost of cleaning to be recovered towards the end of the operating horizon. For example, in the linear fouling

case with a cleaning cost of £4k, the first cleaning action does not occur until 7 months after the start of the operating horizon and there are no cleaning actions in the last 5 months of the operating horizon, as shown in Table 3.4.7.

Similar observations as those in [77] are seen where cleaning actions are cyclic (see Table 3.4.7). For example, in the asymptotic fouling case with a cleaning cost of £4k, after the first cleaning action, subsequent cleanings take place every 4 months. In addition, in this case the schedules are the same, both resulting in a cost value of £222k, as can be seen in Table 3.4.8. This is also applicable to the corresponding linear case. However, for the asymptotic case with a cleaning cost of £0, one less cleaning is performed in our model than in [77]'s (6 *vs.* 7 cleanings) and the schedules are different, with their cleaning actions taking place earlier. In the corresponding linear case, the number of cleaning actions between our model and that of [77] are the same with 4 cleanings take place of which only one is not common, as shown in Table 3.4.7.

The case with £0 cleaning cost is termed the energy maximisation scenario with more cleaning actions taking place, such as in Table 3.4.7, where the total number of cleaning actions increase from 3 to 4 and from 5 to 6 in the linear and asymptotic fouling cases, respectively. This difference is more significant in larger networks, as will be shown in Subsection 3.4.3.

An important observation worth discussing is the bang-bang nature of this problem. Only a small number of fractional $y_{n,p}$ values result from the relaxed MINLP solution, which leads to the objective values using the rounding scheme being very close to the corresponding relaxed MINLP value and in several cases they are completely integer. For example, in the asymptotic fouling case with a cleaning cost of £0, the relaxed MINLP solution is £196k whereas the rounded MINLP solution is only £2k more, as shown in Table 3.4.8. Furthermore, for the corresponding case with a cleaning cost of £4k, these values are almost equivalent (£222k). For the case where $y_{n,p}$ for the relaxed MINLP solution is completely integer, *e.g.* in the linear fouling cases, this is termed a bang-bang solution and is indicated by $*$ in Table 3.4.8.

The schedules featuring the best objective, *i.e.* lowest overall cost, are shown for these cases. However, a number of different schedules with similar objective values are also obtained. For all cases, the range of objective values obtained in the 50 runs is narrow, as shown in Table 3.4.9, where the objective function value varies between £102k up to only £109k for the linear case with a £4k cleaning cost, and between

£222k and £225k for the asymptotic cases with a cleaning cost of £4k. Furthermore, the results are narrowly dispersed about the mean, with a RSD value of 1.2% and 0.4% in the aforementioned corresponding scenarios, respectively. The resource usage varies depending on the cleaning cost, fouling type, method used and problem size. For all of these scenarios, a quick convergence is achieved, where the total CPU time for the 50 runs is a maximum of 9 CPU s, as shown in Table 3.4.9.

3.4.2 Case study B

For the four heat exchanger case over an operating horizon of 12 months, the same schedules are obtained in this work and in the work of [77] (Table 3.4.10), where the cost values are both £106k, as shown in Table 3.4.12. In the longer operating duration of 18 months, the total number of cleaning actions are the same in comparison to the optimum schedule of [77] (6 cleanings in Table 3.4.11). All solutions in the four heat exchanger case are feasible, *i.e.* integer, as shown in Table 3.4.12. Hence, rounding is not needed in these cases.

For the 18 month operating horizon case, a better solution is obtained in our work compared to the work of [77] (£179k *vs.* £183k in Table 3.4.12). When comparing the corresponding schedules in Table 3.4.11, each unit is cleaned the same number of times; however, there is only one common cleaning action and the cleaning actions of [77] are earlier than ours.

In terms of the distribution of the solutions about the mean, the RSD is only 1.6% and 1.2% for the 12 month and 18 month horizons, respectively, and the difference between the maximum and minimum cost values is £5k and £10k (Table 3.4.13) for the corresponding cases, respectively. Therefore, it can be deduced for these cases that only a few runs are sufficient to achieve a good solution. Similarly to case study A, the computational time is very small at a maximum of 23 CPU s for the 18 month case, as shown in Table 3.4.13.

3.4.3 Case study C

For the energy maximisation scenario of the 10 unit HEN case, cleaning actions taking place often, such as in the linear case where the cleaning actions increase from 10 to

Table 3.4.7: Cleaning schedule for the single heat exchanger case using MINLP approach (linear and asymptotic fouling).

Case	Time (months)																								No. of cleaning actions	
	1	2	3	4	5	6	7	8	9	10	11	12	13	14	15	16	17	18	19	20	21	22	23	24	+	◯
Linear fouling, cleaning cost=£0					◯	+				⊕					⊕					⊕					4	4
Linear fouling, cleaning cost=£4k							⊕						⊕						⊕						3	3
Asymptotic fouling, cleaning cost=£0				⊕			◯	+		◯		+	◯		+	◯			⊕			⊕			6	7
Asymptotic fouling, cleaning cost=£4k					⊕				⊕				⊕				⊕				⊕				5	5
cleaning actions: + MINLP rounding scheme; ◯ [77] MILP approach; ⊕ common																										

Table 3.4.8: Economic chart for the single heat exchanger case using MINLP approach.

Case	MINLP model in k£		[77] model in k£
	MINLP rounding scheme solution (relaxed MINLP)	[77] MILP approach solution**	[77] solution
No cleaning, linear fouling	203	203	203
No cleaning, asymptotic fouling	313	313	316
Cleaning cost=£0, linear fouling	90 (90*)	90	90
Cleaning cost=£4k, linear fouling	102 (102*)	102	102
Cleaning cost=£0, asymptotic fouling	198 (196)	195	196
Cleaning cost=£4k, asymptotic fouling	222 (222)	222	225

* relaxed MINLP completely integer, *i.e.* feasible solution. ** [77] MILP approach solution inputted into MINLP model.

Table 3.4.9: Solution metrics for the single heat exchanger case using MINLP approach.

Case	Relaxed MINLP rounding scheme solution				CPU time in s
	Min in k£	Max in k£	Mean in k£	RSD in %	
Cleaning cost=£0, linear fouling	90	96	92	1.2	9
Cleaning cost=£4k, linear fouling	102	109	105	1.2	9
Cleaning cost=£0, asymptotic fouling	196	199	198	0.3	11
Cleaning cost=£4k, asymptotic fouling	222	225	223	0.4	11

Table 3.4.10: Cleaning schedule for the four heat exchanger case using MINLP approach (duration of 12 months, linear fouling, cleaning cost £4k).

HEX	Time (months)												No. of cleaning actions	
	1	2	3	4	5	6	7	8	9	10	11	12	+	◯
1													0	0
2													0	0
3						⊕							1	1
4							⊕						1	1
cleaning actions: + MINLP rounding scheme; ◯ [77] MILP approach; ⊕ common													2	2

18 for the rounding scheme in Tables 3.4.14 and 3.4.15 when the cleaning cost is reduced from £4000 to £0, and increase more than three times from 10 to 31 in the corresponding asymptotic case in Tables 3.4.16 and 3.4.17. A further increase in the cleaning cost would limit the number of cleaning actions even more and increase the objective further. This can be used to determine which cleaning actions and hence exchangers are more important. From Tables 3.4.15 and 3.4.17, it can be seen that exchangers 9 and 10 are cleaned the most frequently, making these exchangers more important in the network, while exchangers 1 and 2 are not cleaned at all. Exchangers 9 and 10 are cleaned more often as they have the highest fouling rates, as shown in Table 3.3.3. Fouling rate is not the only criterion that determines how often cleaning is done. For instance, as shown in Table 3.4.17, despite the similar asymptotic fouling rates of exchangers 5 and 7, the former is not cleaned at all while the latter is cleaned twice during the operating horizon.

Figure 3.4.6 shows the CIT profiles with and without cleaning over time for the linear and asymptotic cases, respectively. For the cleaning scenario, the profile shown is based on the best objective value using the rounding scheme, *i.e.* the schedules in Tables 3.4.15 and 3.4.17. The CIT profiles show that fouling has a significant effect on the performance of the HEN. The larger fouling rates for the asymptotic fouling model result in a steep decline in the CIT, *e.g.* there is a rapid decay in the CIT at the 5^{th}, 9^{th} and 13^{th} months and this is attributed towards unit 10 being cleaned (see Figure 3.4.6b and Table 3.4.17), which has the highest fouling rate.

A cost comparison between our model and [77]'s model only makes sense in the linear fouling case, where the objective value for the no-cleaning scenario is the same. For the asymptotic case, [77] estimates a lower objective value associated with the no-cleaning

Table 3.4.11: Cleaning schedule for the four heat exchanger case using MINLP approach (duration of 18 months, linear fouling, cleaning cost £4k).

HEX	Time (months)																		No. of cleaning actions	
	1	2	3	4	5	6	7	8	9	10	11	12	13	14	15	16	17	18	+	◯
1											◯	+							1	1
2											⊕								1	1
3					◯			+		◯				+					2	2
4						◯	+					◯	+						2	2
cleaning actions: + MINLP rounding scheme; ◯ [77] MILP approach; ⊕ common																			6	6

Table 3.4.12: Economic chart for the four heat exchanger case using MINLP approach.

Case	MINLP model in k£		[77] model in k£
	MINLP rounding scheme solution (relaxed MINLP)	[77] MILP approach solution**	[77] solution
Cleaning cost=£4k, linear fouling, 12 months	106 (106*)	106	106
Cleaning cost=£4k, linear fouling, 18 months	179 (179*)	183	183

* relaxed MINLP completely integer, *i.e.* feasible solution. ** [77] MILP approach solution inputted into MINLP model.

Table 3.4.13: Solution metrics for the four heat exchanger case using MINLP approach.

Case	Relaxed MINLP rounding scheme solution				CPU
	Min in k£	Max in k£	Mean in k£	RSD in %	time in s
Cleaning cost=£4k, linear fouling, 12 months	106	111	108	1.6	16
Cleaning cost=£4k, linear fouling, 18 months	179	189	183	1.2	23

scenario resulting in $< 2\%$ difference (see Table 3.4.18). This is attributed to retaining the nonlinear expressions in our model which is more accurate, whereas, as mentioned in previous sections of this chapter, [77] use standard transformations to obtain linear expressions, thus eliminating the nonlinear expressions by addition of extra variables.

From our results, we observe that in all cases our model produces similar overall costs using both the rounding scheme and B&B method to [77]'s model. The rounding scheme produces a slightly better solution than the B&B method. It is worth noting that [77]'s MILP model is solved to global optimality, whereas our model being a non-convex MINLP model is not. Despite this, we still produce similar results (a difference of £4k in the worst case, as shown in Table 3.4.18). The difference between the maximum and minimum of objective values for all cases is very narrow, this being £16k and £10k in the worst case for the asymptotic fouling case with a cleaning cost of £4k using the rounding scheme and B&B method, respectively (see Table 3.4.19). Therefore, similarly to the previous cases, many runs are not required and a similar objective to that of [77] is obtained within the first run. In these cases, special tuning is not required and the model runs automatically with ease, with only up to 2 infeasible solutions produced out of the 50 runs using the B&B technique, while all solutions produced for the rounding scheme are feasible.

The number of cleaning actions from the three solution methods in the 10 unit HEN case are generally similar. The rounding scheme results in the minimum number of cleaning actions in the energy maximisation scenarios, *e.g.* 18 for the rounding scheme in the linear scenario *vs.* 20 and 21 for B&B method and [77]'s reformulation, respectively. Despite the similarity in the objective values and number of cleaning actions performed, no pattern is observed from the schedules, where cleaning actions occur earlier in some cases and later in others. This further emphasises our earlier findings where there are a number of schedules with similar objective values but different distributions.

Similar to observations from the previous case studies, this problem also exhibits bang-bang behaviour. For the linear fouling cases, the objective values using the rounding scheme are the same value as the corresponding relaxed MINLP values and in some cases are completely integer, as shown in Table 3.4.18. Where fractional $y_{n,p}$ values exist, these solutions are termed bang-singular. The number of singular arcs are minimal with the maximum number of singular arcs produced being 9 out of 180 binary variables in the asymptotic fouling model with £0 cleaning cost. It is worth noting

that in both of the asymptotic fouling cases, the rounded MINLP solution results in a lower objective value in comparison to the relaxed MINLP, as shown in Table 3.4.18 (£362k *vs.* £399k and £460k *vs.* £478k for $C_{cl} = £0$ and $C_{cl} = £4$k, respectively).

Convergence is achieved very quickly in each run and the resource usage is very practical even for the worst case: for the linear fouling case and £4k cleaning cost, only 115 CPU s (1.9 CPU min) is required for 50 runs of the relaxed MINLP. [77] stated that the time to solve the 10 unit HEN case is impractical, therefore, in addition to reformulating their model into a MILP problem, they use a decomposition procedure to decrease the computational time. They also state that they kept the linearity of the expressions with the aim of having better chances of capturing the global optimum. From our findings, these are both clearly not required.

In the next subsection, we will present a 25 unit HEN previously solved by [129] using the BTA and OA methods.

3.4.4 Case study D

Similarly to the asymptotic fouling case in case study C, there is a difference in the uncleaned objective values for both the 24 and 36 month models, as shown in Table 3.4.22. This difference arises from the different numerical methods used to solve the equation sets and represents $< 7\%$ difference and $< 8.5\%$ difference when compared to the BTA algorithm over $NP = 24$ months and $NP = 36$ months, respectively.

The schedules obtained have a limited number of common cleaning actions with that of [129]. For the 2 year operating horizon, the cleaning actions for [129]'s OA method generally take place earlier in the operating horizon as well as closer to the end of the horizon than in our rounding scheme, as shown in Table 3.4.20. In this case, more cleaning actions are performed in their schedule than in ours*, e.g.* 17 in their OA method schedule and 15 in their BTA algorithm schedule compared to 14 in our schedule, as shown in Table 3.4.20. Contrariwise, for the 3 year operating horizon there are more cleaning actions in our schedule than in theirs (36 *vs.* 34, as shown in Table 3.4.21). Some features in common are that most exchangers are cleaned the same number of times as our schedule, and certain exchangers are not cleaned at all (*e.g.* exchangers 3A to 3D in the 2 year schedule, as can be seen in Table 3.4.20).

Table 3.4.14: Cleaning schedule for the 10 unit HEN case using MINLP approach (linear fouling, cleaning cost £0).

HEX	Time (months)																		No. of cleaning actions		
	1	2	3	4	5	6	7	8	9	10	11	12	13	14	15	16	17	18	+	○	×
1								○	+	×									1	1	1
2						○		✳				○		✳					2	2	2
3											⊕	×							1	1	1
4										⊕	×								1	1	1
5					⊗	+			×	○		+		⊗					2	3	3
6							✳	○				○	✳						2	2	2
7						⊗		+		×	○			+	⊗				2	3	3
8					+	⊗				○	+	×			⊕				3	3	2
9					⊗	+			⊗			+		⊗					2	3	3
10							⊛						⊛						2	2	2
cleaning actions: + MINLP rounding scheme; × MINLP B&B technique; ○ [77] MILP approach; ⊛common; ⊗ B&B and [77] common; ⊕ rounding and [77] common; ✳ rounding and B&B common																			18	21	20

Table 3.4.15: Cleaning schedule for the 10 unit HEN case using MINLP approach (linear fouling, cleaning cost £4k).

HEX	Time (months)																		No. of cleaning actions		
	1	2	3	4	5	6	7	8	9	10	11	12	13	14	15	16	17	18	+	◯	×
1																			0	0	0
2																			0	0	0
3									◯	✳									1	1	1
4								+			◯	×							1	1	1
5									◯	✳									1	1	1
6								◯	+		×								1	1	1
7									×	◯	+								1	1	1
8									×	⊕									1	1	1
9						×	⊕						⊗						2	2	2
10						⊕	×					⊕		×					2	2	2
cleaning actions: + MINLP rounding scheme; × MINLP B&B technique; ◯ [77] MILP approach; ⊗common; ⊗ B&B and [77] common; ⊕ rounding and [77] common; ✳ rounding and B&B common																			10	10	10

Table 3.4.16: Cleaning schedule for the 10 unit HEN case using MINLP approach (asymptotic fouling, cleaning cost £0).

HEX	Time (months)																		No. of cleaning actions		
	1	2	3	4	5	6	7	8	9	10	11	12	13	14	15	16	17	18	+	◯	×
1						+	×		◯										1	1	1
2				+	×		◯			✳			◯	✳					3	2	3
3									×		⊕								1	1	1
4						×	+	◯				✳		◯					2	2	2
5			⊛			+	×		◯	✳		◯	×	+		⊗			4	4	5
6				✳		◯		×	+	◯	×		+		⊗				3	3	4
7					⊛			⊕	×		⊕			⊗	+		⊗		4	5	4
8				+	⊗			⊕	×		⊕			⊗	+		◯		4	5	3
9			⊛			⊕	×		◯	✳		◯	×	+	◯	×	+		5	5	5
10				⊗	+		◯	×	+	◯	×		⊕		×	⊕			4	5	4
cleaning actions: + MINLP rounding scheme; × MINLP B&B technique; ◯ [77] MILP approach; ⊛ common; ⊗ B&B and [77] common; ⊕ rounding and [77] common; ✳ rounding and B&B common																			31	33	32

Table 3.4.17: Cleaning schedule for the 10 unit HEN case using MINLP approach (asymptotic fouling, cleaning cost £4k).

HEX	Time (months)																		No. of cleaning actions		
	1	2	3	4	5	6	7	8	9	10	11	12	13	14	15	16	17	18	+	◯	×
1																			0	0	0
2																			0	0	0
3																			0	0	0
4											+	◯							1	1	0
5																			0	0	0
6																			0	0	0
7						◯	✳					◯		+					2	2	1
8							◯			+	×		◯						1	2	1
9				⊛				+	⊗			+		⊗					3	3	3
10					⊛				+	⊗			+		⊗				3	3	3
cleaning actions: + MINLP rounding scheme; × MINLP B&B technique; ◯ [77] MILP approach; ⊛common; ⊗ B&B and [77] common;⊕ rounding and [77] common; ✳ rounding and B&B common																			10	11	8

Table 3.4.18: Economic chart for the 10 unit HEN case using MINLP approach.

Case	MINLP model in k£			[77] model in k£
	MINLP rounding scheme solution (relaxed MINLP)	MINLP B&B technique solution (relaxed MINLP)	[77] MILP approach solution**	[77] solution
No cleaning, linear fouling	361	361	361	361
No cleaning, asymptotic fouling	547	547	547	554
Cleaning cost=£0, linear fouling	204 (204)	204	204	204
Cleaning cost=£4k, linear fouling	258 (258*)	259	258	258
Cleaning cost=£0, asymptotic fouling	362 (399)	399	358	406
Cleaning cost=£4k, asymptotic fouling	460 (478)	477	458	482

* relaxed MINLP completely integer, *i.e.* feasible solution. ** [77] MILP approach solution inputted into MINLP model.

Table 3.4.19: Solution metrics for the 10 unit HEN case using MINLP approach.

Case	relaxed MINLP rounding scheme solution				
	Min in k£	Max in k£	Mean in k£	RSD in %	CPU time in s
Cleaning cost=£0, linear fouling	204	212	207	0.8	111
Cleaning cost=£4k, linear fouling	258	267	263	0.8	115
Cleaning cost=£0, asymptotic fouling	399	408	403	0.4	71
Cleaning cost=£4k, asymptotic fouling	478	494	485	0.7	66
	MINLP B&B technique solution				
Cleaning cost=£0, linear fouling	204	208	206	0.5	111
Cleaning cost=£4k, linear fouling	259	265	261	0.6	112
Cleaning cost=£0, asymptotic fouling	399	404	402	0.4	70
Cleaning cost=£4k, asymptotic fouling	477	487	481	0.4	79

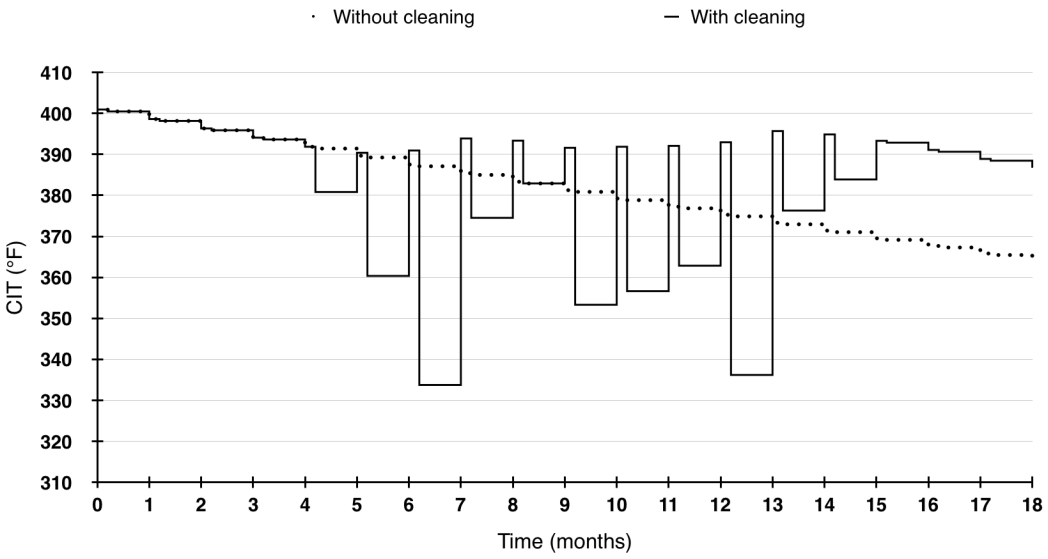

(a)

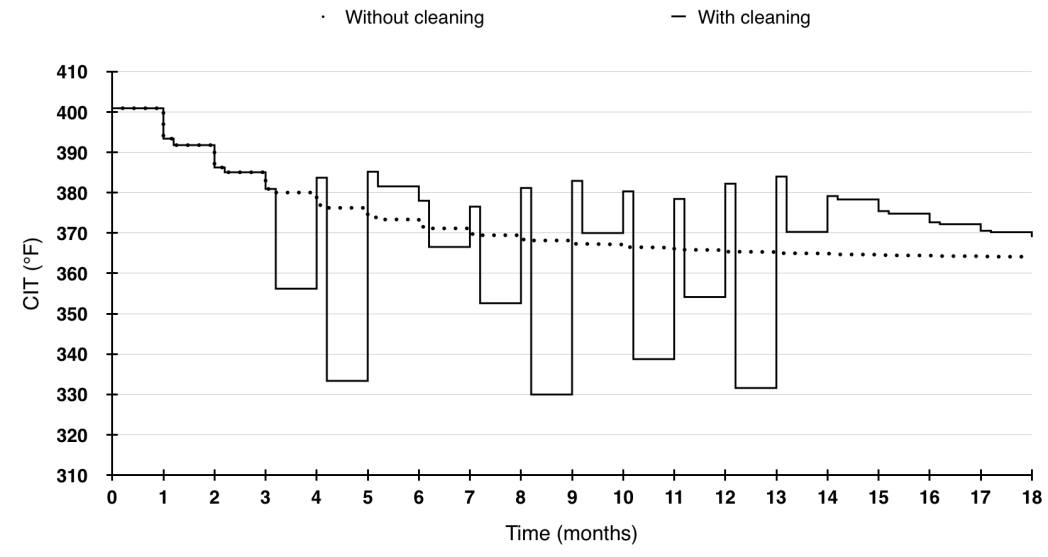

(b)

Figure 3.4.6: CIT profile for the 10 unit HEN case using MINLP rounding approach: (a) linear fouling, cleaning cost=£4k and (b) asymptotic fouling, cleaning cost=£4k

In terms of the economic comparison, the OA method produces the worst objective value, whilst our method produces the best objective value (£535k *vs.* £552k for the 24 month model), as shown in Table 3.4.22. Furthermore, in the same case, the overall cost in our work is slightly better in comparison to [129]'s BTA solution which is £539k. This difference is more notable in the 36 month model, with a cost of £915k in our work compared to £931k in [129]'s BTA solution.

The time required for convergence is minimal in each run and the resource usage is very practical: for the 36 month model, only 252 CPU s (4.2 CPU min overall, ≈ 5 CPU s per run), on a 2014 model MacBook Air, is required for 50 runs, as shown in Table 3.4.23, while the resource usage quoted by [129] for their BTA algorithm is 6,624 CPU for 10 trials (≈ 1.8 CPU hr overall, ≈ 662 CPU s per trial) on a SunSPARC 10 workstation in 2002. As per Moore's law, which is the observation that the number of transistors in a dense integrated circuit doubles every 2 years [91], the convergence time for their method translates to ≈ 10 CPU s per trial in 2014. Hence, the resource usage for their BTA algorithm is 2 times more expensive than the MINLP approach. In addition, they are unable to solve the HEN over 36 months using their proposed OA method.

The objective values vary in a slightly wider range than in the previous case studies, *e.g.* for 3 years of operation the objective varies from £915k to £957k, as shown in Table 3.4.22. In addition, the objective values obtained using the rounding scheme are almost equivalent to the corresponding relaxed MINLP values, at £535k for the 2 year horizon (see Table 3.4.22). Hence, this model also results in a nearly bang-bang solution giving a minimal number of singular arcs. The 24 month operating horizon solution only produces 1 value of $y_{n,p}$ out of 600 which is fractional, whereas the 36 month operating horizon solution produces 16 out of 900 fractional values of $y_{n,p}$.

A 14 unit HEN case study appearing in the work of [128] was also modelled over an operating duration of 3 years. The cost was varied and both linear and asymptotic fouling were considered. Based on the results, similar findings were made to those in the cited work.

Table 3.4.20: Cleaning schedule for the 25 unit HEN case using MINLP approach (linear and fouling, cleaning cost £5k).

HEX	Time (months)																								No. of cleaning actions		
	1	2	3	4	5	6	7	8	9	10	11	12	13	14	15	16	17	18	19	20	21	22	23	24	+	◯	×
1A									×	+					◯										1	1	1
1B										×		◯	+												1	1	1
1C											+	×		◯											1	1	1
1D										◯					✳										1	1	1
2A											+	◯				×									1	1	1
2B													◯	×	+										1	1	1
2C						×				◯			+		×										1	1	2
2D										+	×				◯										1	1	1
3A																									0	0	0
3B																									0	0	0
3C																									0	0	0
3D																									0	0	0
4A								×			◯			+											1	1	1
4B							×					+		◯			×								1	1	2
5A																									0	0	0
5B																									0	0	0
6A												+	◯				×								1	1	1
6B											◯		×	+											1	1	1
7A														◯											0	1	0
7B																									0	0	0
8													×												0	0	1
9A													⊕					×							1	1	1
9B											+	◯	×												1	1	1
10																									0	0	0
11																									0	0	0
cleaning actions: + MINLP rounding scheme; × [129] OA method; ◯ [129] BTA algorithm; ⊗ common; ⊗ B&B and [129] OA common; ⊕ rounding and [129] BTA common; ✳ rounding and [129] OA common																									14	15	17

Table 3.4.21: Cleaning schedule for the 25 unit HEN case using MINLP approach (linear and fouling, cleaning cost £5k).

HEX	Time (months)																																				
	1	2	3	4	5	6	7	8	9	10	11	12	13	14	15	16	17	18	19	20	21	22	23	24	25	26	27	28	29	30	31	32	33	34	35	36
1A												◯					+								+	◯											
1B													+	◯													⊕										
1C												+	◯												◯	+										
1D											◯					+								◯				+									
2A										+					◯								+				◯									
2B														+		◯										⊕										
2C														◯		+								◯			+									
2D												+	◯												⊕											
3A																		+																		
3B															+																					
3C																	+	◯																		
3D																	◯		+																	
4A												◯			+													⊕								
4B									+	◯													◯	+												
5A																	+	◯																		
5B																	◯	+																		
6A										◯				+									◯	+												
6B															+			◯					+													
7A															+		◯																			
7B																		+				◯														
8																			⊕																	
9A																				⊕																
9B												◯	+												◯		+									
10																																				
11																					◯	+														
cleaning actions: + MINLP rounding scheme; ◯ [129] BTA algorithm; ⊕common;																																				

Table 3.4.22: Economic chart for the 25 unit HEN case using MINLP approach.

Case	MINLP model in k£			[129] model in k£	
	MINLP rounding scheme solution (relaxed MINLP)	[129] OA method solution*	[129] BTA algorithm solution**	[129] OA method solution	[129] BTA algorithm solution
No cleaning, linear fouling, 24 months	633	633	633	622	589
No cleaning, linear fouling, 36 months	1376	1376	1376	Not reported	1261
Cleaning cost=£5, linear fouling, 24 months	535 (535)	552	539	525	493
Cleaning cost=£5, linear fouling, 36 months	915 (915)	[129] unable to solve	931	[129] unable to solve	819

* [129] OA method solution inputted into MINLP model. ** [129] BTA algorithm solution inputted into MINLP model.

Table 3.4.23: Solution metrics for the 25 unit HEN case using MINLP approach.

Case	Relaxed MINLP solution				CPU
	Min in k£	Max in k£	Mean in k£	RSD in %	time in s
Cleaning cost=£5k, linear fouling, 24 months	535	540	537	0.2	210
Cleaning cost=£5k, linear fouling, 36 months	915	957	926	0.7	252

3.5 Chapter summary

In this chapter, 2 different methods as an alternative to solving the HEN scheduling cleaning problem are presented. It is shown for the first time that this problem produces nearly bang-bang optimal solutions which can be obtained by simply solving the relaxed MINLP using an IPM followed by a simple rounding scheme. In all the case studies reported, a tight MINLP is formulated thereby making it unnecessary to use a direct B&B approach. The advantages of these methods are that they are quick, robust and reliable with very few infeasible solutions produced. Despite the non-convexity of these models it is shown that only a small number of starting points are needed to attain a good solution. The solutions obtained are compared with three different methods showing that this work's method outperforms the others. Additionally, it is shown that by solving the MINLP problem, as opposed to reformulating the model to an MILP problem, similar solutions are obtained and sometimes even better than the latter approach, despite the fact that the model in this work is not solved to global optimality. This chapter's model is thus more accurate and the full model is solved with minimal resource usage, hence avoiding the need to use a decomposition procedure. The bang-bang nature of this problem is explained further in Chapter 4. In addition, in Chapter 4 another novel method for solving the HEN maintenance scheduling problem is presented, where it is solved as a MIOCP.

Chapter 4

Optimal control approach for multiperiod HEN cleaning scheduling problems

In this chapter a sequential technique for solving the HEN scheduling problem is presented, which is based on the discovery that the HEN cleaning scheduling problem is in actuality a multistage OCP, and further that cleaning actions are the controls which appear linearly in the system equations. The key feature is that these problems exhibit bang-bang behaviour, obviating the need for combinatorial optimisation methods. Similarly to the MINLP approach in Chapter 3, the usual time discretisation approach is implemented; however, the state variables are kept in their true continuous form, thus retaining the model accuracy. Results show that the feasible path approach adopted is stable and efficient in comparison to classical methods which sometimes suffer from failure in convergence.

4.1 Theoretical demonstration of bang-bang optimal control problem property

This section will demonstrate that the HEN cleaning scheduling problem is in actuality a MIOCP. In this problem the controls, *i.e.* cleaning decisions, occur linearly in the

system, thus resulting in a bang-bang solution. Hence, integrality of the solution can be obtained by solving only the relaxed MIOCP as a standard NLP problem. Furthermore, proof of the bang-bang behaviour is shown in this section based on the linearity of the model equations in the controls, *i.e.* cleaning actions.

The basic formulation for an OCP is expressed in Equations (4.1a) to (4.1d) where the performance index is minimised by selection of controls, $u(t)$, subject to differential and algebraic equations involving differential and algebraic state variables, $x(t)$ and $z(t)$, respectively. Equations (4.1b) to (4.1c) describe an index-1 differential algebraic equation (DAE) system given the initial condition, x_0, and a fixed final time, t_F. It is noted that the problem considered involves binary control variables, $u(t)$, thus constituting a MIOCP.

$$\min_{u(\cdot)} W = \phi[x(t_{\mathrm{F}})] + \int_0^{t_{\mathrm{F}}} L[x(t), z(t), u(t), t]\, dt \tag{4.1a}$$

subject to

$$\dot{x}(t) = f[x(t), z(t), u(t), t], \quad x(t_0) = x_0, \tag{4.1b}$$

$$g(x(t), z(t), u(t), t) = 0, \tag{4.1c}$$

$$u(t) \in \mathscr{U}, \quad \mathscr{U} \in \{0,1\} \qquad \forall t \in [0, t_{\mathrm{F}}] \tag{4.1d}$$

The OCP solution is obtained through discretisation of time into periods, where the control profiles are allowed to be discontinuous at a finite number of points, t_p, termed junctions. Period lengths have not been specified. [138] gives a general form of junction conditions between stages (*i.e.* periods) p and $p+1$. This is shown in Equation (4.2)

for the sake of clarity.

$$J_p(\dot{x}_{p+1}(t_p^+), x_{p+1}(t_p^+), z_{p+1}(t_p^+), u_{p+1}(t_p^+), \dot{x}_p(t_p^-), x_p(t_p^-), z_p(t_p^-), u_p(t_p^-), t_p) = 0 \quad \forall p = 1,2,\ldots,NP-1 \tag{4.2}$$

The basic formulation of a multi-period OCP over time periods, $p = 1,\ldots,NP$, where $t \in [t_{p-1}, t_p]$ with $t_{NP} = t_\mathrm{F}$, is shown in Equations (4.3a) to (4.3g).

$$\min_{u(\cdot)} W = \sum_{p=1}^{NP} \left[\phi^{(p)} x(t_p), z^{(p)}(t_p), u^{(p)}, t^{(p)}\right] + \int_{t_{p-1}}^{t_p} L^{(p)} \left[x^{(p)}(t), z^{(p)}(t), u^{(p)}, t\right] dt \tag{4.3a}$$

subject to

$$\dot{x}^{(p)}(t) = f^{(p)}(x^{(p)}(t), z^{(p)}(t), u^{(p)}, t) \tag{4.3b}$$

$$0 = g^{(p)}(x^{(p)}(t), z^{(p)}(t), u^{(p)}, t) \tag{4.3c}$$

$$t_{p-1} \leq t \leq t_p, \quad p = 1,2,\ldots,NP \tag{4.3d}$$

$$x^{(1)}(t_0) = I^{(1)}(u^{(1)}) \tag{4.3e}$$

$$x^{(p)}(t_{p-1}) = I^{(p)}(x^{(p-1)}(t_{p-1}), z^{(p-1)}(t_{p-1}), u^{(p)}) \quad \forall p = 2,3,\ldots,NP \tag{4.3f}$$

$$u(t) \in \mathscr{U}, \quad \mathscr{U} \in \{0,1\} \tag{4.3g}$$

For the HEN cleaning problem the controls, $u^{(p)}(t)$, are considered to be piecewise constant so as to reflect the on/off nature of having a unit cleaning or not. The stage switching times, t_p, are fixed in this initial derivation. The collective vector of controls over all stages is:

$$\boldsymbol{u} = (u^{(1)}, u^{(2)}, \ldots, u^{(NP)})^T \tag{4.4}$$

At the junctions, conditions are set where differential state variables are allowed to be re-initialised based on the control variable value:

$$x^p(t_{p-1}) = u^p(t) \cdot x^{p-1}(t_{p-1}) \qquad \forall p = 2, \ldots NP \tag{4.5}$$

Proof that the control in the relaxed multistage MIOCP for cleaning scheduling is linearly related to the process variables is provided as follows, with acknowledgment to [1] for the derivation corrections.

This multistage adjoint system is a linear time-varying coefficient semi-explicit index-1 DAE system. The performance index in Equation (4.3a) is modified such that the Euler-Lagrange multipliers are introduced:

$$\begin{aligned}
\bar{W} \;=\; & \sum_{p=2}^{NP} \Bigg\{ \\
& \phi^{(p)}(x^{(p)}(t_p), z^{(p)}(t_p), u^{(p)}, t^{(p)}) \\
& + \left(\nu^{(p)}\right)^T \cdot \left(I^{(p)}(x^{(p-1)}(t_{p-1}), z^{(p-1)}(t_{p-1}), u^{(p)}) - x^{(p)}(t_{p-1})\right) \\
& + \int_{t_{p-1}}^{t_p} L^{(p)}(x^{(p)}(t), z^{(p)}(t_p), u^{(p)}, t)\, dt \\
& + \int_{t_{p-1}}^{t_p} \left(\lambda^{(p)}(t)\right)^T \cdot \left(f^{(p)}(x^{(p)}(t), z^{(p)}(t_p), u^{(p)}, t) - \dot{x}^{(p)}(t)\right) dt
\end{aligned}$$

Note, the equation continues on the next page.

$$
\begin{aligned}
&+\int_{t_{p-1}}^{t_p}\left(\mu^{(p)}(t)\right)^T\cdot\left(g^{(p)}(x^{(p)}(t),z^{(p)}(t),u^{(p)},t)\right)dt\\
&\Bigg\}\\
&+\phi^{(1)}(x^{(1)}(t_1),z^{(1)}(t_1),u^{(1)},t^{(1)})\\
&+\left(\nu^{(1)}\right)^T\cdot\left(I^{(1)}(u^{(1)})-x^{(1)}(t_0)\right)\\
&+\int_{t_0}^{t_1}L^{(1)}(x^{(1)}(t),z^{(1)}(t),u^{(1)},t)\,dt\\
&+\int_{t_0}^{t_1}\left(\lambda^{(1)}(t)\right)^T\cdot\left(f^{(1)}(x^{(1)}(t),z^{(1)}(t),u^{(1)},t)-\dot{x}^{(1)}(t)\right)dt\\
&+\int_{t_0}^{t_1}\left(\mu^{(1)}(t)\right)^T\cdot\left(g^{(1)}(x^{(1)}(t),z^{(1)}(t),u^{(1)},t)\right)dt
\end{aligned}
\tag{4.6}
$$

Variations on the parameter set of stage p', of the form $\delta u^{(p')}$, are considered, which result in variations in the state values at all times, as shown in Equation (4.7). Clearly, the state vector of stage p, where $p < p'$, will not be influenced. This results in $\delta x^{(p)}(t) \triangleq 0$ and $\delta z^{(p)}(t) \triangleq 0$.

$$
\begin{aligned}
\delta\bar{W} \;=\; &\sum_{p=2}^{NP}\Bigg\{\\
&\left[\frac{\partial\phi^{(p)}}{\partial x^{(p)}(t_p)}\delta x^{(p)}(t_p)+\frac{\partial\phi^{(p)}}{\partial z^{(p)}(t_p)}\delta z^{(p)}(t_p)+\frac{\partial\phi^{(p)}}{\partial u^{(k)}}\delta u^{(p)}\right]\\
&+\left(\nu^{(p)}\right)^T\cdot\\
&\left(\frac{\partial I^{(p)}}{\partial x^{(p-1)}(t_{p-1})}\delta x^{(p-1)}(t_{p-1})+\frac{\partial I^{(p)}}{\partial z^{(p-1)}(t_{p-1})}\delta z^{(p-1)}(t_{p-1})+\frac{\partial I^{(p)}}{\partial u^{(p)}}\delta u^{(p)}\right.
\end{aligned}
$$

Note, the equation continues on the next page.

$$
\begin{aligned}
&-\delta x^{(p)}(t_{p-1})\Bigg) \\
&+\int_{t_{p-1}}^{t_p} \frac{\partial L^{(p)}}{\partial x^{(p)}(t)}\delta x^{(p)}(t)+\frac{\partial L^{(p)}}{\partial z^{(p)}(t)}\delta z^{(p)}(t)+\frac{\partial L^{(p)}}{\partial u^{(p)}}\delta u^{(p)}\,dt \\
&+\int_{t_{p-1}}^{t_p} \left(\lambda^{(p)}(t)\right)^T \cdot \\
&\left(\frac{\partial f^{(p)}}{\partial x^{(p)}(t)}\delta x^{(p)}(t)+\frac{\partial f^{(p)}}{\partial z^{(p)}(t)}\delta z^{(p)}(t)+\frac{\partial f^{(p)}}{\partial u^{(p)}}\delta u^{(p)}-\delta \dot{x}^{(p)}(t)\right)dt \\
&+\int_{t_{p-1}}^{t_p} \left(\mu^{(p)}(t)\right)^T \cdot \left(\frac{\partial g^{(p)}}{\partial x^{(p)}(t)}\delta x^{(p)}(t)+\frac{\partial g^{(p)}}{\partial z^{(p)}(t)}\delta z^{(p)}(t)+\frac{\partial g^{(p)}}{\partial u^{(p)}}\delta u^{(p)}\right)dt \\
&\Bigg\} \\
&+\left[\frac{\partial \phi^{(1)}}{\partial x^{(1)}(t_1)}\delta x^{(1)}(t_1)+\frac{\partial \phi^{(1)}}{\partial z^{(1)}(t_1)}\delta z^{(1)}(t_1)+\frac{\partial \phi^{(1)}}{\partial u^{(1)}}\delta u^{(1)}\right] \\
&+\left(\nu^{(1)}\right)^T \cdot \left(\frac{\partial I^{(1)}}{\partial u^{(1)}}\delta u^{(1)}-\delta x^{(1)}(t_0)\right) \\
&+\int_{t_0}^{t_1} \frac{\partial L^{(1)}}{\partial x^{(1)}(t)}\delta x^{(1)}(t)+\frac{\partial L^{(1)}}{\partial z^{(1)}(t)}\delta z^{(1)}(t)+\frac{\partial L^{(1)}}{\partial u^{(1)}}\delta u^{(1)}\,dt \\
&+\int_{t_0}^{t_1} \left(\lambda^{(1)}(t)\right)^T \cdot \\
&\left(\frac{\partial f^{(1)}}{\partial x^{(1)}(t)}\delta x^{(1)}(t)+\frac{\partial f^{(1)}}{\partial z^{(1)}(t)}\delta z^{(1)}(t)+\frac{\partial f^{(1)}}{\partial u^{(1)}}\delta u^{(1)}-\delta \dot{x}^{(1)}(t)\right)dt \\
&+\int_{t_0}^{t_1} \left(\mu^{(1)}(t)\right)^T \cdot \left(\frac{\partial g^{(1)}}{\partial x^{(1)}(t)}\delta x^{(1)}(t)+\frac{\partial g^{(1)}}{\partial z^{(1)}(t)}\delta z^{(1)}(t)+\frac{\partial g^{(1)}}{\partial u^{(1)}}\delta u^{(1)}\right)dt \quad (4.7)
\end{aligned}
$$

Integration by parts for the last term in the integrals involving $\delta \dot{x}^{(p)}$ is used to obtain Equation (4.8):

$$
\begin{aligned}
\delta\bar{W} \;=\; & \sum_{p=2}^{NP} \Bigg\{ \\
& \left[\frac{\partial \phi^{(p)}}{\partial x^{(p)}(t_p)} \delta x^{(p)}(t_p) + \frac{\partial \phi^{(p)}}{\partial z^{(p)}(t_p)} \delta z^{(p)}(t_k) + \frac{\partial \phi^{(p)}}{\partial u^{(p)}} \delta u^{(p)} \right] \\
& + \left(\nu^{(p)} \right)^T \cdot \\
& \left(\frac{\partial I^{(p)}}{\partial x^{(p-1)}(t_{p-1})} \delta x^{(p-1)}(t_{p-1}) + \frac{\partial I^{(p)}}{\partial z^{(p-1)}(t_{p-1})} \delta z^{(p-1)}(t_{p-1}) + \frac{\partial I^{(p)}}{\partial u^{(p)}} \delta u^{(p)} \right. \\
& \left. - \delta x^{(p)}(t_{p-1})) \right) \\
& + \int_{t_{p-1}}^{t_p} \frac{\partial L^{(p)}}{\partial x^{(p)}(t)} \delta x^{(p)}(t) + \frac{\partial L^{(p)}}{\partial z^{(p)}(t)} \delta z^{(p)}(t) + \frac{\partial L^{(p)}}{\partial u^{(p)}} \delta u^{(p)} \, dt \\
& + \int_{t_{p-1}}^{t_p} \left(\lambda^{(p)}(t) \right)^T \cdot \\
& \left(\frac{\partial f^{(p)}}{\partial x^{(p)}(t)} \delta x^{(p)}(t) + \frac{\partial f^{(p)}}{\partial z^{(p)}(t)} \delta z^{(p)}(t) + \frac{\partial f^{(p)}}{\partial u^{(p)}} \delta u^{(p)} \right) dt \\
& + \int_{t_{p-1}}^{t_p} \left(\dot{\lambda}^{(p)}(t) \right)^T \delta x^{(p)}(t) \, dt \\
& + \left(\lambda^{(p)}(t_{p-1}) \right)^T \cdot \delta x^{(p)}(t_{p-1}) - \left(\lambda^{(p)}(t_p) \right)^T \cdot \delta x^{(p)}(t_p) \\
& + \int_{t_{p-1}}^{t_p} \left(\mu^{(p)}(t) \right)^T \cdot \left(\frac{\partial g^{(p)}}{\partial x^{(p)}(t)} \delta x^{(p)}(t) + \frac{\partial g^{(p)}}{\partial z^{(p)}(t)} \delta z^{(p)}(t) + \frac{\partial g^{(p)}}{\partial u^{(p)}} \delta u^{(p)} \right) dt \\
& \Bigg\} \\
& + \left[\frac{\partial \phi^{(1)}}{\partial x^{(1)}(t_1)} \delta x^{(1)}(t_1) + \frac{\partial \phi^{(1)}}{\partial z^{(1)}(t_1)} \delta z^{(1)}(t_1) + \frac{\partial \phi^{(1)}}{\partial u^{(1)}} \delta u^{(1)} \right] \\
& + \left(\nu^{(1)} \right)^T \cdot \left(\frac{\partial I^{(1)}}{\partial u^{(1)}} \delta u^{(1)} - \delta x^{(1)}(t_0) \right)
\end{aligned}
$$

Note, the equation continues on the next page.

$$
\begin{aligned}
&+\int_{t_0}^{t_1} \frac{\partial L^{(1)}}{\partial x^{(1)}(t)}\delta x^{(1)}(t)+\frac{\partial L^{(1)}}{\partial z^{(1)}(t)}\delta z^{(1)}(t)+\frac{\partial L^{(1)}}{\partial u^{(1)}}\delta u^{(1)}\,dt \\
&+\int_{t_0}^{t_1} \left(\lambda^{(1)}(t)\right)^T \cdot \\
&\left(\frac{\partial f^{(1)}}{\partial x^{(1)}(t)}\delta x^{(1)}(t)+\frac{\partial f^{(1)}}{\partial z^{(1)}(t)}\delta z^{(1)}(t)+\frac{\partial f^{(1)}}{\partial u^{(1)}}\delta u^{(1)}\right) dt \\
&+\int_{t_0}^{t_1} \left(\dot{\lambda}^{(1)}(t)\right)^T \delta x^{(1)}(t)\,dt \\
&+\left(\lambda^{(1)}(t_0)\right)^T \cdot \delta x^{(1)}(t_0)-\left(\lambda^{(1)}(t_1)\right)^T \cdot \delta x^{(1)}(t_1) \\
&+\int_{t_0}^{t_1} \left(\mu^{(1)}(t)\right)^T \cdot \left(\frac{\partial g^{(1)}}{\partial x^{(1)}(t)}\delta x^{(1)}(t)+\frac{\partial g^{(1)}}{\partial z^{(1)}(t)}\delta z^{(1)}(t)+\frac{\partial g^{(1)}}{\partial u^{(1)}}\delta u^{(1)}\right) dt
\end{aligned} \tag{4.8}
$$

For a stationary point, infinitesimal variations in the right hand side should yield no change to the performance index, *i.e.* $\delta\bar{W}=0$, and hence related terms must be chosen so that they always guarantee this. This leads to the following set of Euler-Lagrange equations and the Pontryagin minimum principle [108].

To cancel the $\delta x^{(1)}(t)$ and $\delta x^{(1)}(t_1)$ terms, the differential equations and final time stage conditions, as shown in Equations (4.9a) to (4.10), must hold, respectively:

$$
\dot{\lambda}^{(1)}(t)=-\left[\frac{\partial f^{(1)}}{\partial x^{(1)}(t)}\right]^T \lambda^{(1)}(t)-\left[\frac{\partial g^{(1)}}{\partial x^{(1)}(t)}\right]^T \mu^{(1)}(t)-\left[\frac{\partial L^{(1)}}{\partial x^{(1)}(t)}\right]^T \tag{4.9a}
$$

$$
t_0 \le t \le t_1 \tag{4.9b}
$$

$$
\lambda^{(1)}(t_1)=\left[\frac{\partial \phi^{(1)}}{\partial x^{(1)}(t_1)}\right]^T+\left[\frac{\partial I^{(2)}}{\partial x^{(1)}(t_1)}\right]^T \nu^{(2)} \tag{4.10}
$$

Algebraic equations and final stage conditions, Equations (4.11a) to (4.12), must hold

in order to cancel the $\delta z^{(1)}(t)$ and $\delta z^{(1)}(t_1)$ terms:

$$\left[\frac{\partial f^{(1)}}{\partial z^{(1)}(t)}\right]^T \lambda^{(1)}(t) + \left[\frac{\partial g^{(1)}}{\partial z^{(1)}(t)}\right]^T \mu^{(1)}(t) + \left[\frac{\partial L^{(1)}}{\partial z^{(1)}(t)}\right]^T = 0 \tag{4.11a}$$

$$t_0 \leq t \leq t_1 \tag{4.11b}$$

$$\left[\frac{\partial \phi^{(1)}}{\partial z^{(1)}(t_1)}\right]^T + \left[\frac{\partial I^{(2)}}{\partial z^{(1)}(t_1)}\right]^T \nu^{(2)} = 0 \tag{4.12}$$

The $\delta x^{(p)}(t)$, $\delta x^{(p)}(t_p)$ and $\delta x^{(p)}(t_{p-1})$ terms are cancelled through the condition that the following differential equations and final time stage conditions are held:

$$\dot{\lambda}^{(p)}(t) = -\left[\frac{\partial f^{(p)}}{\partial x^{(p)}(t)}\right]^T \lambda^{(p)}(t) - \left[\frac{\partial g^{(p)}}{\partial x^{(p)}(t)}\right]^T \mu^{(p)}(t) - \left[\frac{\partial L^{(p)}}{\partial x^{(p)}(t)}\right]^T \tag{4.13a}$$

$$t_{p-1} \leq t \leq t_p \qquad \forall p = 2,3,\ldots NP \tag{4.13b}$$

$$\lambda^{(p)}(t_p) = \left[\frac{\partial \phi^{(p)}}{\partial x^{(p)}(t_p)}\right]^T + \left[\frac{\partial I^{(p+1)}}{\partial x^{(p)}(t_p)}\right]^T \nu^{(p+1)} \qquad \forall p = 2,3,\ldots,NP-1 \tag{4.14a}$$

$$\lambda^{(p)}(t_p) = \left[\frac{\partial \phi^{(p)}}{\partial x^{(p)}(t_p)}\right]^T \qquad \forall p = NP \tag{4.14b}$$

$$\nu^{(p)} = \lambda^{(p)}(t_{p-1}) \qquad \forall p = 2,3,\ldots,NP \tag{4.15}$$

To cancel $\delta z^{(p)}(t)$ and $\delta z^{(p)}(t_p)$ terms, the following algebraic equations must hold:

$$\left[\frac{\partial f^{(p)}}{\partial z^{(p)}(t)}\right]^T \lambda^{(p)}(t) + \left[\frac{\partial g^{(p)}}{\partial z^{(p)}(t)}\right]^T \mu^{(p)}(t) + \left[\frac{\partial L^{(p)}}{\partial z^{(p)}(t)}\right]^T = 0 \tag{4.16a}$$

$$t_{p-1} \leq t \leq t_p \qquad \forall p = 2,3,\dots NP \tag{4.16b}$$

$$\left[\frac{\partial \phi^{(p)}}{\partial z^{(p)}(t_p)}\right]^T + \left[\frac{\partial I^{(p+1)}}{\partial z^{(p)}(t_p)}\right]^T \nu^{(p+1)} = 0 \qquad \forall p = 2,3,\dots,NP-1 \tag{4.17a}$$

$$\left[\frac{\partial \phi^{(p)}}{\partial z^{(p)}(t_p)}\right]^T = 0 \qquad \forall p = NP \tag{4.17b}$$

The terms $\delta u^{(1)}$ and $\delta u^{(p)}$ are cancelled on the condition that Equations (4.18a) to (4.19b) hold. These are equivalent to the Hamiltonian gradient condition:

$$\nabla_{u^{(1)}} H^{(1)} \triangleq \left[\frac{\partial \phi^{(1)}}{\partial u^{(1)}(t_1)}\right]^T + \left[\frac{\partial I^{(1)}}{\partial u^{(1)}}\right]^T \nu^{(1)} \tag{4.18a}$$

$$+ \int_{t_0}^{t_1} \left\{ \left[\frac{\partial L^{(1)}}{\partial u^{(1)}(t)}\right]^T + \left[\frac{\partial f^{(1)}}{\partial u^{(1)}(t)}\right]^T \lambda^{(1)}(t) + \left[\frac{\partial g^{(1)}}{\partial u^{(1)}(t)}\right]^T \mu(t) \right\} dt \triangleq 0$$

$$t_0 \leq t \leq t_1 \tag{4.18b}$$

$$\nabla_{u^{(p)}} H^{(p)} \triangleq \left[\frac{\partial \phi^{(p)}}{\partial u^{(p)}(t_p)}\right]^T + \left[\frac{\partial I^{(p)}}{\partial u^{(p)}}\right]^T \nu^{(p)} \tag{4.19a}$$

$$+ \int_{t_{p-1}}^{t_p} \left\{ \left[\frac{\partial L^{(p)}}{\partial u^{(p)}(t)}\right]^T + \left[\frac{\partial f^{(p)}}{\partial u^{(p)}(t)}\right]^T \lambda^{(p)}(t) + \left[\frac{\partial g^{(p)}}{\partial u^{(p)}(t)}\right]^T \mu(t) \right\} dt \triangleq 0$$

$$t_{p-1} \leq t \leq t_p \qquad \forall p = 2,3,\dots NP \tag{4.19b}$$

When the functions appearing in Equations (4.18a) and (4.19a) are linearly related to the control, the optimal control for the relaxed MIOCP will exhibit bang-bang behaviour (with potential singular arcs). Bang-bang solutions occur when the optimal control action is at either bound of the feasible region [17]. Controls that are not bang-bang, where the control lies between the bounds, are called singular. In this case, singular arcs exist. Pure bang-bang controls are demonstrated in minimum-time problems for linear systems [9] and bilinear systems [89], optimal control of batch reactors [14], optimal thermal control [8], *etc.*

For nonlinear optimisation systems, this bang-bang principle does not always hold. [150] investigated reservoir flooding problems, where the control is linear in relation to the continuous variables, and showed that if the only constraints are upper and lower bounds on the control, then due to their particular structure, these problems will sometimes have bang-bang optimal solutions. This is advantageous since bang-bang solutions can be implemented with simple on–off control valves.

Approaches for optimal control of nonlinear dynamical systems with binary controls (on/off) were reviewed by [118]. To satisfy requirements for bang-bang behaviour, the general OCP is reformulated such that the binary controls are presented linearly in the system dynamics. Solutions in this case may require use of heuristics, *e.g.* rounding up or a sum up rounding strategy, or algorithms such as Branch and Bound, when singular arcs appear [118].

For the cleaning scheduling problem, reformulation is not necessary as the controls involved already have linear presentation in the system. More importantly, the formulation of this problem as an OCP facilitates the solution of the relaxed NLP problem through the feasible path approach, obviating the need to discretise the system equations. This otherwise leads to a very large scale optimisation problem with a strongly nonlinear system of equality constraints. This approach avoids failures of convergence produced by direct solutions of MINLPs resulting from discretisation, such as in previous work of [45] and of [128]. Furthermore, it allows direct handling of nonlinear models without approximation by linearisation, particularly in the case where fouling kinetics may take a highly nonlinear form, *e.g.* in a dual layer fouling model when the growth rates of the layers are functions of temperature [106].

4.2 Problem formulation as an optimal control problem

The objective to be minimised is expressed as in Equation (1.12). The overall heat transfer coefficient can be determined through rearrangement of Equation (1.2) and rewriting it as:

$$U_n = \frac{U_{c,n}}{1 + U_{c,n} R_{f,n}} \qquad \forall n \in NE \tag{4.20}$$

The optimisation of the HEN maintenance scheduling problem is started from a clean condition, *i.e.* $U_{0,n} = U_{c,n}$. Through incorporation of the binary control variable, $y_{n,p}$, the linear and asymptotic fouling resistances in Equations (1.4) and (1.5) can be rewritten as:

$$\dot{R}_{f,n} = y_{n,p} a_n \qquad \forall n \in NE,\, p \in NP \tag{4.21}$$

$$R_{f,n} = R^{\infty}_{f,n} \left(1 - \exp(-t_n^{'}/\tau_n)\right) \qquad n \in NE \tag{4.22a}$$

$$\dot{t_n^{'}} = y_{n,p} \qquad \forall n \in NE,\, p \in NP \tag{4.22b}$$

As the HEN optimisation is started from a clean condition, the initial fouling resistance is 0 for the first period of all heat exchangers. In consecutive periods, the initial fouling resistance is related to the fouling resistance at the end of the previous period by integration in time, and this value is allowed to be reset through a junction condition when cleaning occurs. The junction condition for the linear fouling model is defined in Equation (4.23) where the fouling resistance is reinitialised based on the control variable value.

$$R_{f,n}(t_p^{\text{initial}}) = y_{n,p} R_{f,n}(t_{p-1}^{\text{end}}) \qquad \forall n \in NE,\, p = 2, \ldots NP \tag{4.23}$$

For the asymptotic fouling model, this junction condition is defined in Equation (4.24),

where the elapsed time since the last cleaning is reinitialised based on the control variable value.

$$t_n^{'}(t_p^{\text{initial}}) = y_{n,p} t_n^{'}(t_{p-1}^{\text{end}}) \qquad \forall n \in NE,\, p = 2, \ldots NP \tag{4.24}$$

Similarly, to the MINLP formulation, the NTU effectiveness method is also used in this case. Through rearranging and rewriting of Equations (3.17) and (3.18), the temperature of the cold and hot streams leaving each exchanger can be calculated, via:

$$T_{\text{c},n}^{\text{out}} = T_{\text{c},n}^{\text{in}} + P_n \left(T_{\text{h},n}^{\text{in}} - T_{\text{h},n}^{\text{out}} \right) \qquad \forall n \in NE \tag{4.25}$$

$$\begin{aligned} T_{\text{h},n}^{\text{out}} \;=\; & y_{n,p} \left[\frac{(1-P_n) T_{\text{h},n}^{\text{in}} \exp(-\alpha_n (1-P_n)) + T_{\text{c},n}^{\text{in}} (1 - \exp(-\alpha_n (1-P_n)))}{1 - P_n \exp(-\alpha_n (1-P_n))} \right] \\ & + (1 - y_{n,p}) T_{\text{h},n}^{\text{in}} \qquad \forall n \in NE,\, p \in NP \end{aligned} \tag{4.26}$$

where the effectiveness term can be written from Equation (3.14) as:

$$\alpha_n = \frac{U_n A_n}{F_{\text{h},n} C_{\text{h},n}} \qquad \forall n \in NE \tag{4.27}$$

and the ratio of capacity flow rates for each exchanger, P_n, can be expressed as shown in Equation (3.15).

4.3 Problem solution methodology and implementation

The implementation is performed in MATLAB® R2016b with its Optimisation Toolbox ™ and Parallel Computing Toolbox ™ [134]. It is noteworthy that this methodology cannot be implemented in current commercial simulators directly. For example,

gPROMS^{TM} [110], which is one of the most advanced commercial simulators, does not facilitate multi-period optimal control problem solution, as it does not allow for junction conditions.

The MATLAB® code works as a standard multi-period optimal control problem solver using the feasible path approach (*i.e.* sequential approach) by linking together the Ordinary Differential Equation (ODE) solver ode15s with the optimiser fmincon. The default settings for ode15s are used, with absolute tolerance of 10^{-6} and relative tolerance of 10^{-3}. The optimiser fmincon is used with the Sequential Quadratic Programming (SQP) algorithm option whilst keeping the remaining settings at their default values: constraint, optimality and step tolerances of 10^{-6} using a forward finite difference scheme for the estimation of gradients. Gradient evaluations conducted via finite differences are costly and require repeated simulations of the dynamic process model.

Additionally, since this problem is non-convex, multiple runs with different starting points are performed and the best solution is reported. 50 starting points are generated through a random choice of 0 or 1 for all the control variables' initial points, and this is implemented using the randsample function in MATLAB®. A test was run using the Parallel Computing Toolbox^{TM} to compare the computational time between parallelisation of the gradient evaluations versus parallelising a loop of multiple starting points. On a 4GHz Intel Core i7, 16 GB RAM iMac (2014 model) running on macOS Sierra, the latter was faster than the former. Parallelisation of a loop of 50 runs is performed using the parfor loop in MATLAB®. For cases where singular arcs (*i.e.* fractional control values) appear in the optimal control solution found, a rounding up scheme is employed.

4.4 Computational results and discussion

In this section, computational results for the MIOCP feasible path technique on each of the case studies shown in Section 3.3 are presented. For case studies A and C, a cleaning cost of £4000 is used. The energy maximisation scenario is not considered here; however, this can be easily applied by setting the cleaning cost to £0, as done in the previous chapter. Additionally, for case study D only the longer duration, where $NP = 36$, is considered. For case studies A, B and C, the best solutions obtained are compared in the schedules shown in Tables 4.4.1, 4.4.4, 4.4.5, 4.4.8 and 4.4.9 with

the schedules obtained by [77] using the MILP formulation, while for case study D the best solution is compared in the schedule shown in Table 4.4.9 with the schedule obtained by [129] using the BTA algorithm. In the economic comparison, similarly to the MINLP approach in Chapter 3, we fixed the solutions obtained by [77] and [129], and evaluated them using our model. This is done because the full ODE nonlinear model is used here, and hence the constraints of the model are completely satisfied. This would be even more accentuated in the case of highly nonlinear fouling kinetics, where linearisation would not necessarily satisfy the constraints of the full nonlinear model, let alone produce the same objective function value. These are shown in Tables 4.4.2, 4.4.6, 4.4.10 and 4.4.13, where the best obtained solution is reported for each of the cases. Solution metrics which include the worst cost out of 50 runs of different starting points, mean cost, RSD around the mean value, number of iterations and function evaluations are reported in Tables 4.4.3, 4.4.7, 4.4.11 and 4.4.14. In addition for each case, the best and worst resultant computational time per run is reported in these tables.

4.4.1 Case study A

Similar observations are seen as in Subsection 3.4.1:

(i) Due to the higher initial fouling rates of the asymptotic fouling case in comparison to that of the linear case, the objective for the no-cleaning scenario is much larger in the asymptotic case (*e.g.* £317k *vs.* £203k for the single unit case, as shown in Table 4.4.2).

(ii) More cleaning actions are expected in the asymptotic fouling model case than the corresponding linear one due to the early loss of exchanger efficiencies. This is evident in Table 4.4.1 with the cleaning actions increasing from 3 to 5 in both the MIOCP solution and the solution of [77].

(iii) Cleaning actions occur cyclicly (see Table 4.4.1). For linear fouling, the number of cleaning actions as well as the schedules are very similar; however, the cleanings in our model are performed 1 month earlier than in [77]'s schedule.

Both linear and asymptotic fouling case solutions produced are bang-bang, where the relaxed MIOCP is completely integer and no rounding is needed. This evident in

Table 4.4.2 where the relaxed MIOCP and the MIOCP solutions are £103k and £226k for the linear fouling and asymptotic fouling cases, respectively.

Due to the non-convexity of this problem, a number of local solutions with different schedules are produced. For the linear case, the best cost value obtained is £103k compared to the worst cost being £109k, as shown in Table 4.4.3. The difference between the best and worst objective increases to £15k for the asymptotic behaviour case (£226k to £241k, as shown in Table 4.4.3). The results are narrowly dispersed about the mean, with a RSD value of 1.3% and 1.4% in the linear and asymptotic scenarios, respectively. The resource usage varies depending on the cleaning cost, fouling type, method used and problem size. For all of these scenarios, a quick convergence is achieved, where the total CPU time per run ranges between 15 to 48 CPU s and 9 to 47 CPU s for the linear and asymptotic cases, respectively, as shown in Table 4.4.3.

4.4.2 Case study B

For the four heat exchanger case, the schedule for the 12 month operating horizon is the same as that of the [77] model, resulting in the same cost of £106k, as shown in Tables 4.4.4 and 4.4.6; meanwhile, for the 18 month duration case, the schedules differ although the number of cleaning actions per unit are the same (see Table 4.4.5). No pattern is evident when the schedules are compared, with some cleaning actions occurring earlier in some cases and later in others.

In terms of cost comparison for the case of 18 months operation, the cost of our schedule is slightly less than that reported, with the difference in savings being $<$1.5%. This is because of the existence of multiple local optima. It is noteworthy that [77]'s MILP model is solved to global optimality whereas our model, being a non-convex MINLP (MIOCP) model, is not. Despite this, we still obtain similar results and in some cases even better.

For the 4 unit heat exchanger case over a 12 month length of operation, the resultant savings from cleaning are 19.3% in the worst case compared to 21.5% in the best case scenario (see Table 4.4.7). Therefore, similarly to Subsection 3.4.2, only a few runs are needed to achieve a good solution, where the RSD is even less at only 0.9% and 1.1% for the 12 month and 18 month horizons, respectively. Furthermore, the difference between the maximum and minimum cost value is only £3k for the 4 unit

Table 4.4.1: Cleaning schedule for the single heat exchanger case using MIOCP approach (linear and asymptotic fouling).

Case	Time (months)																							No. of cleaning actions	
	1	2	3	4	5	6	7	8	9	10	11	12	13	14	15	16	17	18	19	20	21	22	23	24	+	◯
Linear fouling, cleaning cost=£4000						+	◯					+	◯					+	◯						3	3
Asymptotic fouling, cleaning cost=£4000					⊕				⊕				⊕				◯	⊕			⊕				5	6
cleaning actions: + MIOCP approach; ◯ [77] MILP approach; ⊕ common																										

Table 4.4.2: Economic chart for the single heat exchanger case using MIOCP approach. All values in k£.

Case	MIOCP model		[77] model
	MIOCP solution (relaxed MIOCP)	[77] MILP approach solution**	[77] solution
No cleaning, linear fouling	203	203	203
No cleaning, asymptotic fouling	317	317	316
Cleaning cost=£4k, linear fouling	103 (103*)	102	102
Cleaning cost=£4k, asymptotic fouling	226 (226*)	225	225

* relaxed MIOCP completely integer, *i.e.* feasible solution. ** [77] MILP approach solution inputted into MIOCP model.

Table 4.4.3: Solution metrics for the single heat exchanger case using MIOCP approach.

Case	Relaxed MIOCP approach solution				No. of iterations			No. of function evaluations (*i.e.* simulations)			CPU time in s		
	Min in k£	Max in k£	Mean in k£	RSD in %	Min	Max	Mean	Min	Max	Mean	Min	Max	Mean
Cleaning cost=£4k, linear fouling	103	109	105	1.3	5	18	11	145	467	286	15	48	30
Cleaning cost=£4k, asymptotic fouling	226	241	233	1.4	2	15	7	72	388	192	9	47	25

Table 4.4.4: Cleaning schedule for the four heat exchanger case using MIOCP approach (duration of 12 months, linear fouling, cleaning cost = £4000)

HEX	Time (months)												No. of cleaning actions	
	1	2	3	4	5	6	7	8	9	10	11	12	+	◯
1													0	0
2													0	0
3						⊕							1	1
4							⊕						1	1
cleaning actions: + MIOCP approach; ◯ [77] MILP approach; ⊕ common													2	2

heat exchanger case over a 12 month operating horizon, and this difference is £10k for the corresponding 18 month operating horizon scenario. The optimisation converges within an average of 34 CPU s and 132 CPU s (≈2.2 CPU min) for the four heat exchanger case over 12 months and 18 months duration, respectively (see Table 4.4.7). In addition, it is evident from Table 4.4.7 that only a few iterations are required to achieve convergence (a maximum of 12 and 22 major iterations of the SQP algorithm for the 12 month and 18 month cases, respectively).

4.4.3 Case study C

For the 10 unit HEN case, the economic chart (Table 4.4.10) shows that the cost for the linear fouling case is similar to that of [77] (£259k *vs.* £258k). In terms of the schedules, although a general relation is seen in [77]'s schedule, where cleaning actions increase in the asymptotic fouling case *vs.* the linear one (from 10 to 11 cleanings), this drops down by 4 cleaning actions in our schedule, as shown in Tables 4.4.8 and 4.4.9. Only the last 3 units are cleaned here whilst there is a more distributed cleaning of units in the schedule of [77], with half the units in the network undergoing cleaning during the operational horizon. Consequently, the cost of their schedule is slightly less than ours (£484k *vs.* £493k as shown in Table 4.4.10). This is a small difference of just over 1.5% in savings (11.2% saving in the MIOCP solution compared to 12.8% in [77]'s MILP one).

Both cases result in the solution of the relaxed models being completely integer, *i.e.* a bang-bang control solution, indicated by $*$ in Table 4.4.10. Thus, the proposed rounding up scheme was not performed here. However, given the non-convex nature of this

Table 4.4.5: Cleaning schedule for the four heat exchanger case using MIOCP approach (duration of 18 months, linear fouling, cleaning cost = £4k)

HEX	Time (months)																		No. of cleaning actions	
	1	2	3	4	5	6	7	8	9	10	11	12	13	14	15	16	17	18	+	◯
1										+	◯								1	1
2											⊕								1	1
3					◯		+			◯				+					2	2
4						⊕						⊕							2	2
cleaning actions: + MIOCP approach; ◯ [77] MILP approach; ⊕ common																			6	6

Table 4.4.6: Economic chart for the four heat exchangers case using MIOCP approach. All values in k£.

Case	MIOCP model		[77] model
	MIOCP solution (relaxed MIOCP)	[77] MILP approach solution**	[77] solution
No cleaning, linear fouling, 12 months	135	135	Not reported
No cleaning, linear fouling, 18 months	289	289	Not reported
Cleaning cost = £4k, linear fouling, 12 months	106 (106*)	106	106
Cleaning cost = £4k, linear fouling, 18 months	179 (179*)	183	183

* relaxed MIOCP completely integer, *i.e.* feasible solution. ** [77] MILP approach solution inputted into MIOCP model.

Table 4.4.7: Solution metrics for the four heat exchanger case using MIOCP approach.

Case	Relaxed MIOCP approach solution				No. of iterations			No. of function evaluations (*i.e.* simulations)			CPU time in s		
	Min in k£	Max in k£	Mean in k£	RSD in %	Min	Max	Mean	Min	Max	Mean	Min	Max	Mean
4 units, linear fouling, 12 months	106	109	107	0.9	5	12	8	270	592	404	22	48	34
4 units, linear fouling, 18 months	179	189	182	1.1	11	22	15	835	1,609	1,141	97	190	132

problem, a number of bang-singular solutions are obtained, where the objective values are similar but different orders of cleaning actions are obtained.

Figure 4.4.1 shows the CIT profiles with and without cleaning over time for the linear and asymptotic cases, respectively. For the cleaning scenario, the profile shown is based on the best objective value using the MIOCP feasible path approach, *i.e.* the schedules in Tables 4.4.8 and 4.4.9. Similarly to Figure 3.4.6, the CIT profiles in Figure 4.4.1 show that fouling has a significant effect on the performance of the HEN, where, for the asymptotic fouling model, there are a couple of instances where there is a rapid decay in the CIT which reaches as low as 327°F, due to the unit with the highest fouling rate (unit 10) being cleaned in the 4^{th}, 8^{th} and 12^{th} months (see Figure 4.4.1b and Table 4.4.9).

The range of objective values obtained in the 50 runs is quite narrow for the linear case, as shown in Table 4.4.11, where the objective values only vary by a maximum of £11k. For the 10 unit asymptotic HEN case study, this range widens up to £42k from a minimum of £493k to a maximum of £535k. Hence, for less complex networks and/or fouling models many runs at different starting points are not required to obtain a good solution. In terms of the distribution of the objective values for the 50 runs performed in each case, the results for each of the cases are narrowly dispersed around the associated mean value, where the RSD of the local optima for each of the cases considered lies in a narrow range of 1% and 1.5% (see Table 4.4.11). For the 10 unit HEN case subject to asymptotic fouling, the worst run results in a saving of 3.6% compared to 11.2% for the best solution achieved.

From Table 4.4.11, it can be seen that the resource usage is practical even for the worst case: the 10 unit HEN with asymptotic fouling model required 942 CPU s (≈15.7 CPU min), with the corresponding best case for this model being a modest 91 CPU s (≈1.5 CPU min).

4.4.4 Case study D

For the 25 unit HEN case study, [129] reported a lower objective associated with the no-cleaning scenario representing <11% difference (see Table 4.4.13). This is partly attributed to our model retaining the fouling expressions in their dynamic form, which is more accurate. [129] discretised the system equations and thus assumed that

Table 4.4.8: Cleaning schedule for the 10 unit HEN case using MIOCP approach (linear fouling, cleaning cost = £4k).

HEX	Time (months)																		No. of cleaning actions	
	1	2	3	4	5	6	7	8	9	10	11	12	13	14	15	16	17	18	+	◯
1																			0	0
2																			0	0
3									⊕										1	1
4											⊕								1	1
5									◯	+									1	1
6								◯			+								1	1
7									+	◯									1	1
8										⊕									1	1
9							⊕						⊕						2	2
10						⊕						⊕							2	2
cleaning actions: + MIOCP approach; ◯ [77] MILP approach; ⊕ common																			10	10

Table 4.4.9: Cleaning schedule for the 10 unit HEN case using MIOCP approach (asymptotic fouling, cleaning cost = £4k).

HEX	Time (months)																		No. of cleaning actions	
	1	2	3	4	5	6	7	8	9	10	11	12	13	14	15	16	17	18	+	◯
1																			0	0
2																			0	0
3																			0	0
4												◯							0	1
5																			0	0
6																			0	0
7						◯						◯							0	2
8							◯				+		◯						1	2
9				◯		+			◯	+				◯					2	3
10				+	◯			+		◯		+			◯				3	3
cleaning actions: + MIOCP approach; ◯ [77] MILP approach; ⊕ common																			6	11

Table 4.4.10: Economic chart for the 10 unit HEN case using MIOCP approach. All values in k£.

Case	MIOCP model		[77] model
	MIOCP solution (relaxed MIOCP)	[77] MILP approach solution**	[77] solution
No cleaning, linear fouling	361	361	361
No cleaning, asymptotic fouling	555	555	554
Cleaning cost = £4k, linear fouling	259 (259*)	258	258
Cleaning cost = £4k, asymptotic fouling	493 (493*)	484	482

* relaxed MIOCP completely integer, *i.e.* feasible solution. ** [77] MILP approach solution inputted into MIOCP model.

Table 4.4.11: Solution metrics for 10 unit HEN case using MIOCP approach.

Case	Relaxed MIOCP approach solution				No. of iterations			No. of function evaluations (*i.e.* simulations)			CPU time in s		
	Min in k£	Max in k£	Mean in k£	RSD in %	Min	Max	Mean	Min	Max	Mean	Min	Max	Mean
10 unit HEN, linear fouling, 18 months	259	270	264	1.0	9	25	16	1,581	4,322	2,782	298	822	535
10 unit HEN, asymptotic fouling, 18 months	493	535	512	1.5	2	19	7	343	3,292	1,298	91	942	343

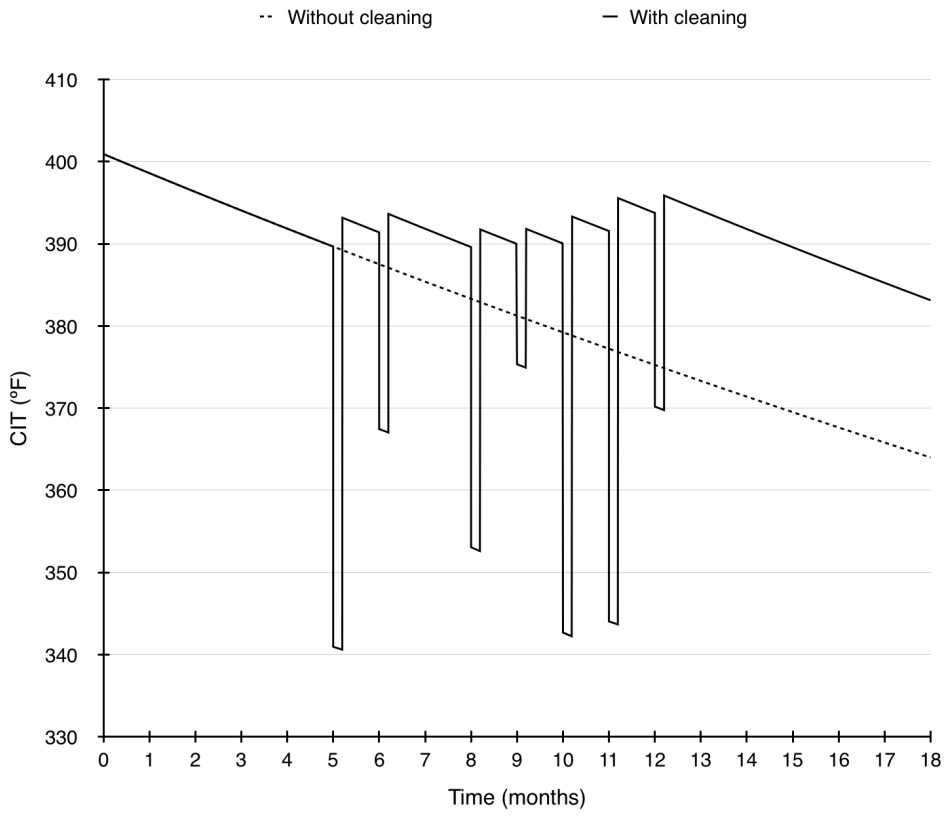

(a)

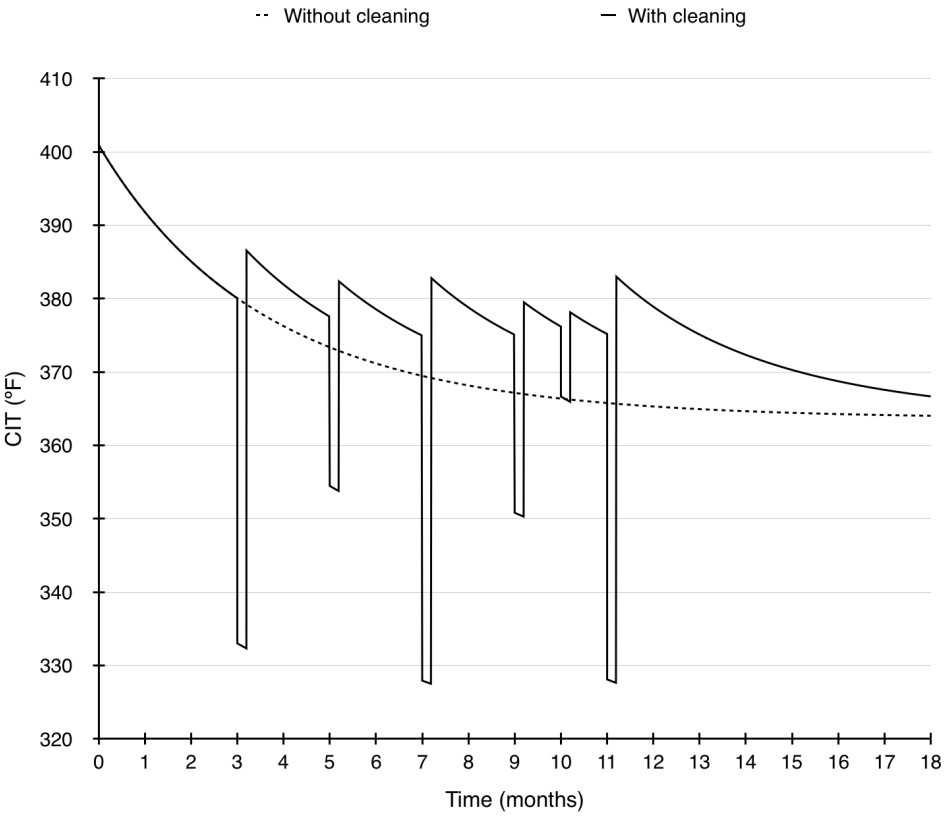

(b)

Figure 4.4.1: CIT profile for the 10 unit HEN case using MIOCP approach: (a) linear fouling, cleaning cost=£4k and (b) asymptotic fouling, cleaning cost=£4k

variables, such as the temperatures of the hot and cold streams, are fixed within each sub-period, which is not a good approximation for large complex networks with extensive feedback of hot/cold streams. Temperatures in our model are interpreted continuously over time. The difference in the objective for the no-cleaning scenario in the 25 unit HEN is also attributed to the different numerical methods used to the solve the equation sets.

The MIOCP solution yields a saving of 36.2% with an overall cost of £902k, whereas the best reported cost produced by [129] using their BTA algorithm is £917k. The associated schedule has a small number of cleaning actions in common with that of [129]. Similarly to the 4 units over 18 months case study, no pattern is evident in the cleaning actions for the [129] method. More cleaning actions are performed in our schedule (37 *vs.* 34, as shown in Table 4.4.12). Some features in common are that most exchangers are cleaned the same number of times as our schedule and certain exchangers are not cleaned at all (*e.g.* exchanger 10).

Figure 4.4.2 shows the CIT profiles with and without cleaning over time for the case of 36 months of operation. For the cleaning scenario, the profile shown is based on the best objective value using the MIOCP feasible path approach, *i.e.* the schedule in Table 4.4.12. Towards the centre of this profile, there are multiple instances where the CIT steeply declines. This is due to the frequent cleanings (37 as per Table 4.4.12) taking place towards the middle of the operating horizon. Units with the highest fouling rates, *e.g.* 1A to 1D, as well as units which are important in the network (based on their location), result in the most rapid decays in the CIT.

In terms of the solution metrics, out of the 50 different starting points performed, the range of objective values varies by up to £28k, from £902k to £930k. Similarly to previous cases, the RSD about the mean is small (only 0.8%, as shown in Table 4.4.14). The resource usage becomes expensive for the 25 unit HEN case study, requiring 55,243 CPU s (≈15.3 CPU hr) with 38,603 function evaluations in the worst case. This is due to the implementation approach whereby gradients are calculated using finite differences in the MATLAB® optimiser. The computational cost is proportional to the number of finite difference calculations required, with each finite difference calculation requiring a full dynamic system simulation; for larger problems, this leads to a significant computational cost. For example, for the single heat exchanger case under linear fouling for an operating horizon of 24 periods, an average of 11 gradient calculations is required with each one requiring 24 finite difference calculations, as

shown in Table 4.4.3. This accounts for the average computational cost of 30 CPU s. The case of the 25 unit HEN under linear fouling over 36 periods results in a much larger average computational time of 39,611 CPU s (≈11 CPU hr). In this case, there is an average of 31 gradient calculations each of them requiring 900 finite difference calculations (see Table 4.4.14).

Future applications of the multistage optimal control approach will include the reduction of CPU time such that it becomes significantly smaller in larger and more complex networks. This will be achieved through gradient calculation using sensitivity equations. Furthermore, future work will involve extending the range of case studies in HENs to include pressure drop constraints, variable throughput, and optimisation of operating conditions such as the consumption of utilities.

4.5 Critique

This chapter has demonstrated that the HEN cleaning scheduling problem as posed, considering all potential cleaning actions, can be solved for large networks and larger numbers of actions than previously achieved through the recognition of the task as an OCP where the solutions fit bang-bang characteristics. Here, we review which aspects of the scheduling problem, which may be encountered in practice, have been included in the work, and those which have not, in order to identify the scope and potential for further development.

Aspects which have been included are: the distribution of heat duties within networks in response to cleaning actions, and their evolution; linear and nonlinear (asymptotic) fouling behaviour; and constraints on the selection of combination of cleaning actions representing pump-around targets, rundown temperature targets, flash temperature maintenance, *etc.* Aspects presented by other workers which could be included, but require more detailed modelling and therefore solution time, include the choice between two types of cleaning actions [106] and temperature target constraints (*e.g.* desalter temperature, see [60]).

Those not included can be grouped as follows:

(i) Nonlinearity arising from fouling phenomena.

Table 4.4.12: Cleaning schedule for the 25 unit HEN case using MIOCP approach (linear fouling, cleaning cost = £5k).

HEX	Time (months)																																		
	1	2	3	4	5	6	7	8	9	10	11	12	13	14	15	16	17	18	19	20	21	22	23	24	25	26	27	28	29	30	31	32	33	34	35	36
1A												◯					+								+	◯										
1B													+	◯													⊕									
1C												+	◯												◯	+										
1D											◯					+								◯				+								
2A										+					◯								+				◯									
2B														+		◯										⊕										
2C														◯		+								◯			+									
2D												+	◯												⊕											
3A																		+																		
3B															+																					
3C																	+	◯																		
3D																	◯		+																	
4A												◯			+													⊕								
4B									+	◯													◯	+												
5A																	+	◯																		
5B																	◯	+																		
6A										◯				+									◯	+												
6B															+			◯					+													
7A															+		◯																			
7B																		+				◯														
8																			⊕																	
9A																				⊕																
9B												◯	+												◯		+									
10																																				
11																					◯	+														
cleaning actions: + MIOCP approach; ◯ [129] BTA algorithm; ⊕ common																																				

Table 4.4.13: Economic chart for the 25 unit HEN case using MIOCP approach. All values in k£.

Case	MIOCP model		[129] model	
	MIOCP solution (relaxed MIOCP)	[129] OA method solution**	[129] BTA algorithm solution***	[129] OA method solution	[129] BTA algorithm solution
No cleaning, 36 months	1,413	1,413	1,413	Not reported	1,261
Cleaning cost = £5k, 36 months	902 (902*)	[129] unable to solve	917	[129] unable to solve	819

* relaxed MIOCP completely integer, *i.e.* feasible solution. ** [129] OA method solution inputted into MIOCP model.
*** [129] BTA algorithm solution inputted into MIOCP model.

Table 4.4.14: Solution metrics for the 25 unit HEN case using MIOCP approach.

Case	Relaxed MIOCP approach solution				No. of iterations			No. of function evaluations (*i.e.* simulations)			CPU time in s		
	Min in k£	Max in k£	Mean in k£	RSD in %	Min	Max	Mean	Min	Max	Mean	Min	Max	Mean
25 unit HEN, linear fouling, 36 months	902	930	915	0.8	25	43	31	21,944	38,603	28,042	30,670	55,243	39,611

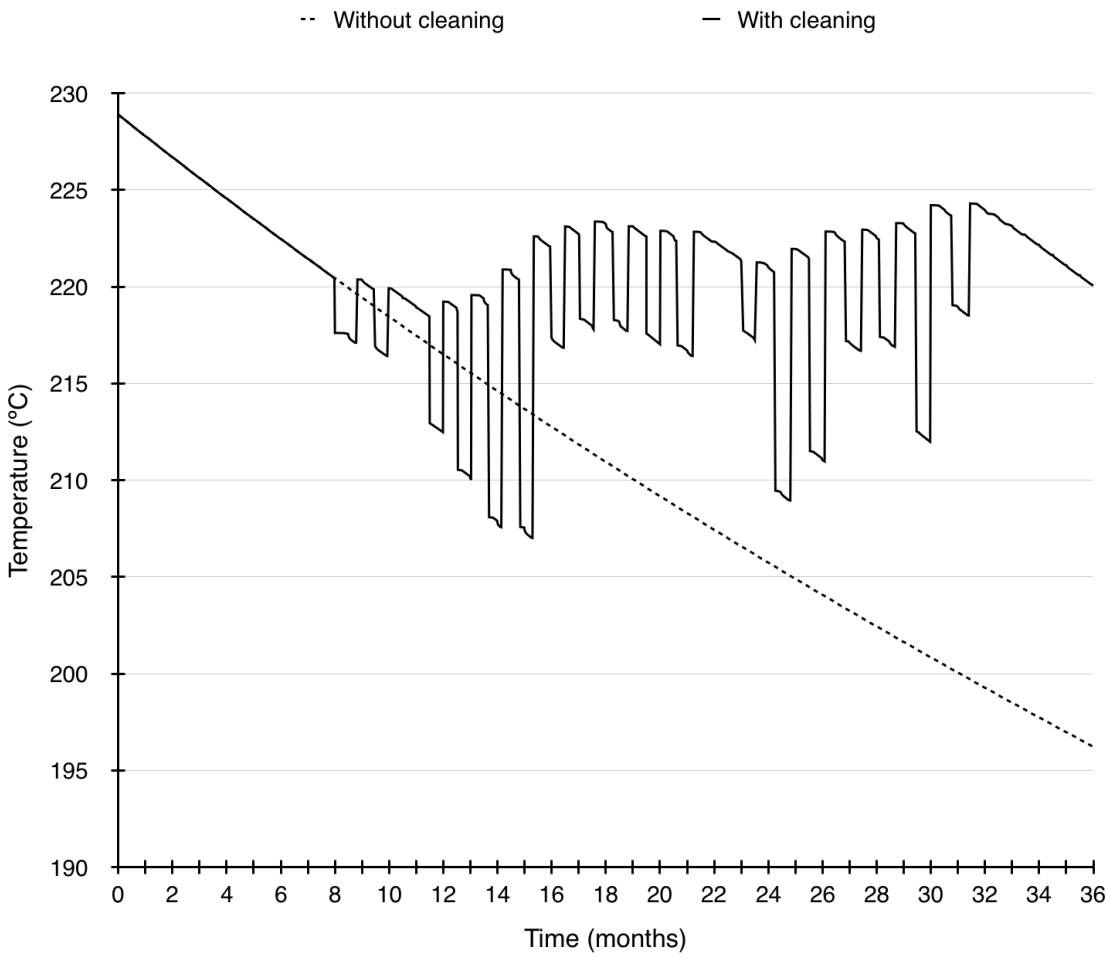

Figure 4.4.2: CIT profile for the 25 unit HEN case using MIOCP approach (36 months)

Fouling rates are known to depend strongly on temperature, and will therefore vary in an exchanger over time as fouling changes the temperature distribution within a network. This level of detailed modelling can be incorporated in greedy [63] and genetic algorithm approaches [114], at the expense of ensuring global optimality, as well as in these total horizon approaches.

(ii) Nonlinearity arising from network dynamics.

Fouling deposits change the pressure drop across a heat exchanger as well as its heat transfer performance. The network model presented here assumes constant stream flow rates, but fouling in practice can give rise to flow redistribution between parallel streams, as well as throughput reduction, as a result of pumping limitations [62, 147]. Changes in flow rate affect both local fouling rates and the objective function, and network models incorporating pressure drop and throughput dynamics have been constructed. The relationship between fouling resistance, pressure drop and throughput is not linear: depending on the network configuration, it can feature a threshold followed by a quasi-parabolic region. The heat duty in the objective function (Equation (1.12)) then contains a product of two variables ($\dot{F}_c$ and CIT), and with an appropriate formulation, this is amenable to the total horizon approach.

(iii) Uncertainty in fouling models and model parameters.

There is a conflict between aspects (i) and (ii) and (iii): the increased model complexity in the former means that multiple condition testing, as required by (iii), will require considerable resource. The desire to account for known, deterministic phenomena must be balanced against the limitations to tractability introduced by those phenomena. From an engineering perspective, the question to be asked is which essential features of the problem must be included, at a suitable level of detail, to achieve the desired outcome.

Aspects (i) and (ii) will require special reformulation to be incorporated in a suitable level of detail for some practical cases with total horizon approaches, such as the one described in this chapter. These approaches are, however, ideally suited for combination with algorithms for designing HENs, as they can generate estimates for expecting optimal operating performance, including considerations of uncertainty in fouling (and operating parameters).

For the case of a crude PHT, the initial network design would yield temperature and flow rate conditions for which fouling rates could be estimated. The operation of this network, with cleaning schedules calculated for a portfolio of fouling rates, could then be quantified (and key exchangers identified for design attention), and this information used to update the design. [141] employed simulated annealing approaches to identify fouling resistant preheat train designs, but did not incorporate cleaning aspects in their consideration of network performance: the MIOCP solution methodology now makes this a tractable problem and one worthy of attention.

Current network complexities may prohibit application of a full optimisation based methodology for the scheduling of cleaning, and hence currently the preference in industry is to use heuristic or greedy approaches. However, the contribution of this chapter is to show that optimisation based methodologies can be general enough to encapsulate both complexity and different operating modes and this will be explored further in future work.

4.6 Chapter summary

An alternative methodology to the solution of the HEN cleaning scheduling problem is presented here by recognising, for the first time, that this optimisation model is in actuality a MIOCP which exhibits bang-bang behaviour. This proves to be an efficient and robust approach and has been compared with 3 different methods: a direct MINLP approach (OA), reformulation of the MINLP to an MILP model, and a stochastic optimisation technique (BTA algorithm).

The multistage optimal control formulation using the feasible path approach does not suffer from failures in convergence and is thus reliable, in contrast to the OA method which fails to produce a solution in larger and more complex networks. The feasible path approach as implemented is shown to be very competitive. Optimal solutions reported here are all bang-bang in the controls. As a result, these particular case studies did not require any heuristic approaches to be applied. In comparison to the classical methods, economic values are similar and in some instances better than those reported in the open literature. The cleaning schedules showed several conventional characteristics, with key exchangers being cleaned more often. However, the allocation of cleaning actions was often not systematic, *i.e.* unpredictable.

This approach is not limited to HENs, and, in the next chapter, the feasible path MIOCP methodology is applied to the optimisation of general scheduling maintenance problems, specifically, scheduling the maintenance of reverse osmosis membrane networks.

Chapter 5

Maintenance scheduling of reverse osmosis membrane networks

This chapter will demonstrate that the methodology used to solve the HEN cleaning scheduling problem can be generalised to other maintenance problems with decaying performance processes. Here, the feasible path MIOCP approach is applied to determine the optimal regeneration schedules for RO module units in seawater desalination and wastewater treatment systems. Similarly to the previous chapter, this scheduling problem is formulated using a discretised interval analysis to allocate cleaning and operating periods whilst keeping the state variables in their original continuous state. An exponential decay in membrane permeability over time is considered. Results show that the feasible path approach can be utilised for other maintenance scheduling problems with declining performance characteristics.

5.1 Introduction and motivation

For the sustainability of human life fresh water is of paramount necessity. The demand for fresh water has increased over the years at a rate of about 1% per year as a function of population growth, economic development, changing consumption patterns, *etc.* In addition, the industrial and domestic demand for water is increasing significantly, with the vast increase in demand for water occurring in developing countries. Moreover, due to climate change, long durations of drought are occurring, with drier regions

becoming ever drier. Currently, approximately 3.6 billion of the world's population live in potentially water-scarce areas at least one month per year. Furthermore, water quality has deteriorated over the years due to pollution, primarily affecting countries with higher population and economic growth, as well as lack of wastewater management systems [136]. Therefore, there is a great need to find alternative affordable sources for fresh water in order to accommodate the current demand not only for human consumption, but also for industrial use.

Desalination is an alternative way to provide a reliable and sustainable source of water due to the large availability of seawater. [137] reported that the Persian Gulf area has the biggest concentration of installed desalination capacity in the world, totalling around 9.2 million megalitres per year, with 96% of this capacity located in the Gulf Cooperation Council (GCC).

Seawater desalination involves the use of RO for the selective purification of seawater from impurities such as ions, molecules and larger particles. This is achieved by raising the hydrostatic pressure of the seawater above its osmotic pressure, thus reversing the flow of seawater due to osmosis through a semi-permeable membrane. The osmotic pressure is determined through the presence of ions such as $Na^{+}$and Cl^{-}. Pure water emerges from the low pressure side, known as the permeate stream, whilst the reject stream, known as brine, exits from the high pressure side. This is shown in Figure 5.1.1 where the symbols F, Co and Pr denote flow rate, concentration and pressure, respectively, while subscripts f, r, perm, b and w indicate the feed, reject, permeate, bulk and wall, respectively. The brine is rejected in a number of ways depending on location, cost and environmental impact [124]:

(i) Discharge back into the sea.

(ii) Disposal to evaporation ponds.

(iii) Injection into deep subsurface wells.

Typically, RO networks feature RO modules, booster pumps and turbines for energy recovery.

Fouling is a major issue in RO networks as it causes the decay in membrane performance over time. Fouling in seawater desalination is caused by precipitation of

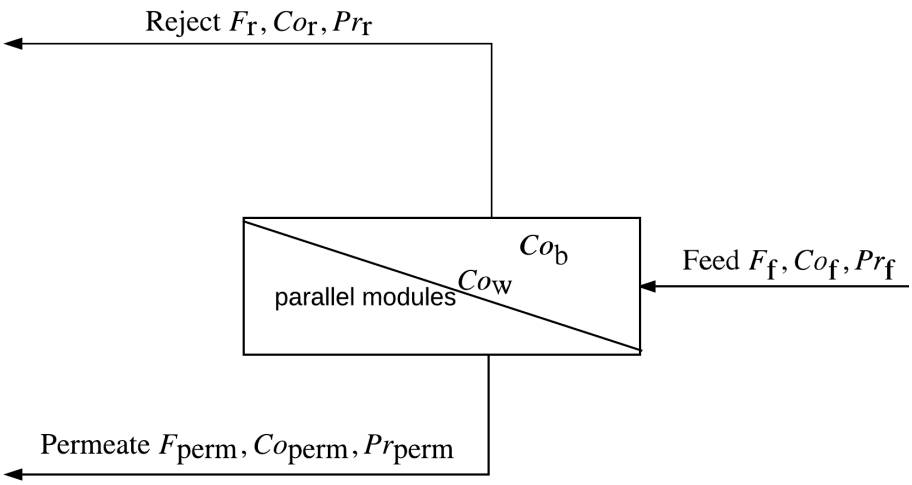

Figure 5.1.1: Reverse osmosis process schematic

insoluble salts and the growth of bacteria on the membrane surface, which results in a restriction to the flow of water through the membrane. Membranes are required to be cleaned in order to regenerate their performance, so product requirements, such as the concentration and flow rate demand are met. Cleaning of membranes can be either mechanically, by introducing a high shear rate at the membrane surface through periodical back-flushing, or chemically, by acid washing and using biocides to remove precipitates and destroy bacterial growth, respectively [135]. This is costly and can constitute a significant proportion of operating costs. Therefore, the economics of the process can be immensely affected by cleaning considerations [124]. Currently, in practice simple greedy heuristics are used to determine the cleaning schedules for reverse osmosis networks (RONs), which results in poor solutions that negatively impact the process economics.

5.2 Problem formulation as an optimal control problem

The effect of fouling is modelled through an exponential decay in the membrane permeability, Km, which is described as in Equation (5.1):

$$Km = Km^0 \exp\left(\frac{-t'}{\tau}\right) \tag{5.1}$$

where Km^0 is the permeability in the initial clean condition, *i.e.* when the membrane is regenerated, τ is the decay constant and t' is the elapsed time since the last cleaning which is defined as follows

$$\dot{t'} = 1 \tag{5.2}$$

The type of membranes considered are DuPont B-10 hollow fibre RO modules and their performance is modelled using the unified RO performance model (UROPM), which was developed by [37] based on the Kimura-Sourirajan analysis (KSA) model for RO desalination plants using a graphical analytical method. This model applies to highly rejecting RO membranes, where $Co_{\mathrm{w}} \gg Co_{\mathrm{perm}}$. Using this model, the permeate flow rate, F_{perm}, can be predicted via Equation (5.3), which features the membrane permeability, Km, the number of RO modules, Nm, the membrane surface area, Sm, the net pressure difference between the bulk operating pressure and that of the permeate streams, ΔPr, the osmotic pressure difference between the membrane wall and permeate streams, $\Delta\pi$, and the membrane correction factor, γ.

$$F_{\mathrm{perm}} = NmSmKm(\Delta Pr - \Delta\pi)\gamma \tag{5.3}$$

The pressure difference across the membrane, ΔPr, is calculated as shown in Equation (5.4):

$$\Delta Pr = Pr_{\mathrm{b}} - Pr_{\mathrm{perm}} \tag{5.4}$$

The bulk pressure can be defined as the arithmetic mean value of the operating pressure on the high pressure side of the membrane, *i.e.* feed and reject streams, as shown in Equation (5.5):

$$Pr_{\mathrm{b}} = \frac{Pr_{\mathrm{f}} + Pr_{\mathrm{r}}}{2} \tag{5.5}$$

Since the permeate operating pressure is much less than that of the bulk operating pressure, Pr_{perm} can be ignored in Equation (5.4) with insignificant loss in accuracy. Therefore, the pressure difference across the membrane can be simplified as

$$\Delta Pr = \frac{Pr_{\mathrm{f}} + Pr_{\mathrm{r}}}{2} \tag{5.6}$$

The pressure drop across the membrane modules depends on the membrane type [152] and is also a function of the membrane permeability. The increase in pressure drop as a result of fouling will need to be compensated by increasing the feed pressure and/or restricting the feed flow rate to meet the product quality requirements. For attaining results that can be compared to published ones from case studies in literature, the pressure drop across the membrane modules is assumed to be constant, as is shown in Equation (5.7):

$$Pr_{\mathrm{f}} - Pr_{\mathrm{r}} = Pr^{drop} \tag{5.7}$$

The osmotic pressure difference across the membrane, $\Delta\pi$, is expressed through Equation (5.8).

$$\Delta\pi = \pi_{\mathrm{w}} - \pi_{\mathrm{perm}} \tag{5.8}$$

where the membrane wall osmotic pressure can be considered to be equal to the bulk osmotic pressure, π_{b}, as under normal operating conditions the membrane wall concentration, Co_{w}, is only 2% greater than the membrane bulk concentration, Co_{b}, [55]. Therefore, π_{w} can be defined as the arithmetic mean value of the osmotic pressure of

the solute on the high pressure side of the membrane:

$$\pi_{\mathrm{w}} = \frac{\pi_{\mathrm{f}} + \pi_{\mathrm{r}}}{2} \tag{5.9}$$

The osmotic pressure,$\pi_{\mathrm{f,r\,or\,perm}}$, of each stream is linearly related to its concentration, via

$$\pi_{\mathrm{f,r\,or\,perm}} = \pi_o Co_{\mathrm{f,r\,or\,perm}} \tag{5.10}$$

In the above equation, π_o is the osmotic pressure constant. Since the membrane wall concentration, Co_{w}, is normally one hundred times bigger than the permeate concentration, Co_{perm}, in highly rejecting membranes, Co_{perm} can be ignored with only minimal loss in accuracy of Equation (5.8). Hence, Equation (5.8) becomes

$$\Delta\pi = \frac{\pi_o(Co_{\mathrm{f}} + Co_{\mathrm{r}})}{2} \tag{5.11}$$

For hollow fibre membranes, ΔPr is not constant due to the small inner radius of the fibres. Therefore, a correction factor, γ, which is a function of membrane geometry must be included in order to take the mean overall driving force through the hollow fibre membrane into account. This factor was developed by [6] and is defined in Equation (5.12).

$$\gamma = \frac{\eta}{1 + \frac{16Km\mu_v r_o l_f l_s}{r_i^4 \rho_{\mathrm{f}}}} \tag{5.12}$$

where μ_v is the dynamic viscosity of water, r_o is the outer radius of the membrane fibre, r_i is the inner radius of the membrane fibre, l_f is the membrane fibre length, l_s is the membrane fibre seal length, ρ_{f} is the density of water at the inlet, and η is the membrane specific coefficient.

The density of the feed, *i.e.* seawater, can be calculated using Equation (5.13):

$$\rho_{\mathrm{f}} = \rho^{water} + 0.001 Co_{\mathrm{f}} \tag{5.13}$$

where ρ^{water} is the density of pure water (1000kg/m^3) and Co_f is the solute concentration measured in ppm.

The membrane specific coefficient, η, is determined via

$$\eta = \frac{\tanh\left[\left(\frac{16Km\mu_v r_o}{r_i^2 \rho_\mathrm{f}}\right)^{0.5}\left(\frac{l_f}{l_s}\right)\right]}{\left(\frac{16Km\mu_v r_o}{r_i^2 \rho_\mathrm{f}}\right)^{0.5}\left(\frac{l_f}{l_s}\right)} \tag{5.14}$$

Using the UROPM, the permeate concentration can be predicted through Equation (5.15).

$$Co_\mathrm{perm} = \frac{DmCo_\mathrm{b}}{Km(\Delta Pr - \Delta\pi)\gamma} \tag{5.15}$$

where Dm is the solute transport parameter and the membrane bulk concentration, Co_b, is assumed to be equal to the arithmetic mean concentration across the high pressure side, Co^{ave}. This assumption holds due to the low permeability of the hollow fibre membranes and the relatively low permeate concentration which leads to an insignificant concentration polarisation [38]. The arithmetic mean concentration across the high pressure side is calculated via

$$Co^{ave} = \frac{Co_\mathrm{f} + Co_\mathrm{r}}{2} \tag{5.16}$$

The flow and material balances within an RO membrane unit can be expressed through Equations (5.17) and (5.18), respectively.

$$F_\mathrm{f} = F_\mathrm{r} + F_\mathrm{perm} \tag{5.17}$$

$$F_\mathrm{f}Co_\mathrm{f} = F_\mathrm{r}Co_\mathrm{r} + F_\mathrm{perm}Co_\mathrm{perm} \tag{5.18}$$

The operating cost (OC) to be minimised is the total operating costs which consists of the sum of the operating costs due to membrane cleaning or regeneration (MOC),

the energy consumption by the booster pump (POC) minus the energy recovered by the turbine (TOC). The general objective is shown in Equation (5.19):

$$OC = MOC + POC - TOC \tag{5.19}$$

A network consisting of four RO membrane units is considered here (units A, B, C and D). Using the time discretisation scheme outlined in Figure (1.2.4) and binary variables $y_{n,p}$, shown in Equation (1.11), the objective can be written as

$$\begin{aligned} OC &= \sum_{p=1}^{NP} \left[C_{FC} \left(1 - y_{A,p} y_{B,p} y_{C,p} y_{D,p}\right) + \sum_{n=1}^{NU} C_{VC} N m_n (1 - y_{n,p}) \right] \\ &\quad + C_{EL} \int_0^{t_F} (KW_b(t) - KW_t(t))\, dt \qquad \forall n, p \end{aligned} \tag{5.20}$$

In Equation (5.20), the membrane regeneration cost consists of: (i) a fixed cost, C_{FC}, for each period in which cleaning occurs despite the number of units (NU) being cleaned in any period, and (ii) a variable cost per module, C_{VC}. Hence, this cost model boosts simultaneous cleaning actions in any given period rather than single cleaning actions. KW_b and KW_t are the electrical duties of the booster pump and turbine, respectively. The same value of electrical power cost, C_{EL}, is associated with both the booster pump and turbine.

The electrical duty of the booster pump is defined as follows

$$KW_b = \frac{F_{b,\text{in}} (Pr_{b,\text{out}} - Pr_{b,\text{in}})}{1000 \eta_{eff} \rho_{b,\text{in}}} \tag{5.21}$$

where $F_{b,\text{in}}$ is the booster pump feed mass flow rate, $Pr_{b,\text{in}}$ is the booster pump inlet pressure, $Pr_{b,\text{out}}$ is the booster pump outlet pressure, η_{eff} is the efficiency of the booster pump, $\rho_{b,\text{in}}$ is the density of seawater at the inlet of the booster pump, and the unit 1000 converts power from W into kW.

The electrical duty of the turbine can be defined as Equation (5.22).

$$KW_t = \frac{F_{t,\text{in}}\eta_{eff}(Pr_{t,\text{in}} - Pr_{t,\text{out}})}{1000\rho_{t,\text{in}}} \tag{5.22}$$

where $F_{t,\text{in}}$ is the turbine feed mass flow rate, $Pr_{t,\text{in}}$ is the turbine inlet pressure, $Pr_{t,\text{out}}$ is the turbine outlet pressure, η_{eff} is the efficiency of the turbine, $\rho_{t,\text{in}}$ is the density of brine at the inlet of the turbine, and the unit 1000 is used to convert the power from W into kW. In order to obtain results which can be compared with those in the open literature, the pump and turbine are assumed to feature the same efficiency value.

The problem is reformulated as a MIOCP in which, for a network of membranes, the membrane permeability of membrane unit n is calculated by rewriting Equation (5.1) as follows

$$Km_n = Km_n^0 \exp\left(\frac{-t'_n}{\tau}\right) \qquad \forall n \in NU \tag{5.23}$$

where the elapsed time since the last cleaning action for membrane unit n is equivalent to

$$\dot{t}'_n = y_{n,p} \qquad \forall n \in NU,\, p \in NP \tag{5.24}$$

As the RO membrane network optimisation is started from a clean condition, the initial membrane permeability is Km_n^0 for the first period for all membranes. In consecutive periods, the initial membrane permeability is related to the membrane permeability at the end of the previous period by integration in time, and this value is allowed to be reset through a junction condition when regeneration occurs. This junction condition for the defined exponential fouling model is presented in Equation (5.25), where the elapsed time since the last cleaning is reinitialised based on the control variable value.

$$t'_n(t_p^{\text{initial}}) = y_{n,p}t'_n(t_{p-1}^{\text{end}}) \qquad \forall n \in NE,\, p = 2,\ldots NP \tag{5.25}$$

The flow of the permeate is rewritten from Equation (5.3) as

$$F_{\text{perm},n} = Nm_n SmKm_n(\Delta Pr_n - \Delta\pi_n)\gamma_n \qquad \forall n \in NU \tag{5.26}$$

where the pressure difference across the membrane is

$$\Delta Pr_n = \frac{Pr_{\text{f},n} + Pr_{\text{r},n}}{2} \qquad \forall n \in NU \tag{5.27}$$

the osmotic pressure difference across the membrane is

$$\Delta\pi_n = \frac{\pi_o(Co_{\text{f},n} + Co_{\text{r},n})}{2} \qquad \forall n \in NU \tag{5.28}$$

the membrane geometric correction factor is

$$\gamma_n = \frac{\eta_n}{1 + \frac{16Km_n\mu_v r_o l_f l_s}{r_i^4 \rho_{\text{f},n}}} \qquad \forall n \in NU \tag{5.29}$$

the membrane specific coefficient is

$$\eta_n = \frac{\tanh\left[\left(\frac{16Km_n\mu_v r_o}{r_i^2\rho_{\text{f},n}}\right)^{0.5}\left(\frac{l_f}{l_s}\right)\right]}{\left(\frac{16Km_n\mu_v r_o}{r_i^2\rho_{\text{f},n}}\right)^{0.5}\left(\frac{l_f}{l_s}\right)} \qquad \forall n \in NU \tag{5.30}$$

and the density of the water at the feed is

$$\rho_{\text{f},n} = \rho^{water} + 0.001Co_{\text{f},n} \qquad \forall n \in NU \tag{5.31}$$

The permeate concentration for unit n is calculated by rewriting and combining Equations (5.15) and (5.16) as

$$Co_{\text{perm},n} = \frac{Dm(Co_{\text{f},n} + Co_{\text{r},n})}{2Km_n(\Delta Pr_n - \Delta\pi_n)\gamma_n} \tag{5.32}$$

The flow and material balances for membrane unit n are calculated by rewriting Equations (5.17) and (5.18), respectively, as

$$F_{\mathrm{f},n} = F_{\mathrm{r},n} + F_{\mathrm{perm},n} \qquad \forall n \in NU \tag{5.33}$$

$$F_{\mathrm{f},n} Co_{\mathrm{f},n} = F_{\mathrm{r},n} Co_{\mathrm{r},n} + F_{\mathrm{perm},n} Co_{\mathrm{perm},n} \qquad \forall n \in NU \tag{5.34}$$

Operational constraints are added such that cleaning in consecutive periods is not permitted. This is expressed in Equation (5.35):

$$y_{n,p} + y_{n,p-1} \geq 1 \qquad \forall n \in NU,\, p = 2,\ldots,NP \tag{5.35}$$

Furthermore, all membrane units are set to be online, *i.e.* operating, during the first period of the horizon.

$$y_{n,p} = 1 \qquad \forall n \in NU,\, p = 1 \tag{5.36}$$

Other operational constraints are added based on the product quality requirements, *e.g.* overall flow rate and concentration of permeate stream leaving the membrane network. This is shown in Equations (5.37) and (5.38):

$$F_{perm} > F_{perm,\min} \tag{5.37}$$

$$Co_{perm} < Co_{perm,\max} \tag{5.38}$$

5.3 Similarities with HEN maintenance scheduling problems

This section highlights the similarities between the HEN maintenance scheduling problems and the RO membrane network maintenance problem.

Both of the aforementioned problems feature decaying performance processes. The HEN maintenance scheduling problem consists of a linear/asymptotic fouling model in which the overall heat transfer coefficient declines over time. Similarly, the RO membrane network maintenance scheduling problem consists of an exponential fouling model in which the membrane permeability decays over time.

Additionally, in these scheduling maintenance problems a discretised binary control variable, $y_{n,p}$, is defined where a decision is made for which heat exchanger unit or RO membrane unit, n, is cleaned and in which period, p, cleaning takes place. Fouling is not the only necessary justification for cleaning of units; other reasons include remaining within operational limitations and achieving product quality requirements. For HEN maintenance scheduling problems this includes temperature targets, pump-around targets, among others, whereas for the RO membrane network maintenance scheduling problem there is a minimum required product flow rate and also a maximum acceptable concentration for this product stream.

The most important feature that is similar in these problems is the appearance of the control in relation to the system. In both of these problems, the control appears linearly in the system thereby leading to bang-bang solutions. Thus, like the HEN maintenance scheduling problems, the RO membrane network maintenance scheduling problem can be solved as a MIOCP using a sequential feasible path approach. Assuming not many singular arcs occur in the relaxed MIOCP optimal solution, a simple rounding up scheme can be used as was performed in the HEN maintenance scheduling problems.

5.4 Problem solution methodology and implementation

Similarly to the HEN maintenance scheduling problems in Chapter 4, the implementation is performed in MATLAB® R2016b with its Optimisation Toolbox™ and Parallel Computing Toolbox™ [134]. The implementation details are repeated here from Section (4.3) for the sake of clarity.

The MATLAB® code works as a standard multi-period OCP solver using the feasible path approach (*i.e.* sequential approach) by linking together the ODE solver ode15s

with the optimiser fmincon. The default settings for ode15s are used, with absolute tolerance of 10^{-6} and relative tolerance of 10^{-3}. The optimiser fmincon is used with the SQP algorithm option whilst keeping the remaining settings at their default values: constraint, optimality and step tolerances of 10^{-6} using a forward finite difference scheme for the estimation of gradients. Gradient evaluations conducted via finite differences are costly and require repeated simulations of the dynamic process model.

Additionally, since this problem is non-convex, 50 runs with different reasonable starting points, which are generated using the randsample function in MATLAB®, are performed and the best solution is reported. The implementation is performed on a 4GHz Intel Core i7, 16 GB RAM iMac (2014 model) running on macOS Sierra. Parallelisation of a loop of 50 runs is performed using the parfor loop in MATLAB®. For cases where singular arcs appear in the control, the rounding up scheme is employed.

5.5 Case study description

In this section, the case study for the scheduling of cleaning actions in RO membrane networks is introduced along with its associated data.

A RO membrane network from [124] is considered. The network compromises 94 Du Pont B-10 RO modules arranged in 4 units, n, where $n \in NU$ ($NU = \{A, B, C, D\}$) in a 2 by 2 layout, as shown in Figure 5.5.2. The intake seawater salinity is assumed to be constant at 35,000ppm and the input flow rate is fixed at $48\text{m}^3/\text{hr}$. Likewise, the booster pump pressure is fixed at 62atm. The modules in each of the units are in a parallel configuration and the number of modules per unit is $Nm_n = \{27, 27, 20, 20\}$. The number of periods considered is $NP = 37$ for this network.

For this case, the cleaning mode considered is perfect cleaning, the number of days of operation, $\Delta t^{\text{OP}} = 10\,\text{days}$, and no downtime for regeneration is considered, so $\Delta t^{\text{CL}} = 0\,\text{days}$. Practically, this is not valid as imperfect cleaning, as well as downtime for cleaning, will need to be considered. In the case where downtime for cleaning is taken into account, the product quality requirements must be relaxed as the network is unlikely to meet product specifications. This is because, when a unit is taken offline, the permeate flow rate would be significantly reduced. Hence, the product flow rate requirements will need to be reduced during any cleaning sub-period.

Furthermore, the feed flow rate and operating pressure will need to be manipulated between defined limits in order to maintain the required quality and flow rate. For the purpose of achieving results that can be compared to published ones from case studies in the open literature, perfect cleaning is assumed, the feed conditions are kept fixed and no downtime is considered. To eliminate downtime, Equation (5.24) is modified to Equation (5.39):

$$i' = 1 \qquad \forall n \in NU \tag{5.39}$$

In this study, both the density, ρ, and dynamic viscosity, μ_v, were assumed to be constant instead of taking the average between the feed and brine solutions. This decision was made as their values were not expected to vary by much. [124] showed that there is an error of less than 7% when these parameters are kept constant for a two-stage RO network. Furthermore, this reduces the nonlinearity of the model as the membrane geometry correction factor, γ, becomes practically constant, and only changes slightly with Km. Input data, solute characteristics, process constraints and cost parameters for the investigated case study are shown in Table 5.5.1. Constraints shown in Equations (5.35) to (5.38) are imposed, where the network has to produce a minimum of 21.6m^3/hr of product water with salinity below 570 ppm at all times. In addition, a lower bound on the permeability, Km_n, is imposed such that the permeability is not allowed to fall below 1.2×10^{-10} kg/sN for each of the units at all times.

5.6 Computational results and discussion

In this section, computational results for the MIOCP feasible path technique on the case study shown in Section 5.5 are presented. The best solution obtained is compared in the schedule shown in Table 5.6.2 with the schedule obtained by [124] using an MINLP formulation. [124] solved this scheduling problem using a discrete and continuous optimiser, DICOPT++ under the GAMS environment. Their optimisation solution technique is based on an OA/ER approach.

In the economic comparison, we fixed the solution obtained by [124] and evaluated it using our model. This is shown in Table 5.6.3 where the best obtained solution is reported for the case study. Solution metrics, which include the worst cost out of

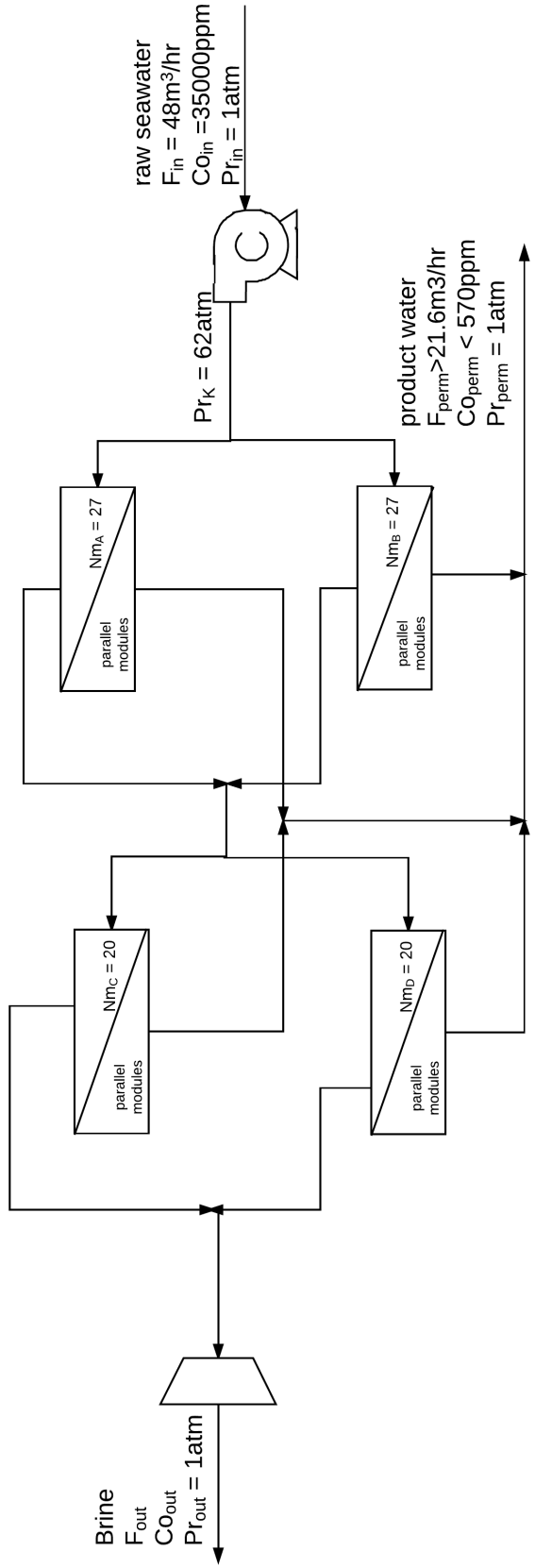

Figure 5.5.2: 4 unit reverse osmosis membrane network case. Adapted from [124].

Table 5.5.1: Solute characteristics, process constraints, membrane characteristics and cost parameters for the RO membrane network maintenance scheduling problem. Adapted from [124].

Parameter	Value
Solute characteristics:	
π_o [atm/ppm]	7.85×10^{-4}
ρ_{f} [kg/m^3]	1035
μ_v [kg/ms]	1.08×10^{-3}
Process constraints:	
$F_{perm,\min}$ [m^3/hr]	21.6
$Co_{perm,\max}$ [ppm]	570
Pr^{drop} [atm]	0.22
Membrane characteristics:	
Km_n^0 [kg/sN]	3×10^{-10}
Dm [kg/m^{2}s]	4×10^{-6}
Sm [m^2]	152
τ [day]	328
l_f [m]	0.75
l_s [m]	0.075
r_o [m]	50×10^{-6}
r_i [m]	21×10^{-6}
Cost data:	
C_{EL} [$/kWh]	0.07
C_{FC} [$]	10,000
C_{VC} [$]	450
η_{eff}	0.65

50 runs of different starting points, mean cost, RSD about the mean value, number of iterations and function evaluations, are reported in Table 5.6.4. In addition, the best and worst resultant computational time per run is reported in this table. The optimum profiles of the membrane permeability, total permeate flow rate and total permeate concentration are presented in Figures 5.6.3, 5.6.4 and 5.6.5, respectively.

Due to the non-convexity of this problem, a number of local solutions with different schedules are produced. For the 50 runs performed, the local solutions produced are nearly bang-bang and in some case entirely bang-bang, in which the relaxed solution is completely integer. The best solution is produced during the first run where only 4 decision variables out of 148 are fractional. The relaxed MIOCP and the MIOCP results for the best solution are \$197k and \$196k, respectively, as shown in Figure 5.6.3. It is worth noting that, in this case, rounding of the relaxed MIOCP results in an even better solution in which the cost is reduced by \$1k.

Our best solution is the same as that produced by [124] in terms of not only economic value but also the cleaning schedule, as shown in Table 5.6.2, where all cleaning actions are common. The optimal schedule consists of a total of 7 cleaning actions, where membrane units A, B and C are cleaned twice throughout the horizon while membrane unit D is cleaned only once after 200 days of operation. Membrane unit C is also cleaned after 200 days of operation as this model encourages simultaneous cleaning actions.

Generally, cleaning actions are centralised towards the middle of the operating horizon, where the first cleaning action does not take place until after 100 days of operation and the final cleaning action takes place after 310 days of operation. This is because, like the HEN maintenance scheduling problem, at the start of the operating horizon there is little motive to clean a relatively clean unit and at the end of the horizon there is insufficient time to recover losses or costs after cleaning. Cleaning only occurs when fouling and process constraints force cleaning, in order to maintain operability of the network. For example, the permeability of unit D reaches a low value, close to 1.6 kg/sN at 200 days, as shown in Figure 5.6.3. Consequently, unit D is cleaned in the next period to restore its permeability to a clean condition, bringing the total flow rate of the permeate stream from 22m^3/hr up to 23.8m^3/hr (see Figure 5.6.4) and reducing the salinity from 459ppm down to 433ppm (see Figure 5.6.5).

At the start of operation, due to the high permeability of the membrane units, a large

permeate flow rate with low permeate salinity is produced, resulting in a total permeate flow rate and concentration of 24.7 m^3/hr and 435 ppm, respectively. This is shown in Figures 5.6.4 and 5.6.5, respectively. With the continuous decay in the membrane performance due to exponential fouling, the performance of the network deteriorates over time, producing poorer permeate quality, which has a higher salinity and causes a reduction in the product water flow rate from the first stage units, *i.e.* A and B. Thus, this results in a higher flow rate to units in the second stage, *i.e.* units C and D, slightly increasing the product water flow rate from the second stage. Consecutive cleaning of the membrane units can restore their performance, as shown in Figure 5.6.3, where the membrane permeability is restored to a clean state (3×10^{-10} kg/sN), and as shown in Figure 5.6.4, where the total permeate flow rate produced is increased, as well as in Figure 5.6.5, where the total permeate salinity is reduced to meet the product quality requirements.

Similarly to our approach, [124] solved the problem by running multiple scenarios through varying the initial conditions and selecting the solution that yields the lowest objective function. However, [124] did not report how many runs were performed and important details, such as the worst solution, mean value of the solutions, RSD, *etc.*, were also not reported. In terms of the solution metrics, out of the 50 different starting points performed, the range of objective values varies by up to \$50k from \$197k to \$247k with a mean value of \$224k, as shown in Table 5.6.4. The RSD about the mean is larger than that of the HEN maintenance scheduling problems but still relatively small (6.4% as shown in Table 5.6.4).

The resource usage per run varies significantly in this case study, requiring from 383 CPU s (≈6.4 CPU min) on a 2014 model iMac, with 290 function evaluations in the best case scenario, up to 11,982 CPU s (≈3.3 CPU hr), with 4,502 function evaluations in the worst case. [124] only reported the convergence time associated with their best run which was 2,073 CPU s (≈35 CPU min) on a SunSPARC 10 workstation in 2002. As per Moore's law [91], this reported convergence time corresponds to ≈32 CPU s in 2014. Thus, the resource usage is more expensive in the MIOCP approach than that reported by [124] using the OA/ER method. This is because, as explained in the previous chapter, optimisation gradients are calculated using finite differences in the MATLAB® fmincon optimiser, whereas these are computed using sensitivity equations in the GAMS DICOPT++ optimiser, which take less computational time. From our results, the variation in CPU time between the best and worst cases is by

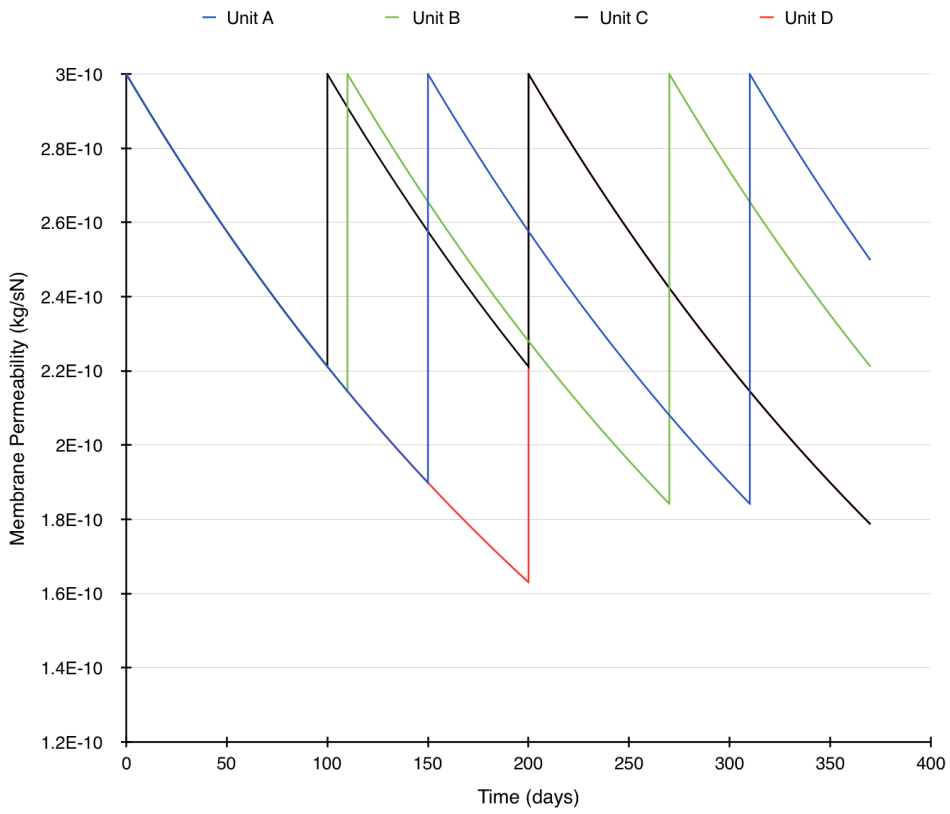

Figure 5.6.3: Optimum operating profiles of the membrane permeability for the RO membrane network.

more than 30-fold, therefore practically it is insufficient to only report the convergence time for the best solution or that associated with a limited number of runs.

5.7 Chapter summary

In this chapter, it has been shown that the feasible path MIOCP approach is not limited to HEN maintenance scheduling problems, and can be generalised to other maintenance scheduling problems with decaying performance, where the control appears linearly in the system. A 4 unit RO membrane network which undergoes exponential fouling has been modelled and the schedule of cleaning actions has been optimised. The solution through this approach was compared with that of an OA/ER method and economic results were shown to be similar. The approach put forward in this thesis proves to be a robust and reliable one, in which the model runs automatically

Table 5.6.2: Cleaning schedule for the RO membrane network maintenance scheduling problem using MIOCP approach.

Times (days)	Membrane Unit			
	A	B	C	D
10				
20				
30				
40				
50				
60				
70				
80				
90				
100				
110			⊕	
120		⊕		
130				
140				
150				
160	⊕			
170				
180				
190				
200				
210			⊕	⊕
220				
230				
240				
250				
260				
270				
280		⊕		
290				
300				
310				
320	⊕			
330				
340				
350				
360				
370				
No. of cleaning actions	2	2	2	1
cleaning actions: + MIOCP approach; ◯ [124]OA/ER approach; ⊕ common				

Table 5.6.3: Economic chart for the RO membrane network maintenance scheduling problem using MIOCP approach. All values in k$

Case	MIOCP model		[124] model
	MIOCP solution (relaxed MIOCP)	[124] OA/ER approach solution*	[124] solution
4 units, exponential fouling, 370 days	196 (197)	196	197

* [124] OA/ER approach solution inputted into MIOCP model

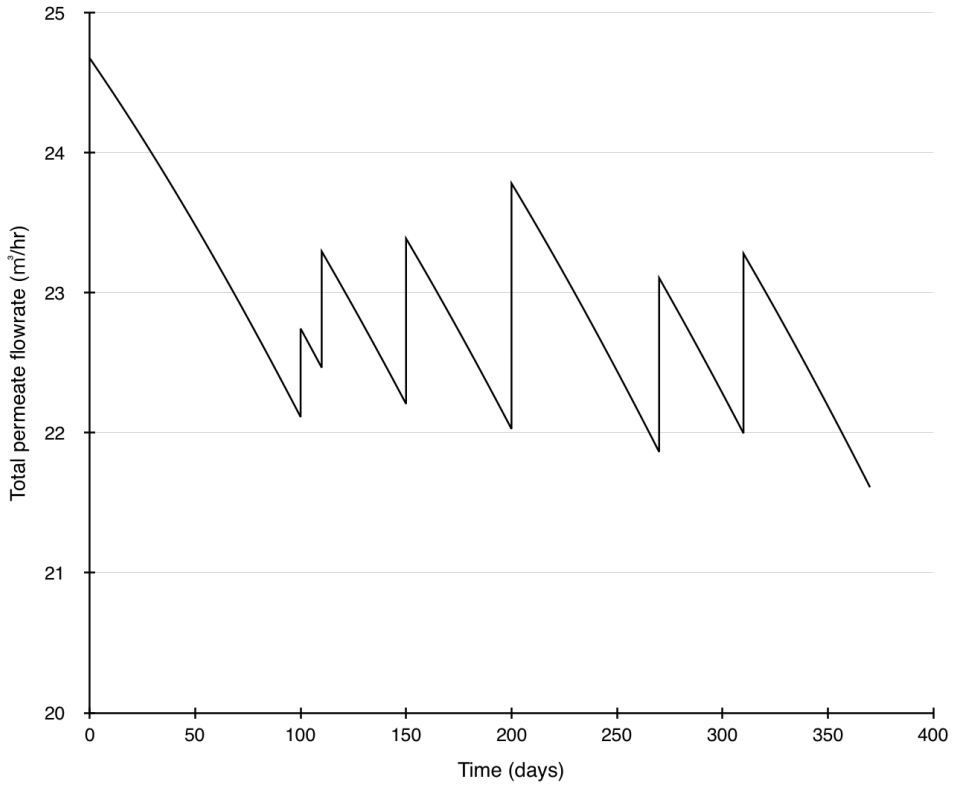

Figure 5.6.4: Optimum operating profile of the total permeate flow rate for the RO membrane network.

Table 5.6.4: Solution metrics for the RO membrane network maintenance scheduling problem using MIOCP approach.

Case	Relaxed MIOCP approach solution				No. of iterations			No. of function evaluations (*i.e.* simulations)			CPU time in s		
	Min in k$	Max in k$	Mean in k$	RSD in %	Min	Max	Mean	Min	Max	Mean	Min	Max	Mean
4 units, exponential fouling, 370 days	197	247	224	6.4	1	30	8	290	4,502	1171	383	11,982	3,211

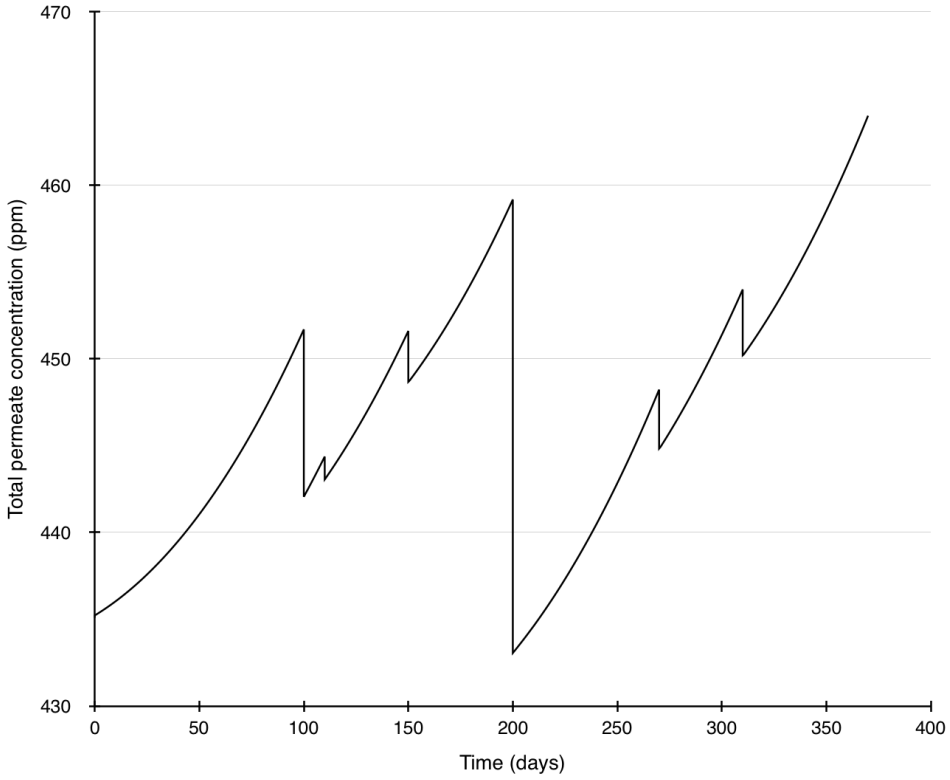

Figure 5.6.5: Optimum operating profile of the total permeate concentration for the RO membrane network.

with ease.

The optimal solutions for the RO membrane network maintenance scheduling problem are nearly bang-bang. Although this case study required the application of heuristic approaches, the resulting MIOCP solution is very close to the relaxed one and in some cases even better.

In the next chapter, an approach for the optimisation of the cleaning schedule in HENs subject to fouling considering the impact of uncertainty is presented.

Chapter 6

Scheduling maintenance operations with parametric uncertainty in HENs

In this chapter, a parametric uncertainty version of the MIOCP formulated models from Chapter 4 is developed and applied to crude distillation unit PHTs situated in oil refineries. The sensitivity of the overall cost due to fouling to the fouling rate parameters, overall heat transfer coefficient in the clean condition and fuel cost are examined. A multi-scenario approach coupled with a feasible path MIOCP approach is considered for the optimisation of the cleaning schedule with parametric uncertainty. This is implemented in two case studies: (i) a network consisting of 10 heat exchangers considering both linear and asymptotic fouling and (ii) a larger network of 25 units with linear fouling. Results show that for some parameters even small changes in value can have a large impact on the overall cost due to fouling. Therefore, it is vital to take parametric uncertainty into account during optimisation of cleaning schedules for HENs.

6.1 Parametric uncertainty in HEN maintenance scheduling problems

The performance of heat exchangers is directly impacted by uncertainties in data. Heat exchangers are typically over-designed by 70–80%, with 30–50% of which being

attributed to fouling [3]. Fouling is subject to many parameters with inherent uncertainty, which can be systematic (*e.g.* the form of the fouling model, and whether it should incorporate deposit ageing [105]) and quasi-random (*e.g.* variation in processed fluid composition over time [130]). Extending lab results to real systems is not straightforward.

Recently, [143] reviewed the progress in quantitative fouling models for crude oil fouling. They reported three areas where systematic uncertainty arises in models for predicting the fouling rates in crude oil:

(i) The fouling models are semi-empirical and the relationship to crude oil composition and characteristics has yet to be established, so one cannot predict, for example, whether linear or asymptotic fouling will be observed in a given unit.

(ii) Fouling rates for complex fluids such as crude oil are rarely studied under controlled conditions. In practice, many operators use fouling models constructed from reconciliation and interpretation of plant fouling data. These are subject to uncertainties in measurement and calculation, so the accuracy of the fouling rate data is low.

(iii) The relationship between fouling rates and crude composition (*e.g.* source, blending) is not currently known. In the majority of applications there is variation in the fouling rate over time, due to changes in the crude being processed. This is one of the reasons why plant fouling data, used to quantify fouling model parameters, contain noticeable scatter and variation.

These areas mean that, in practice, scheduling calculations must be able to consider a range of likely fouling rates.

Heat exchanger design is highly reliant on physical properties, *e.g.* density, specific heat capacity, viscosity, thermal conductivity, *etc.* for estimating heat transfer coefficients and therefore performing overall heat transfer coefficient calculations. Such physical properties are susceptible to a certain degree of uncertainty due to measurement errors, extrapolation and interpolation errors, estimation errors, *etc.* Furthermore, in the standard methods for heat exchanger analysis, such as the NTU-effectiveness method, the overall heat transfer coefficient is assumed to be constant and uniform throughout the heat exchanger. In practice, this coefficient changes along the length of the heat

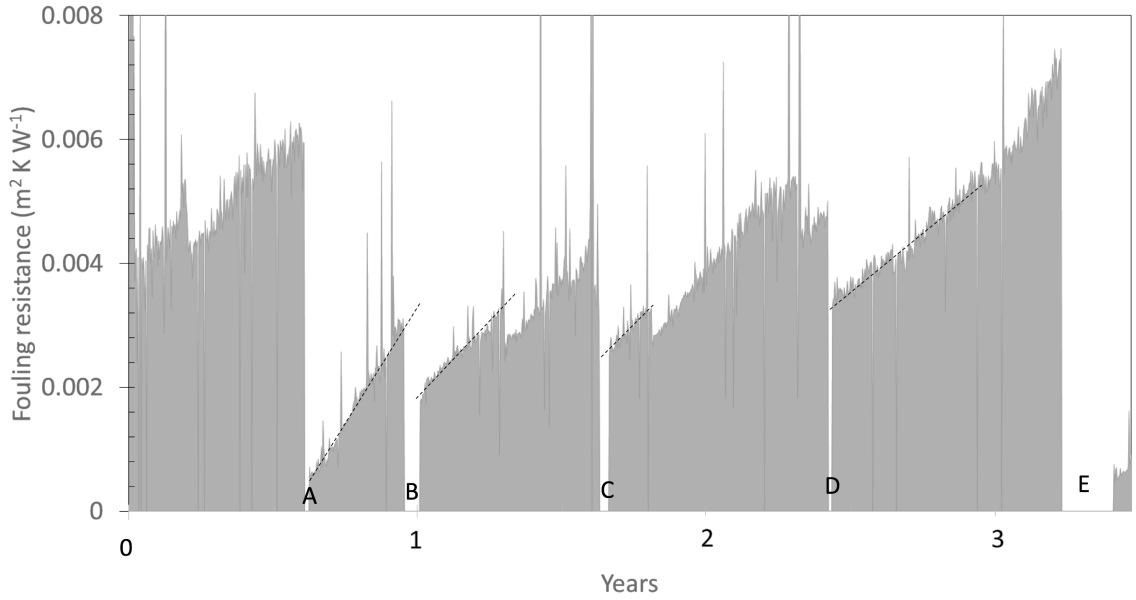

Figure 6.1.1: Evolution of fouling resistance in a refinery heat exchanger over a 40 month period. Letters indicate when the unit was cleaned. Rigorous cleaning was performed at A and E: less intensive cleaning at B, C and D. Dashed lines show simple linear fits to data following cleaning. Reproduced from [59].

exchanger and is strongly dependent on a number of factors including the fluid thermophysical properties and the flow Reynolds number. In a viscous liquid heat exchanger, the heat transfer coefficient can vary by 10-fold. This occurs when the flow pattern encompasses laminar, transition and turbulent regions on one side, which leads to the variation of the overall heat transfer coefficient [126]. [109] highlighted that experimental and/or empirical data for heat transfer coefficients are usually subject to large uncertainties of over 50% for overall heat transfer coefficients.

These features are evident in Figure 6.1.1, which shows a time series of the fouling resistance calculated for an industrial shell-and-tube heat exchanger in fouling service. The instantaneous fluctuations arise from the uncertainties in measurement, data, collection and calculation. Pseudo-linear trends are evident between each cleaning event, but the gradient, *i.e.* the fouling rate, differs in each case.

The scheduling of cleaning actions in HENs is highly dependent on fouling model parameters and Figure 6.1.1 demonstrates how there can be considerable uncertainty in these inputs.

Although general scheduling problems with uncertainty have been considered by sev-

eral authors [35, 42, 58, 70, 83, 125], there has been limited work on HEN cleaning scheduling with uncertainty. A search through the literature found a few publications, such as [76, 78]. [76] extended a reformulated MILP model for the planning of HEN cleaning in chemical plants to include uncertainty in the data. Although the fouling coefficients, cleaning costs, plant turnaround horizons and the processing of different crudes at different times are uncertain parameters, they only considered uncertainty in energy prices. [76] used the standard two-stage stochastic programming model [7, 24] and constructed the scenarios through sampling energy prices. The sampling was done assuming normal distributions, with increasing standard deviation for similar months of the year as the time horizon increases. They compared their stochastic solutions to deterministic and heuristic solutions and discussed financial risk management options. [78] studied the effects of uncertainty in parameters, including the future fuel price used in the furnace, the change of feedstock and the fouling rate of the crude processed, on the cleaning schedule. They used a reformulated MILP model coupled with a multi-scenario based approach and showed how the optimal cleaning schedule can vary when different parameters are considered uncertain simultaneously. Furthermore, their results showed how the model helped determine the best cleaning schedule to apply when risk is involved.

6.2 Solution procedures for the HEN maintenance scheduling problem with parametric uncertainty

In this section, an overview of the different mathematical approaches used to describe uncertain parameters is given. This is followed by a literature review of the methodologies commonly used for solving optimisation problems with uncertainty.

Several methods have been employed to describe uncertain parameters within optimisation models. Three of these methods were reviewed by [79]:

(i) Bounded form, which is applicable in cases where there is insufficient data to make use of probabilistic models to describe the uncertain parameters of the probability distribution. Here, the uncertain parameters, x, are described by an

interval $x \in [x_{\min}, x_{\max}]$, which describes the range of all possible realisations of the uncertain parameters. $x_{\min}$ and $x_{\max}$ can be determined based on experimental or historical data. In addition, market considerations can be taken into account to determine these bounds.

(ii) Probabilistic approach, in which uncertainties are characterised by probabilities associated with events. The probability distribution of the uncertain parameter can be described by its probability distribution function if it is random and discrete. However, if the uncertain parameter is random and continuous, the probability distribution can be described by its probability density function, *i.e.* the probability that the uncertain parameter falls within a particular interval.

(iii) Fuzzy description, in which a fuzzy set, based on possibility theory, is defined. This set is a function which measures the degree of membership to a set. A high value of the membership function implies a high possibility, whereas a low value implies a poor possibility. Fuzzy sets are particularly useful for the description of uncertain parameters in situations where probabilistic data are not readily available. [4] highlighted that the use of the fuzzy description for uncertain parameters is advantageous over the probabilistic approach as complex integration schemes, which are needed for the continuous probabilistic models, are not required. In addition, they highlighted that unlike fuzzy sets, discrete probabilistic models need a large number of scenarios. Thus, the solution for these models requires a high computational expense.

Numerous authors have reviewed the variety of approaches available for dealing with uncertainty in optimisation problems, including stochastic programming with fixed recourse, robust optimisation methods, fuzzy programming methods, sensitivity analysis, parametric programming, among others [4, 21, 30, 49, 79, 119].

6.2.1 Stochastic programming with fixed recourse

Stochastic based programming methods are programs in which data may be considered uncertain. Here, the deterministic model is transformed into a stochastic model in which probabilistic distributions are used. The uncertainties are treated as stochastic variables. Stochastic optimisation has an important assumption, *i.e.* the true probability distribution of uncertain data must be known or estimated [47].

The classical two stage stochastic based approach with fixed recourse was developed by [7, 24]. Recourse based approaches are those in which some decisions or recourse actions can be taken after uncertainty is disclosed. In the two stage stochastic based approach with fixed recourse, decision variables are partitioned into two stages, where the first stage decision variables are those that have to be taken prior to the experiment, *i.e.* prior to the actual realisation of the uncertain parameters. The second stage decision variables, also known as recourse decision variables, are those that can be taken after the experiment, *i.e.* after the actual realisation of the uncertain parameters [13]. The second stage decision variables can be interpreted as corrective measures or recourse against any infeasibilities arising due to a particular realisation of uncertainty. They can also be interpreted as an operational level decision following a first stage decision and the uncertainty realisation. Furthermore, the two stage formulation can be readily extended to a multistage formulation [119].

Two stage and multistage stochastic programming approaches with fixed recourse have been applied to several areas in research and practice, such as the design of distributed energy systems under uncertainty [87, 146], scheduling of energy systems under uncertainty [88, 99], multi-activity tour scheduling under uncertainty [113], lot sizing and scheduling under uncertainty [58], petroleum refinery planning under uncertainty [71], blood supply chain planning under uncertainty [149], among others.

6.2.2 Robust optimisation methods

Robust optimisation, which was developed by [96], is a proactive approach, whereby goal programming formulations are integrated with a scenario based description of problem data. This method generates a series of solutions that are progressively less sensitive to realisations of the model data from a scenario set. Unlike stochastic programming, robust optimisation involves the introduction of a penalty function for dealing with uncertain data. The penalty function is used to penalise violations of the control constraints under some of the scenarios. The control constraints are those that involve the control decision variables, *i.e.* the variables that are subject to adjustment once the uncertain parameters are realised.

The robust optimisation model takes a multi-criteria objective, where the first term measures optimality robustness and the second term, which is the penalty term, is a

measure of model robustness. The solution to the robust optimisation model is defined as solution robust and model robust if it remains close to optimal for all scenarios of the input data and if it remains almost feasible for all scenarios, respectively. The multi-criteria objective involves a goal programming weight, which is introduced as a product of the penalty function and is used to derive a spectrum of answers that trade-off solution for model robustness [96]. Robust optimisation methods are advantageous compared to stochastic programming as no assumptions are needed regarding the underlying probability distribution of the uncertain data. Furthermore, it provides a way of incorporating different attitudes toward risk [79].

Robust optimisation methods have been used in many applications, including: (i) classical logistics problems, such as the capacitated vehicle routing problem with demand uncertainty [132] and the robust traveling salesman problem with interval data [90], (ii) supply chain problems, *e.g.* the determination of a joint optimal bundle of price and order quantity for a retailer in a two stage supply chain under uncertainty of parameters in demand and purchase cost functions [80], (iii) scheduling problems, such as in the work of [145], who used robust optimisation and considered passenger choice behaviours and uncertain market demands in inter-city bus scheduling models, and in the work of [54], who considered robust scheduling and robustness measures for the discrete time/cost trade-off problem, *etc.*

6.2.3 Fuzzy programming methods

Fuzzy set theory can be used to describe uncertainties in parameters in cases where the information for describing the uncertainties in parameters in terms of probabilistic models is unavailable. Fuzzy programming can be applied to optimisation problems with uncertainty. In fuzzy programming, the random parameters and constraints are considered as fuzzy numbers and fuzzy sets, respectively. A certain level of constraint violation is allowed and the degree of satisfaction of the constraint is described by the membership function of the constraint. Here, the objective functions are treated as constraints, in which the lower and upper bounds of these constraints represent the decision makers' expectations [79].

Fuzzy programming approaches have been applied to scheduling problems with uncertainty. For example, [92] applied fuzzy programming to a multi-objective patient

appointment scheduling problem with uncertainty in a large hospital. The main aims of this scheduling problem were to minimise the admission dates of patients along with the duration of their hospital stay. They formulated this scheduling problem as an integer linear programming model. Since a significant level of uncertainty exists in terms of the amount of availability of clinical services in each time frame, [92] used fuzzy programming to address this multi-objective patient appointment scheduling problem. Based on their numerical results, they concluded that their proposed model is a promising approach to the solution of these problems.

Also, [101] applied a fuzzy logic based decision support system to a parallel machine scheduling/rescheduling problem in a pottery company with uncertain disruptions. The uncertain disruption they considered was glaze shortage and this was defined by the number of glaze shortage occurrences as well as the glaze shortage duration. To deal with the glaze shortage disruption, [101] implemented a predictive–reactive scheduling approach, which was defined by a two-step procedure: (i) The generation of a predictive schedule that can absorb the impact of the glaze shortage duration and (ii) the application of rescheduling to cases when the impact of the glaze shortage disruption is too high. For the rescheduling decision making, they applied fuzzy rules to determine when to reschedule and to determine which rescheduling method to use. From their results, they showed that the predictive schedules have good performance in the presence of uncertain disruptions. In addition, they showed that the fuzzy inference generates appropriate rescheduling decisions. Other examples where fuzzy programming methods have been applied include [19, 20, 40, 94, 148, 151], among others.

6.2.4 Sensitivity analysis and parametric programming

An alternative way for dealing with uncertainty in optimisation problems is to use analytical tools such as sensitivity analysis (SA) and parametric programming methods. SA is a useful tool to determine how a given model solution depends upon the input parameters [79]. [79] described SA as an "important method for checking the quality of a given model, as well as a powerful tool for checking the robustness and reliability of any solution". Online scheduling can be used to potentially correct the offline scheduling problem solution by accounting for the actual real-time values. SA in scheduling problems is useful for analysing the variation of the scheduling problem

solution relative to the variations at the execution time of the estimated values used by the scheduling policy [100]. SA has been applied to different applications by several authors, including [51, 52, 65, 81, 121, 144], *etc.*

Similarly to SA, parametric programming is an analytical tool in which uncertainty in optimisation problems can be accounted for. The foundation of parametric programming is the consideration of how the solution of a constrained optimisation problem changes as a function of a parameter [85]. Numerous researchers have contributed to the single parametric programming case, *i.e.* how the solution of a constrained optimisation problem changes if a change occurs in a single parameter of the problem formulation, such as [26, 66, 82, 116], among others. However, with the availability of faster computational power and the development of efficient and robust optimisation software, this enabled the consideration of multi-parametric programming, *i.e.* how the solution of a constrained optimisation problem changes if changes occur in multiple parameters of the problem formulation [98]. The multi-parametric programming formulation has been applied by numerous authors to a variety of problems, including model predictive control [10, 48, 103], the integration of design, scheduling and control [29, 102, 120], moving horizon estimation [27, 32, 112], bilevel programming [31, 39, 117], *etc.*

6.3 Problem solution methodology and implementation

A multiple scenario based approach is proposed due to its simplicity and direct implementation to the MIOCP approach. Here, a simulation is used to evaluate a batch of scenarios based on the level of uncertainty in each of the parameters in question. An analysis of the impact of the number of scenarios produced in this scheduling cleaning problem on the cost due to fouling is conducted. The impact of uncertainty in the fouling rate parameters, which includes the linear fouling constant, a, asymptotic fouling resistance, R_f^{∞}, and decay constant, τ, on the cost due to fouling is assessed. The sensitivity of the cost due to fouling to the overall heat transfer coefficient in the clean condition, U_{c}, and fuel cost, C_{E}, are also analysed. This analysis is performed by considering uncertainty in one parameter at a time whilst keeping the other parameters fixed. For the parametric uncertainty problem, uncertainty is considered in all

of the aforementioned parameters simultaneously.

This multiple scenario approach gives a larger DAE system by stacking many realisations of the HEN multiperiod problem whilst applying the same control action among all scenarios. In the simulation phase, the DAE integrator is overloaded while the optimisation problem remains at the same size as a single scenario presented to the optimiser. Here, the number of decision variables is the same among the multiple scenarios which are solved using the feasible path approach. Hence, the optimiser is presented with effectively an unconstrained problem, whether a single-scenario case is used or a multiple-scenario case. The only constraints that may be present in these formulations are the ones that are associated with the binary variables which are not dependent on the number of scenarios. This highlights the potency of the proposed feasible path methodology, in that it can be used effectively to tackle the maintenance scheduling problem with uncertainty. This strategy is used for the sake of keeping both the optimisation problem size under control, as well as contributing to reducing computational time to a practical level. Computational time can be further reduced owing to this approach being highly parallelisable.

Similarly to the previous chapter, the implementation is performed in MATLAB® R2016b with its Optimisation Toolbox ™ and Parallel Computing Toolbox ™ [134]. The ODE solver, ode15s, and the optimiser fmincon are used with the SQP algorithm. All other settings are kept at their default values. Gradient calculations are parallelised using the Parallel Computing Toolbox™ and all case studies are performed on a 4GHz Intel Core i7, 16 GB RAM iMac running on macOS Sierra. Single optimisations are performed for each scenario, *i.e.* from a single starting point. Here, all the control variables' initial points are set to 1.

6.4 Modification of problem formulation

A similar formulation to the one presented in Section 4.2, where the problem is formulated as an OCP, is used for the HEN maintenance scheduling problem with parametric uncertainty along with a few modifications:

(i) Multiple scenarios, s, where $s \in S$, are created by generating random values normally distributed about the mean of each of the uncertain parameters ($\bar{a}$,

$\bar{R}_f^{\infty}$, $\bar{\tau}$, $\bar{U}_c$, and $\bar{C}_E$), *i.e.* a totally random sampling of space and not a systematic one. This is achieved using the normrnd function in MATLAB®.

(ii) The objective function is modified from Equation (1.12) to Equation (6.1), where this is now a summation of the mean operating cost from all scenarios and the cleaning cost.

(iii) The same control action is applied to all scenarios as given in Equation (6.1).

$$Obj = \left(\sum_{s=1}^{S} \int_{0}^{t_F} \frac{C_E^s Q_F^s(t)}{\eta_f} dt \right) / S + \sum_{p=1}^{NP} \sum_{n=1}^{NE} C_{cl}(1 - y_{n,p}) \tag{6.1}$$

6.5 Modification of case studies

Case studies C and D from Subsections 3.3.3 and 3.3.4, respectively are considered. Modifications are implemented for the purpose of converting these problems from a deterministic case to one with parametric uncertainty. In this section, these amendments are presented.

6.5.1 Case study C

Modifications for this case study are as follows: The linear fouling constant, a, asymptotic fouling resistance, R_f^{∞}, decay constant, τ, and overall heat transfer coefficient in the clean condition, U_c parameters, which appear in Table 3.3.3, are redefined as the mean of the associated parameters with uncertainty (see Table 6.5.1). Furthermore, the cost of fuel, C_E, is redefined as the mean fuel cost with uncertainty, $\bar{C}_E$, and is £2.93/MMBtu. A sensitivity analysis is performed in this case study for each of the aforementioned parameters with uncertainty to evaluate the impact of the parameter on the cost due to fouling. In this analysis, RSD values of 5, 10, 15 and 20% about the mean of each of the examined parameters are considered, and 30 scenarios are generated.

The impact of the number of scenarios on this scheduling problem is also assessed. Here, the RSD for each uncertain parameter is set at 10%, while the range of $10 \leq$

$S \leq 50$ scenarios is considered in this study. A single realisation for the scheduling of HEN cleaning actions with parametric uncertainty with linear and asymptotic fouling models is performed. In these cases, the RSD for each uncertain parameter is set at 10% and 30 scenarios are generated.

6.5.2 Case study D

Similarly, for case study D, the U_c and a parameters are redefined as shown in Table 6.5.2. The mean furnace fuel cost with uncertainty, $\bar{C}_E$, is £0.34/kW day. A single realisation for the scheduling of HEN cleaning actions with parametric uncertainty is conducted, where the RSD of the uncertain parameters are set at 10% and 30 scenarios are produced.

6.6 Computational results

In this section, the following computational results are presented: (i) the sensitivity analysis of the overall cost due to fouling to the parameters with uncertainty, and (ii) the HEN maintenance scheduling optimisation with parametric uncertainty.

For the 10 unit HEN case study with linear fouling, numerical and graphical results relating to the sensitivity analysis of the cost due to fouling to the linear fouling constant, clean overall heat transfer coefficient, and fuel cost parameters are shown in Tables 6.6.4 to 6.6.5, respectively, as well as in Figures 6.6.3 to 6.6.4, respectively. In addition for this case, results for the impact of number of scenarios on the cost due to fouling are shown in Table 6.6.3 and Figure 6.6.2. Numerical results consist of the minimum, maximum, mean costs for each deviation in the parameter as well as the associated RSD.

The same is applicable to the 10 unit HEN case with asymptotic fouling where the results for the sensitivity analysis of the cost due to fouling to the asymptotic fouling resistance, decay constant, clean overall heat transfer coefficient, fuel cost parameters and number of scenarios are shown in Tables 6.6.10 to 6.6.9, respectively, and Figures 6.6.8 to 6.6.7, respectively.

Table 6.5.1: Data for 10 unit HEN case with parametric uncertainty.

Parameter	Heat Exchanger									
	1	2	3	4	5	6	7	8	9	10
$\bar{a}$ (linear fouling, $\times 10^7$) [ft^2°F/Btu]	1.23	1.84	1.23	1.64	3.07	2.25	3.07	3.27	3.68	3.88
$\bar{R}_f^{\infty}$ (asymptotic fouling, $\times 10^3$) [hft^2°F/Btu]	1.61	2.41	1.61	2.14	4.02	2.95	4.02	4.29	4.82	5.09
$\bar{\tau}$ (decay constant) [month]	4									
$\bar{U}_c$ [Btu/hft^2°F]	88.1									

Table 6.5.2: Data for 25 unit HEN case with parametric uncertainty.

HEX	$\bar{U}_c$ (kW $m^{-2}K^{-1}$)	$\bar{a} \times 10^{11}$ (m^2KJ^{-1})
1A	0.5	1.9
2A	0.5	1.8
3A	0.5	1.6
1B	0.5	1.9
2B	0.5	1.8
3B	0.5	1.6
3C	0.5	1.9
2C	0.5	1.8
3C	0.5	1.6
1D	0.5	1.9
2D	0.5	1.8
3D	0.5	1.6
4A	0.5	1.5
5A	0.5	1.1
6A	0.5	1.5
4B	0.5	1.6
5B	0.5	1.1
6B	0.5	1.5
7A	0.5	0.8
7B	0.5	0.8
8	0.5	0.8
9A	0.5	0.9
9B	0.5	0.9
10	0.5	0.6
11	0.5	0.6

Results for the 10 unit HEN scheduling maintenance problem with parametric uncertainty are shown in Table 6.6.7, Table 6.6.8 and Figure 6.6.6. Table 6.6.7 summarises the best, worst, average costs as well as the associated weighted average cost, whereas Table 6.6.8 shows the optimum cleaning schedule associated with the mean cost. Figure 6.6.6 displays the associated cost against probability curve. The same is applicable to the 10 unit HEN case study with asymptotic fouling, where results are displayed in Table 6.6.14, Table 6.6.15 and Figure 6.6.12, as well as the 25 unit HEN case study in which the results are shown in Table 6.6.16, Table 6.6.17 and Figure 6.6.13.

6.6.1 Case study C

For the 10 unit HEN linear case, the deterministic cost, *i.e.* the overall minimised cost without uncertainty, is £260k. Graphical results for the impact of the number of scenarios on the overall cost due to fouling are shown in Figure 6.6.2, which displays the spread of the cleaning costs from the mean value for each sample set. Symbol $\times$ indicates the mean cost and is applicable to all figures in this section.

There is no direct correlation between mean overall cost due to fouling and number of samples. Although the mean cost increases by £62k when the number of samples are increased from 10 to 40, this value decreases by £8k from 40 to 50 samples (see Table 6.6.3). This is because of the way in which the sample sets are generated. The set of samples are independent from each other, *i.e.* they are not produced by the addition of 10 more samples to the previous set repeatedly. Sample sets are created in the same manner for the asymptotic fouling case. The costs due to fouling for each sample set are broadly dispersed about their mean value. Here, the RSD ranges from 31.1% up to 53.7%, with the largest deviation corresponding to the least number of samples. In addition, the difference between maximum and minimum cost value for each sample set is large, ranging from £321k to £500k, as shown in Figure 6.6.2. The total number of cleanings for the deterministic case is 11, while this ranges from 9 to 11 cleanings with a mode of 10 cleanings when the number of samples are varied (see Table 6.6.3).

Results concerning the sensitivity of the cost due to fouling to the linear fouling constant, a, show that the sensitivity of the cost is limited. Table 6.6.4 and Figure 6.6.3 show that the mean cost varies by only £4k when the deviation of the linear fouling rate about its mean is increased from 5% to 20%.

Moreover, the results are narrowly dispersed about the mean cost, where the variation in the RSD value lies within the range of 1.1% to 4%. The largest difference between the maximum and minimum cost is £45.6k for the 20% deviation scenario. The variation in the number of cleanings between each case is small, increasing from 10 cleanings for the 5% and 10% deviation scenarios to 11 for the 15% and 20% scenarios (see Table 6.6.4).

Table 6.6.5 and Figure 6.6.4 show that the cost due to fouling is sensitive to C_{E}; the RSD rises from 4.7% to 15.5% as the deviation of the fuel cost parameter is increased from 5% to 20%. Furthermore, the difference between the maximum and minimum value of the overall cost for fouling increases by more than a factor of 3, from £47.4k to £159k. The overall costs due to fouling are more scattered in this parameter than the linear fouling rate. In this scenario, the mean cost due to fouling increases by £12k, from £261k to £273k, when the deviation of the fuel cost parameter is increased from 5% to 20%.

As expected, the maximum cost increases when the deviation of C_{E} is increased. However, although the minimum cost decreases, from £157k to £67k, when the deviation of C_{E} is increased from 5% to 10%, this value increases to £109k when the deviation is increased by 10% further. Generally, the minimum cost should decrease with increase in deviation for well sampled scenarios. This is also observed in the results for the sensitivity of the cost due to fouling to U_{c} (see Table 6.6.6) and in the asymptotic case (see Tables 6.6.10 to 6.6.13) . In contrast to the impact of a on the schedule, the number of cleanings here does not change with the level of deviation in C_{E} and remains constant at 10 cleanings.

Results for the sensitivity of the cost due to fouling to the overall heat transfer coefficient in the clean condition, shown in Table 6.6.6 and Figure 6.6.5, reveal that the cost associated with the HEN cleaning problem is highly sensitive to this parameter. The RSD increases from 17.2% to 60.7% when the deviation of this parameter is increased from 5% to 20%. Moreover for each scenario, there is a large difference between the maximum and minimum cost, *e.g.* over 7 times and over 16 times in the 10% and 20% deviation scenarios, respectively. Generally, the number of cleaning actions required here remain constant at 10 and only increases by 1 in the 20% deviation scenario.

For the case with parametric uncertainty, we show one realisation where each of a, U_{c} and C_{E} parameters are considered uncertain simultaneously. Here, we set the deviation

of each of these parameters to 10% with a fixed number of samples, of 30. The results in Table 6.6.7 show the P90, P50 and P10 cost values. The P90 is the cost level with 10% probability of exceeding and 90% probability to under run. This value is £397k, as shown in Table 6.6.7, and is considered a conservative estimate of the cost due to fouling. P10 is the cost value with 90% probability of exceeding and 10% probability to under run; this more optimistic value is £168k. The P50 cost, also known as the 50^{th} percentile, is the median and is £276k. In this case, this value is equivalent to the mean cost due to fouling resulting in a normal curve, *i.e.* symmetrical distribution of a cost against probability curve with no skew, as shown in Figure 6.6.6. The associated full width at half maximum (FWHM) and standard deviation (SD) is £202k and £86k, respectively. The weighted average cost is the sum of all outcomes times the respective probabilities, and given that we have a normal curve, this value is very similar to that of the P50, with only £1k difference, as shown in Table 6.6.7 . Overall, the anticipated cost associated with this realisation is £277k $\pm$ 31.1% in comparison to a cost of £260k without parametric uncertainty.

Table 6.6.8 compares the cleaning schedules for the linear fouling case with and without parametric uncertainty. All exchangers except unit 2 are cleaned the same number of times in each scenario. In the parametric uncertainty case, unit 2 is not cleaned at all, while it is cleaned once in the deterministic case. There is a limited number of common cleaning actions with only 1 for unit 10 during the 12^{th} month. Moreover, the parametric uncertainty cleanings actions sometimes take place earlier than the deterministic ones and other times later. However, these cleanings are always within 2 periods of each other.

In terms of resource usage, convergence for the deterministic problem of the linear fouling case required 446 CPU s (7.4 CPU min) over 13 SQP major iterations and 2,269 function evaluations, *i.e.* simulations. The corresponding problem with parametric uncertainty required $\approx$36 times more resource usage totalling 16,160 CPU s (4.5 CPU hr) with 16 SQP major iterations and 2,921 function evaluations.

Results for the effect of the number of samples on the cost due to asymptotic fouling displayed in Table 6.6.9 show that the mean cost due to fouling varies from £476k to £552k in comparison to £507k for the deterministic case. As with the linear fouling case, due to the sample sets being independent from each other, there is no direct relation between the mean cost due to fouling and the number of samples considered. In this case, with every increase of 10 samples there is an increase in the mean cost

Table 6.6.3: Effect of number of samples for 10 unit HEN case (linear fouling).

No. of samples	10	20	30	40	50
Mean cost [k£]	234	274	276	296	288
RSD [%]	53.7	34.3	31.1	34.6	36.0
Minimum cost [k£]	40.8	94.0	87.1	98.9	43.7
Maximum cost [k£]	523	519	408	546	544
No. of cleanings	9	10	10	11	10

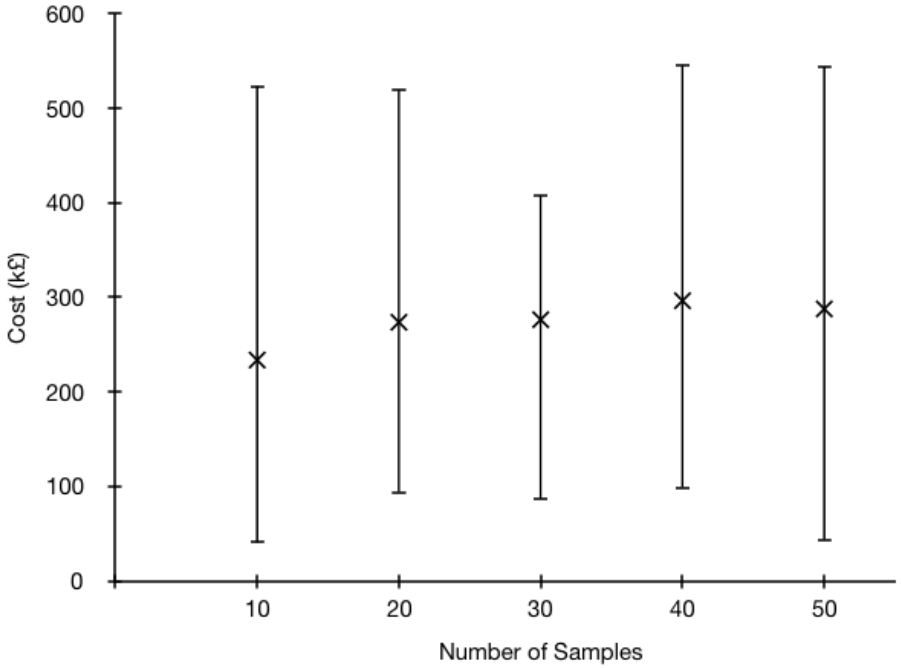

Figure 6.6.2: Effect of number of samples for 10 unit HEN case (linear fouling).

Table 6.6.4: Sensitivity of linear fouling rate for 10 unit HEN case.

Deviation of linear fouling constant [%]	5	10	15	20
Mean cost [k£]	262	266	265	266
RSD [%]	1.1	2.2	3.2	4.0
Minimum cost [k£]	257	254	247	247
Maximum cost in [k£]	267	275	279	293
No. of cleanings	10	10	11	11

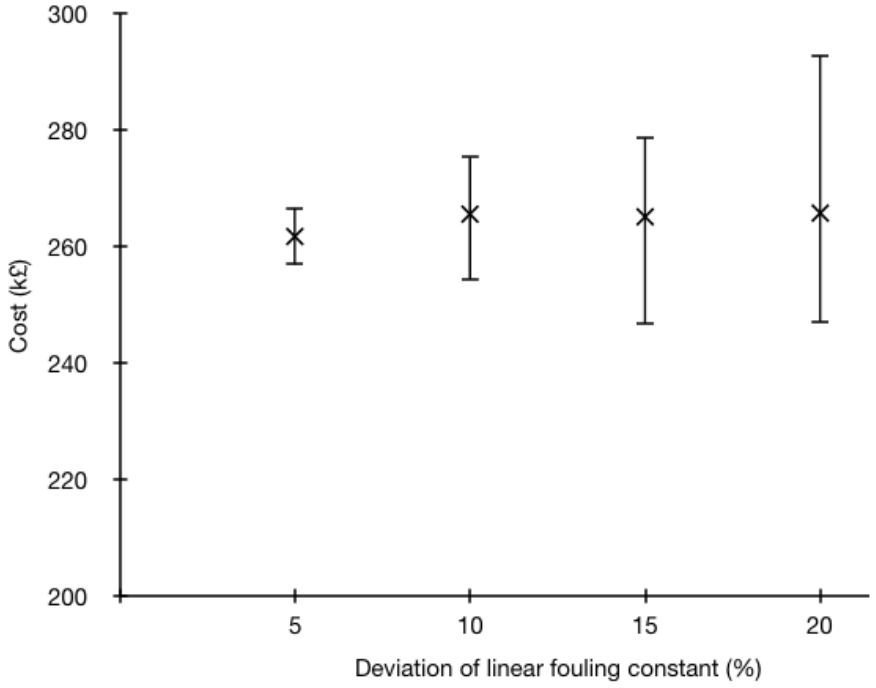

Figure 6.6.3: Effect of linear fouling rate for 10 unit HEN case.

Table 6.6.5: Sensitivity of fuel cost parameter for 10 unit HEN case (linear fouling).

Deviation of fuel cost parameter [%]	5	10	15	20
Mean cost [k£]	261	266	265	273
RSD [%]	4.7	8.7	13.5	15.5
Minimum cost [k£]	235	215	180	196
Maximum cost [k£]	283	311	338	355
No. of cleanings	10	10	10	10

Table 6.6.6: Sensitivity of overall heat transfer coefficient parameter for 10 unit HEN case (linear fouling).

Deviation of overall heat transfer coefficient parameter [%]	5	10	15	20
Mean cost [k£]	252	269	299	303
RSD [%]	17.2	38.2	43.0	60.7
Minimum cost [k£]	157	67.4	109	50.2
Maximum cost in [k£]	338	483	620	836
No. of cleanings	10	10	10	11

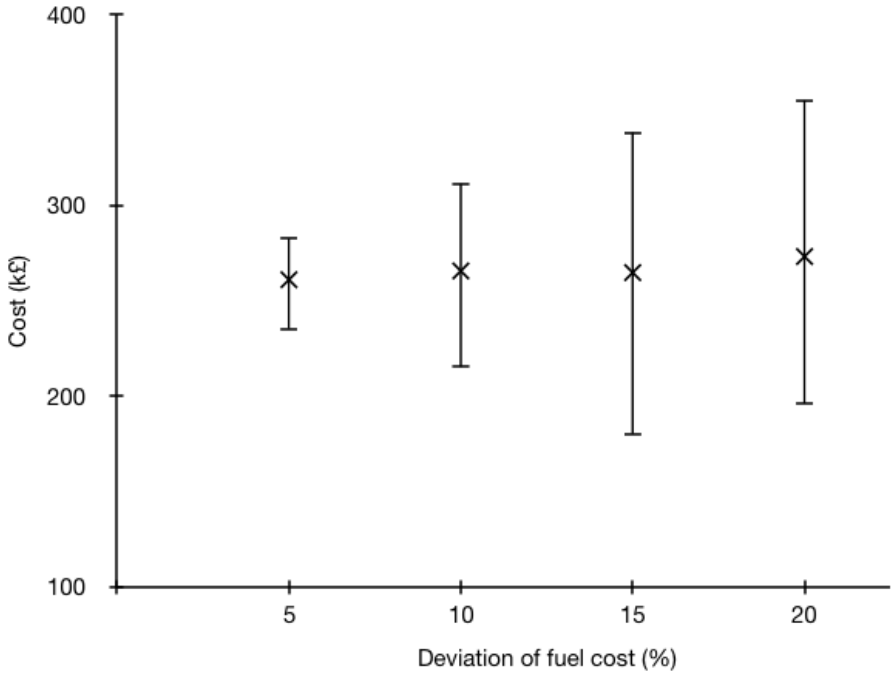

Figure 6.6.4: Effect of fuel cost parameter for 10 unit HEN case (linear fouling).

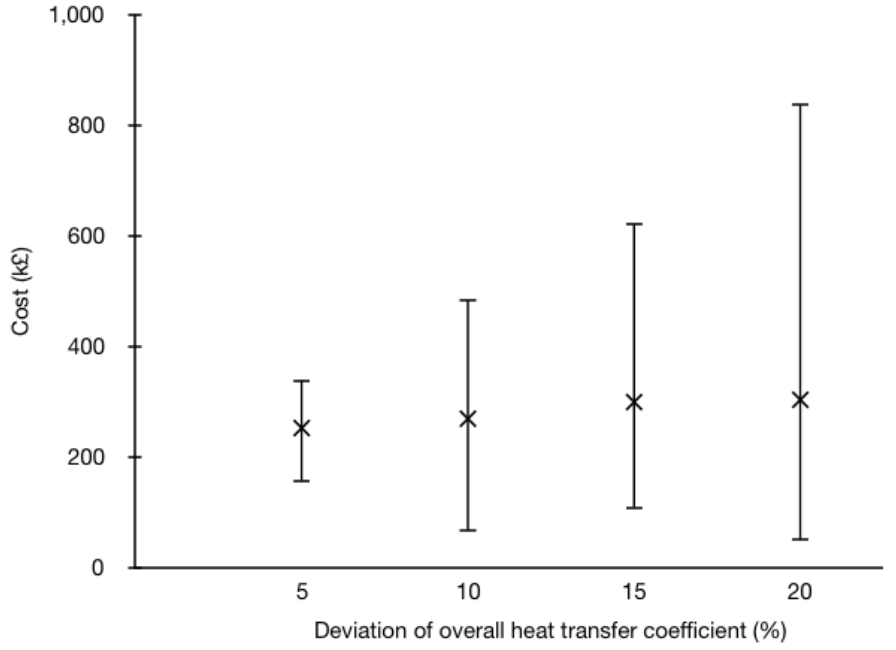

Figure 6.6.5: Effect of overall heat transfer coefficient parameter for 10 unit HEN case (linear fouling).

Table 6.6.7: Cleaning scheduling with parametric uncertainty for 10 unit HEN case (linear fouling).

Mean cost [k£]	276
RSD [%]	31.1
Minimum cost [k£]	87.1
Maximum cost [k£]	458
P90 [k£]	397
P50 [k£]	276
P10 [k£]	168
Weighted average cost [k£]	277

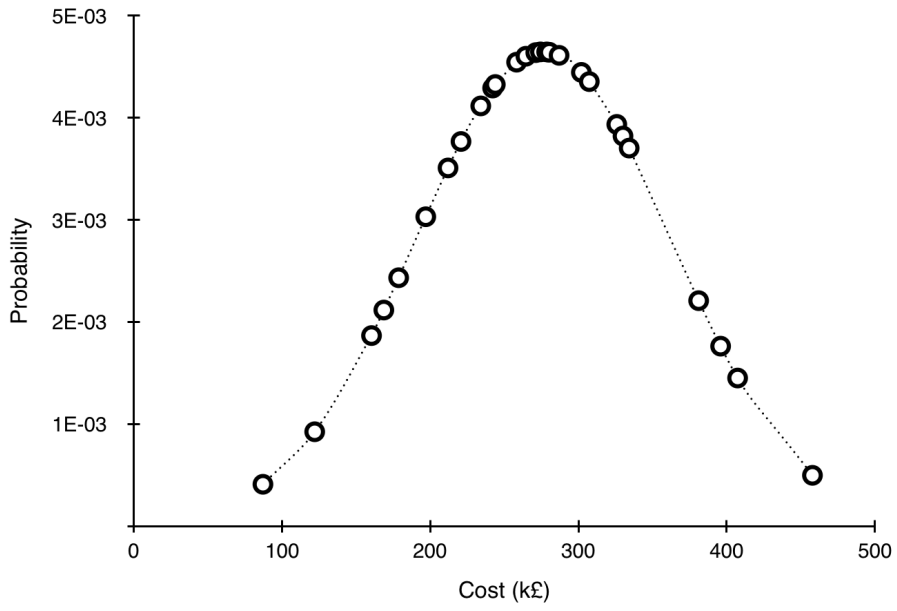

Figure 6.6.6: Cost versus probability curve for 10 unit HEN case (linear fouling).

Table 6.6.8: Cleaning schedule for the 10 unit HEN case with parametric uncertainty (linear fouling, cleaning cost = £4k).

Exchanger No.	Time (months)																		No. of cleaning actions	
	1	2	3	4	5	6	7	8	9	10	11	12	13	14	15	16	17	18	+	◯
1																			0	0
2								◯											0	1
3									◯	+									1	1
4									+	◯									1	1
5									◯		+								1	1
6									+	◯									1	1
7								◯		+									1	1
8									+		◯								1	1
9						+	◯				+	◯							2	2
10						◯		+				⊕							2	2
cleaning actions: + parametric uncertainty case; ◯ deterministic case; ⊕ common																			10	11

followed by a decrease in this value, *e.g.* the mean cost increases by £48k when the sample size is increased from 10 to 20, but decreases by £17k when the sample size is increased further to 30.

The overall costs due to fouling are scattered about their mean value (as shown in Figure 6.6.7) and consequently the RSD varies from 18.2% to up to 21.8% (see Table 6.6.9). In comparison to the linear fouling case, these costs are less dispersed (21.8% maximum in this case *vs.* 53.7% maximum in the linear fouling case), with the largest RSD corresponding to the largest number of samples. The total number of cleanings for the deterministic case and parametric uncertainty case are similar (4 *vs.* a mode of 3 cleanings).

There are a couple of similarities in the results concerning the sensitivity analysis of asymptotic fouling parameters, the asymptotic fouling resistance and decay constant with the linear fouling case:

(i) The sensitivity of the cost to the asymptotic fouling parameters is limited, such that the mean cost only varies by £13k and £17k across a deviation of 5 to 20% for the asymptotic fouling resistance and decay constant parameters, respectively (shown in Tables 6.6.10and 6.6.11).

(ii) There is a tight spread of results about the mean cost (shown in Figures 6.6.8 and 6.6.9), where the RSD reaches a peak of 4.9% and 7% when the deviation of the asymptotic fouling resistance and decay constant parameters are increased to 20%, respectively.

However, in contrast to the linear fouling constant, there is a larger variation in the number of cleanings required for the asymptotic fouling resistance, where this ranges from 3 up to 6 cleaning actions. This is not the case for the decay constant parameter which shows a limited variation (3 to 4 cleaning actions).

Results for the effect of fuel cost parameter show that the overall cost is more sensitive to this parameter than the asymptotic fouling parameters. This is shown in Table 6.6.12 and Figure 6.6.10, where the RSD varies up to 17.7% for a deviation of 20% of the fuel cost parameter. In addition, there is an increase in the difference between the maximum and minimum cost of more than 4 times, from £78.4k to £334k, over the range of 5 to 20% deviation in the fuel cost parameter. Therefore, there is

more of a spread in the cost than that associated with the asymptotic fouling parameters. Unlike the linear fouling case, a decrease in the mean cost is observed when the deviation of the fuel cost parameter is increased from 5% to 20%. The number of cleaning actions required is almost constant and only varies from 3 to 4 in this case.

Similarly to the linear fouling case, the HEN cleaning scheduling problem's cost is highly sensitive to U_c, in which the RSD is 36.4% when the deviation of this parameter is increased to 20% (see Table 6.6.13 and Figure 6.6.11). Moreover, the difference between the maximum and minimum cost is over 4 times in the 20% deviation scenario. The number of cleaning actions required is almost constant (3 to 4).

Furthermore, similarly to the linear fouling case, for the asymptotic fouling problem with parametric uncertainty, we show one realisation where each of the asymptotic fouling, decay constant, overall heat transfer coefficient and fuel cost parameters are considered uncertain simultaneously. Again, we set the deviation of each of these parameters to 10% and fixed the number of samples to 30. The P90, P50 and P10 values are £666k, £502k and £401k, respectively, as shown in Table 6.6.14. In this case the mean cost is £5k higher than the P50 value at £507k, resulting in a slightly positively skewed cost against probability curve, as shown in Figure 6.6.12. As this curve is only slightly skewed, *i.e.* has an almost symmetrical distribution, the weighted average cost is equal to the P50 value. Hence, the expected cost associated with this realisation is £502k± 20.6% in comparison to a cost of £507k without parametric uncertainty.

The comparison of the cleaning schedules with and without parametric uncertainty in Table 6.6.15 shows that only exchangers 9 and 10 are cleaned over the horizon of 18 months. Exchanger 9 is cleaned one less time in the parametric uncertainty case than the deterministic one, giving a total of 3 cleaning actions in the former *vs.* 4 cleaning actions in the latter. There are 2 common cleaning actions taking place just before the midpoint of the horizon.

In terms of resource usage, convergence for the deterministic problem with asymptotic fouling required 461 CPU s (7.7 CPU min) with 11 SQP major iterations and 2,055 function evaluations. Convergence for the parametric uncertainty case required 8,722 CPU s (2.4 CPU hr) with 7 SQP major iterations and 1,370 function evaluations.

Table 6.6.9: Effect of number of samples for 10 unit HEN case (asymptotic fouling).

No. of samples	10	20	30	40	50
Mean cost [k£]	476	524	507	552	534
RSD [%]	18.2	16.9	20.6	17.2	21.8
Minimum cost [k£]	316	352	310	360	327
Maximum cost [k£]	635	718	732	795	769
No. of cleanings	4	3	3	3	4

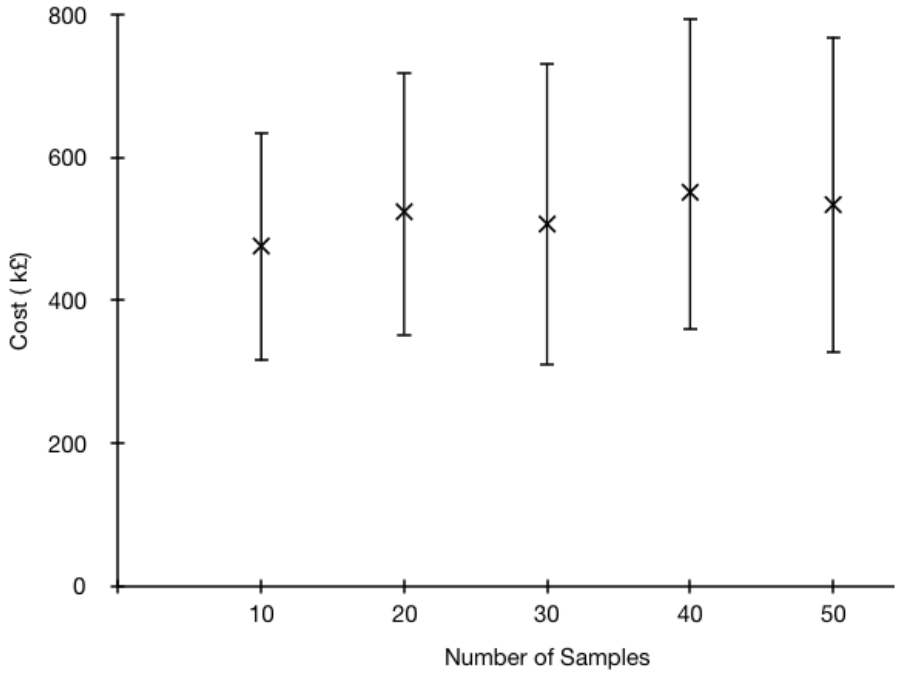

Figure 6.6.7: Effect of number of samples for 10 unit HEN case (asymptotic fouling).

Table 6.6.10: Sensitivity of asymptotic fouling resistance for 10 unit HEN case.

Deviation of asymptotic fouling resistance [%]	5	10	15	20
Mean cost [k£]	508	499	511	512
RSD [%]	1.2	2.5	4.3	4.9
Minimum cost [k£]	493	475	454	457
Maximum cost [k£]	519	528	543	568
No. of cleanings	3	6	4	3

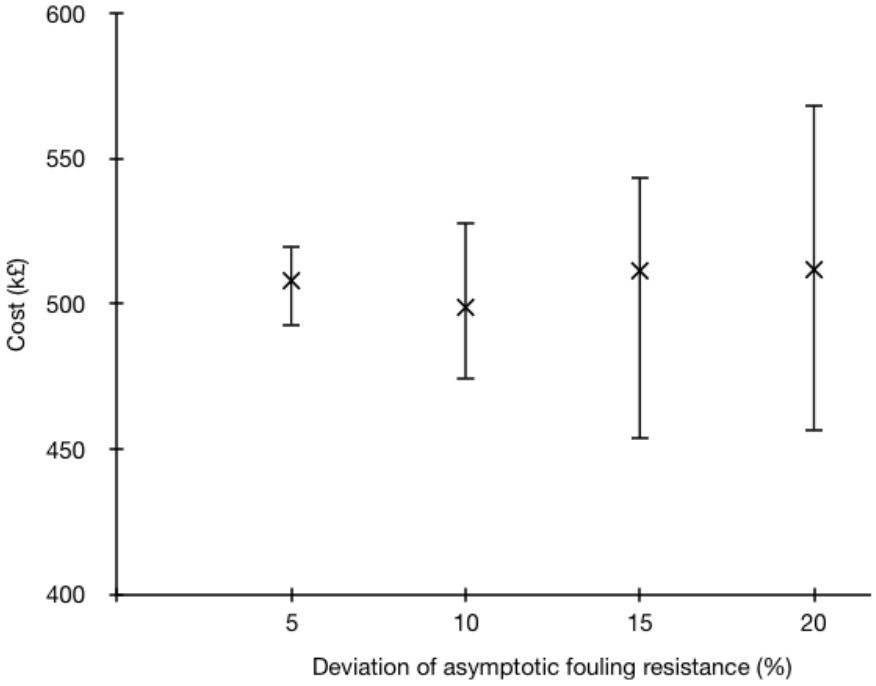

Figure 6.6.8: Effect of asymptotic fouling resistance for 10 unit HEN case.

Table 6.6.11: Sensitivity of decay constant for 10 unit HEN case (asymptotic fouling).

Deviation of decay constant [%]	5	10	15	20
Mean cost [k£]	508	518	501	508
RSD [%]	1.5	3.0	5.4	7.0
Minimum cost [k£]	493	490	424	428
Maximum cost [k£]	522	546	552	581
No. of cleanings	4	3	4	3

Table 6.6.12: Sensitivity of fuel cost parameter for 10 unit HEN case (asymptotic fouling).

Deviation of fuel cost parameter [%]	5	10	15	20
Mean cost [k£]	504	503	498	499
RSD [%]	4.3	9.7	13.9	17.7
Minimum cost [k£]	466	404	307	302
Maximum cost [k£]	545	590	641	620
No. of cleanings	4	4	3	4

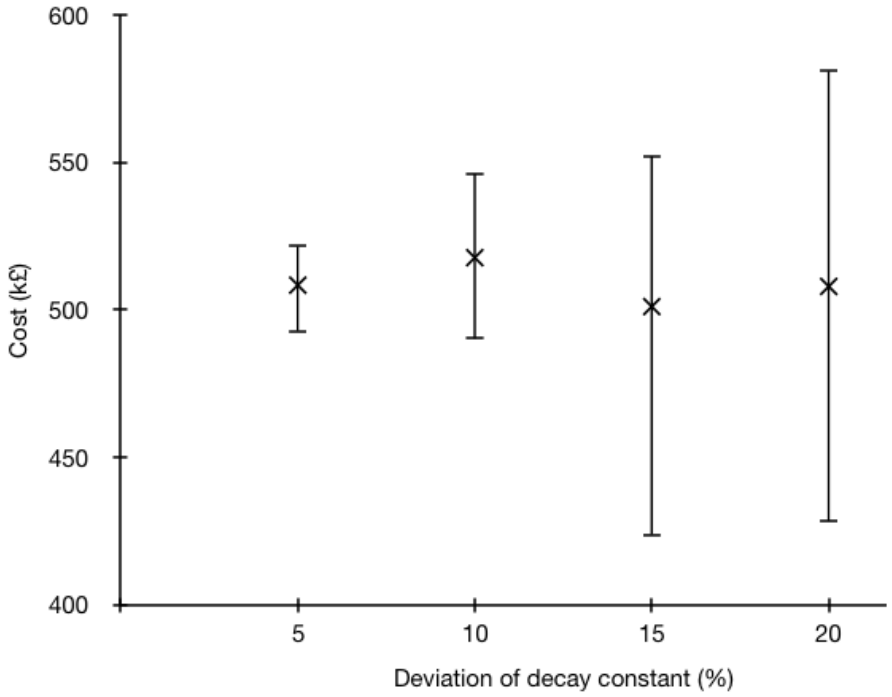

Figure 6.6.9: Effect of decay constant for 10 unit HEN case (asymptotic fouling).

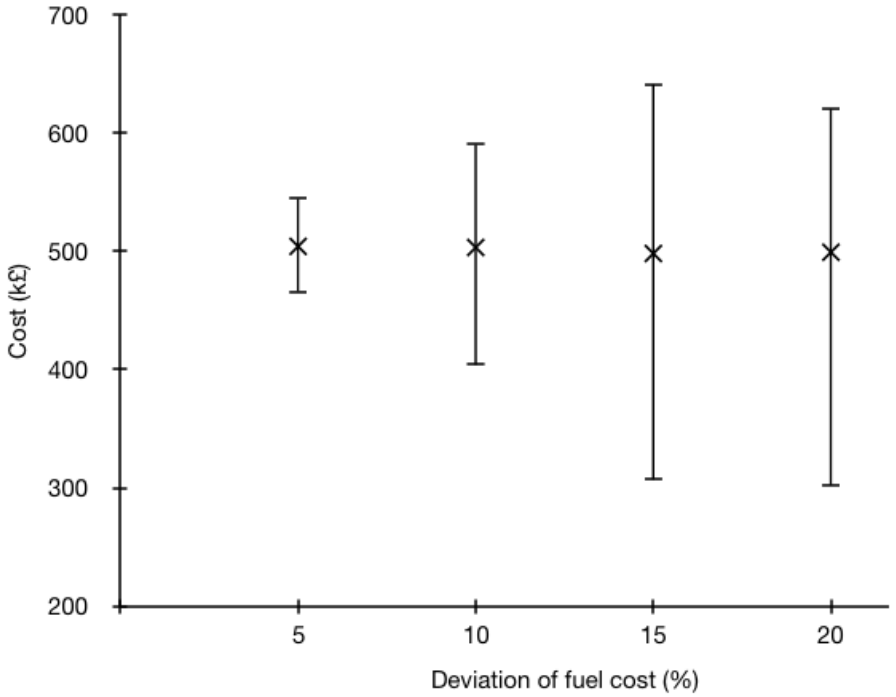

Figure 6.6.10: Effect of fuel cost parameter for 10 unit HEN case (asymptotic fouling).

Table 6.6.13: Sensitivity of overall heat transfer coefficient parameter for 10 unit HEN case (asymptotic fouling).

Deviation of overall heat transfer coefficient parameter [%]	5	10	15	20
Mean cost [k£]	523	530	587	515
RSD [%]	6.4	18.6	17.5	36.4
Minimum cost [k£]	462	347	411	218
Maximum cost [k£]	590	763	806	895
No. of cleanings	4	4	3	4

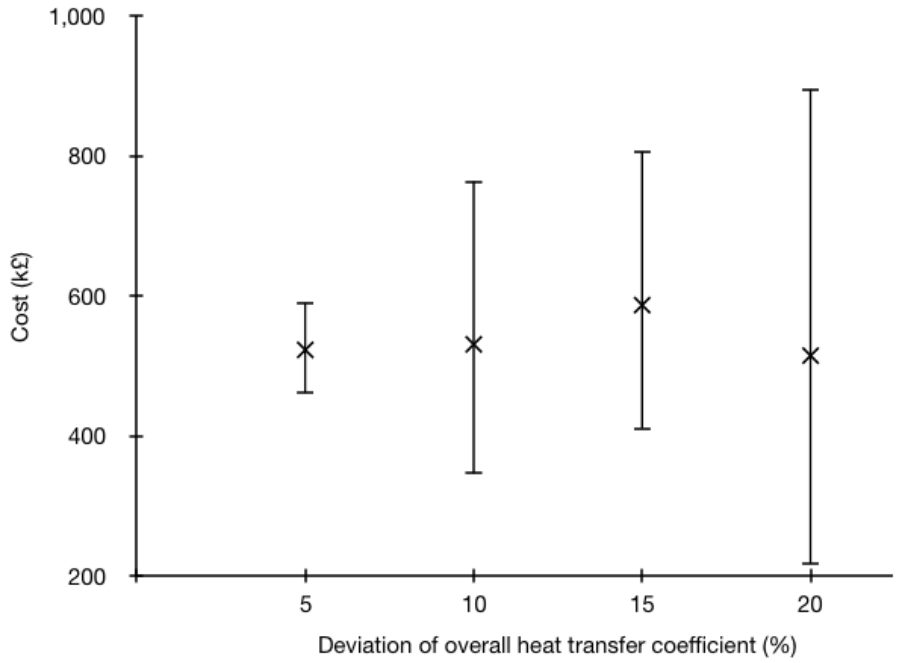

Figure 6.6.11: Effect of overall heat transfer coefficient parameter for 10 unit HEN case (asymptotic fouling).

Table 6.6.14: Cleaning scheduling with parametric uncertainty for 10 unit HEN case (asymptotic fouling).

Mean cost [k£]	507
RSD [%]	20.6
Minimum cost [k£]	310
Maximum cost in [k£]	732
P90 [k£]	666
P50 [k£]	502
P10 [k£]	401
Weighted average cost [k£]	502

Table 6.6.15: Cleaning schedule for the 10 unit HEN case with parametric uncertainty (asymptotic fouling, cleaning cost = £4k).

Exchanger No.	Time (months)																		No. of cleaning actions	
	1	2	3	4	5	6	7	8	9	10	11	12	13	14	15	16	17	18	+	◯
1																			0	0
2																			0	0
3																			0	0
4																			0	0
5																			0	0
6																			0	0
7																			0	0
8																			0	0
9				◯				⊕											1	2
10							⊕				◯	+							2	2
cleaning actions: + parametric uncertainty case; ◯ deterministic case; ⊕ common																			3	4

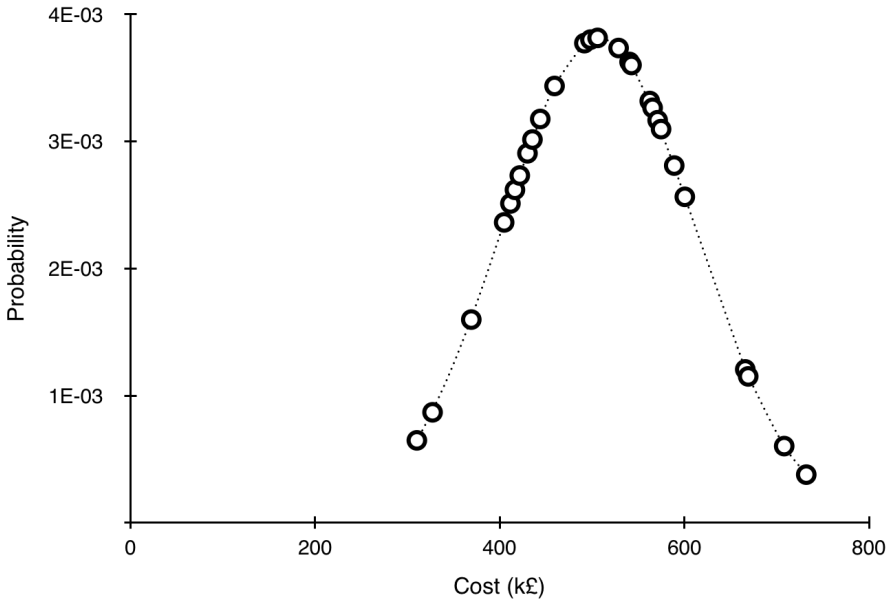

Figure 6.6.12: Cost versus probability curve for 10 unit HEN case (asymptotic fouling).

6.6.2 Case study D

For the 25 unit HEN cleaning scheduling problem with parametric uncertainty, one realisation is performed where each of the linear fouling constant, overall heat transfer coefficient and fuel cost parameters are considered uncertain simultaneously. Again, we set the deviation of each of these parameters to 10% and fixed the number of samples to 30. The P90, P50 and P10 values are £1140k, £925k and £804k, respectively, as shown in Table 6.6.16. The mean cost is £29k higher than the P50 value at £954k resulting in the cost *vs.* probability curve being positively skewed, as shown in Figure 6.6.13. Here, the weighted average cost is £10k more than the P50 value. Hence, the expected cost associated with this realisation is £935k$\pm$ 16.3% in comparison to a cost of £896k for the deterministic case.

The cleaning schedules for the case with and without parametric uncertainty displayed in Table 6.6.17 differ. No pattern is observed here and cleaning actions occur earlier for some units in the parametric uncertainty case in comparison to the deterministic one and later for other units. There are only 6 common cleaning actions out of a total of 39 and 37 cleaning actions for the parametric uncertainty and deterministic cases, respectively.

Table 6.6.16: Cleaning scheduling with parametric uncertainty for 25 unit HEN case.

Mean cost [k£]	954
RSD [%]	16.3
Minimum cost [k£]	654
Maximum cost in [k£]	1305
P90 [k£]	1140
P50 [k£]	925
P10 [k£]	804
Weighted average cost [k£]	935

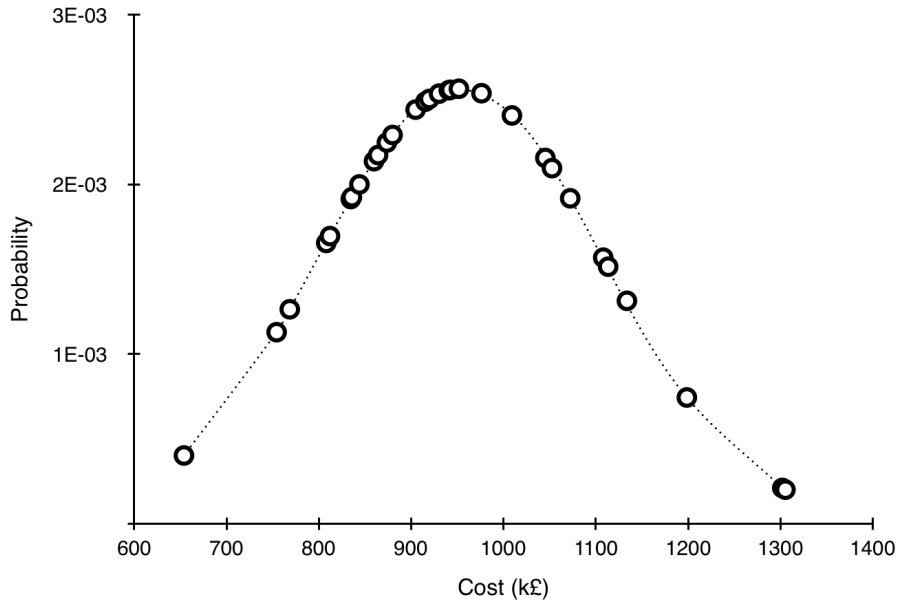

Figure 6.6.13: Cost versus probability curve for 25 unit HEN case.

The resource usage is 29,173 CPU s (≈8.1 CPU hr) and 1.26MM CPU s (≈14.6 CPU day) for the deterministic and parametric uncertainty cases, respectively. For the former case, convergence required 26 SQP major iterations and 23,696 function evaluations. For the latter case, convergence required 38 SQP major iterations and 34,208 function evaluations.

Table 6.6.17: Cleaning schedule for the 25 unit HEN case with parametric uncertainty.

HEX	Time (months)																																			
	1	2	3	4	5	6	7	8	9	10	11	12	13	14	15	16	17	18	19	20	21	22	23	24	25	26	27	28	29	30	31	32	33	34	35	36
1A													◯			+							+	◯													
1B												+		◯							+							⊕									
1C											◯				+										+				◯								
1D										◯							+					◯		+													
2A											◯			+					◯							+											
2B										◯							+				◯								+								
2C										+		◯									+				◯			+									
2D													+	◯										◯	+												
3A																	+				◯																
3B																				+		◯															
3C																+			◯																		
3D																		⊕																			
4A											+		◯										◯				+										
4B												+				◯								+		◯											
5A																			+	◯																	
5B															+		◯																				
6A									⊕							◯										⊕											
6B														+	◯				+								⊕										
7A																⊕																					
7B																	+			◯																	
8																					◯		+														
9A																		+	◯																		
9B																		◯		+																	
10																																				
11																					+		◯													

cleaning actions: + parametric uncertainty case; ◯ deterministic case; ⊕ common

6.7 Discussion

The case studies in this chapter have demonstrated how finding that HEN cleaning scheduling problems exhibit bang-bang control characteristics allows the uncertainty associated with fouling behaviour and other input parameters to be incorporated in scheduling calculations. This allows the impact of uncertainty in the fouling behaviour(s) to be quantified alongside the sensitivity of the results to the costing parameters that appear in the objective function. The former can be considered as a 'natural' variation, while the latter can vary simply as a result of budget and market considerations. The latter are also likely to vary between installations owing to differences in network configuration, availability of fuel and other factors.

The methodology presented here therefore allows the significance of each source of uncertainty to be established and the sensitivity of these factors to be compared. For instance, if the source of uncertainty in fouling model parameterisation is dominated by the absence of reliable data, the results can be used to justify the cost of installing new instrumentation. Likewise, if the schedule is strongly dependent on the costing parameter, management decisions can be made on the basis of forecasts over the anticipated operating period.

Furthermore, it is important to highlight that the methodology presented in this chapter is based on an offline scheduling approach. Adaptive scheduling can be used for the HEN cleaning scheduling problem, where estimates for the fouling data and cost data can be refined in 'real' time, *i.e.* online, as one goes along. This will ultimately reduce the impact of uncertainty in these parameters on the overall cost due to fouling.

6.8 Chapter summary

In this chapter, for the first time a multiple scenario feasible path MIOCP approach is developed and applied to the scheduling of cleaning actions in HENs which undergo fouling. The parametric uncertainty model runs automatically with ease without any failures. Results show that some parameters, specifically the cost of fuel and the clean overall heat transfer coefficient, have a strong influence on the overall cost due

to fouling in HEN maintenance scheduling problems. Consequently, comparison of results with and without parametric uncertainty shows that there is a large difference in economics for the deterministic case versus the parametric uncertainty one. Therefore, it is imperative that uncertainty be taken into account during the optimisation of schedules for HEN maintenance problems and all other general maintenance scheduling problems where there is uncertainty in the data.

More detailed conclusions and further research directions are presented in Chapter 7.

Chapter 7

Conclusions and future work

7.1 Overview of research work in this thesis

The work presented in this thesis aims to investigate and solve maintenance scheduling problems for HENs undergoing fouling and operating continuously over time. The aim of this research is to:

- Design novel strategies for the multiperiod optimisation of scheduling cleaning actions in the HEN maintenance problem.
- Demonstrate that the strategies developed can be generalised to other decaying performance maintenance scheduling problems.
- Utilise stochastic programming techniques to deal with uncertainty in data which directly impacts the HEN maintenance scheduling problem.

The aim was achieved through the following 3 keys points:

(i) Development of an efficient, robust feasible path MIOCP approach based on the observation that the HEN maintenance scheduling problem exhibits bang-bang behaviour (Chapters 3 and 4).

(ii) Application of this feasible path MIOCP technique to the scheduling of membrane regeneration in RO membrane network problems (Chapter 5).

(iii) Development of a stochastic programming version of the feasible path MIOCP strategy through a multi-scenario approach in order to apply it to the scheduling of HEN cleaning actions under parametric uncertainty (Chapter 6).

The detailed conclusions for each objective are summarised below.

7.2 Conclusions

7.2.1 Novel reliable techniques for the multiperiod HEN maintenance scheduling problem

To accomplish objective I in Chapter 2, a new method for the scheduling of HEN cleaning actions with the use of the bang-bang behaviour observation is developed. In Chapter 3, a direct MINLP approach was applied to a range of these case studies situated in refinery crude oil PHTs using the IPOPT solver in Python: (i) a single unit, (ii) four units in a serial arrangement, (ii) a 10 unit HEN, and (iv) a larger 25 unit HEN. Both linear fouling and asymptotic fouling models were considered here. It was observed from the relaxed MINLP solution that these problems exhibit bang-bang behaviour, and thus can be solved through simple heuristic strategies or B&B techniques when many singular arcs occur and a rounding up approach is no longer sufficient to obtain a good solution.

Bang-bang behaviour occurs when the decision variables appear linearly in the system and is a characteristic of an OCP. As such, the HEN maintenance scheduling problem is in actuality a MIOCP problem. Hence, in Chapter 4 this problem was solved for the first time using a feasible path sequential MIOCP strategy coupled with a rounding up scheme. Junction conditions were introduced, whereby the fouling resistance is reset to zero when a unit is cleaned. This strategy was applied to all four aforementioned HEN case studies located in refinery PHTs using the SQP optimiser in MATLAB®.

The quality of the solutions using this feasible path sequential MIOCP approach developed were compared with that of stochastic search approaches, specifically the BTA algorithm, and direct MINLP as well as MILP strategies. It was shown that this technique is highly competitive as it is reliable, robust, and the model runs automatically with ease. Additionally, convergence is achieved without any failures.

7.2.2 Generalisation to other maintenance scheduling problems

To fulfil objective II in Chapter 2, the developed feasible path sequential MIOCP approach with a rounding scheme was applied to the optimisation of membrane regeneration schedules for RO membrane networks situated in desalination plants in Chapter 5. In this case study, there is a decaying performance process whereby the membrane permeability declines over time due to fouling which must be offset through cleaning of the membranes in order to restore performance to meet operability and product quality requirements.

Like the HEN maintenance scheduling problems, this RO membrane maintenance scheduling problem exhibited bang-bang behaviour as the control variable also appeared linearly in the system here. In addition, similarly to the HEN maintenance scheduling problem, results here proved that this procedure is robust, efficient and can be generalised to any other maintenance scheduling problem which possesses a decaying performance process in which the control appears linearly in the system.

7.2.3 Extension of the technique to include a stochastic programming version of the multiperiod HEN maintenance scheduling problem

There is a significant level of uncertainty in some parameters appearing in the HEN maintenance scheduling problem. These parameters directly impact the economics associated with the overall costs due to fouling. Therefore, it is vital that uncertainty be taken into account when optimising the schedules of HEN maintenance problems. In order to achieve objective III from Chapter 2, a stochastic programming version of the feasible path sequential approach is developed in Chapter 6 using a multiple scenario approach. In this case, the original objective to be minimised is modified whereby the overall objective is the mean of all scenarios investigated. The control variable to be optimised is shared among all scenarios developed.

The optimisation of HEN maintenance scheduling under parametric uncertainty is applied to two case studies situated in refinery PHTs: (i) a 10 unit HEN undergoing

linear and asymptotic fouling, and (ii) a larger, more complex 25 unit HEN. In terms of the economic results, the overall expected cost varied by up to just over 30% in the worst case. Therefore, it is crucial that uncertainty in data is taken into account when considering the scheduling of HEN maintenance problems, and in addition other maintenance scheduling problems with decaying performance processes in which data are highly uncertain.

7.3 Future work

7.3.1 Computational efficiency

In the majority of the work in this thesis, the SQP solver in MATLAB ® has been used whereby optimisation gradients are calculated through a finite difference method. In Chapter 4, it has been discussed that gradient evaluations conducted via finite differences are costly and require repeated simulations of the dynamic process model. The computational effort is proportional to the number of finite difference calculations needed and each finite difference calculation necessitates a full dynamic system simulation. For large problems, this results in a significant computational effort.

Instead of obtaining gradients needed from the standard finite difference approximation, gradients can be computed using sensitivity equations. The advantage of this procedure is that computation time can be markedly reduced. Moreover, the accuracy and precision of gradient calculations can be increased further. [2] showed that the gradient computational time can range from a 10-fold decrease for a simple model when compared to a finite difference method, to a significant 100-fold decrease for a complex model when compared to finite differences. The IPOPT solver in Python utilises sensitivity equations for the computation of gradients. The computational time taken for the 25 unit HEN maintenance scheduling problem was ≈15.3 CPU hr in the worst case for the sequential approach in MATLAB® using finite differences for gradient calculations (shown in Chapter 4), whilst this was an average of ≈ 5 CPU s per run when using sensitivity equations for gradient calculations in the direct MINLP technique in Python (shown in Chapter 3). Therefore, significant improvements in computation effort can be achieved by amending the methodology for gradient computation in these problems.

7.3.2 Extension to more practical scheduling maintenance models

In this thesis, it was important to benchmark solutions for HEN maintenance scheduling problems against those in the open literature. As such, certain assumptions were made to achieve results which can be compared economically with other solution methodologies. In some cases, these assumptions are deemed impractical. For example, as mentioned in Chapter 1, the cleaning cost is fixed and taken to be independent of the exchanger size and duty. In practice this is not the case, as units with a larger heat exchanger area take more effort to clean and will hence have a higher value in cost per cleaning action.

Another example worth noting is concerned with the scheduling of RO membrane network maintenance problems. In this case study, no downtime for regeneration is considered for the sake of comparison purposes. Practically, a downtime would be needed to be included when cleaning takes place and as such product quality requirements would need to be relaxed. Otherwise, the network is unlikely to meet the product specifications if downtime is to be considered.

Future work in this area includes the extension of these maintenance scheduling models to more practical ones that are not limited to case studies from the open literature which are in many ways artificially constrained.

7.3.3 Generalisation of feasible path approach to preventive maintenance problems

Two applications have been explored and applied in this thesis: (i) HENs in PHTs located in refineries and (ii) RO membrane networks in desalination plants. The feasible path MIOCP approach is not limited to these two areas and can be applied to other very important multiperiod maintenance scheduling problems which are based on discrete decision making.

Applications can be extended to include the generator maintenance scheduling (GMS) problem which addresses the issue of finding the optimal schedule for planned maintenance outages of generating units in a power system. Regular preventive maintenance of

generating units prolongs their life-expectancy, ensures safe operating conditions, and reduces the risk of unplanned outages caused by their failure. There is an increased difficulty of finding the optimal maintenance schedule for larger power systems, specifically with increasing demand for electricity leading to a highly constrained system [122].

Additionally, the feasible path sequential approach can be generalised to the production and scheduling of catalyst replacement in catalytic bed reactor processes with decaying performance. [57] considered the maximisation of profit from these processes based on selection of the best operating policies over time given the model for decay in catalyst activity and production. Their optimisation model also ensured that seasonal customer demands and minimum inventory levels were met.

Further work will consider the aforementioned areas as well as other applications.

7.3.4 Investigation of alternative methods for uncertainty quantification

In this thesis, the HEN maintenance scheduling problem was extended to include parametric uncertainty. A multi-scenario based MIOCP feasible path method was proposed and applied to the HEN maintenance scheduling problem with uncertainty. Alternative approaches for uncertainty quantification were reviewed in Section 6.2, *e.g.* robust optimisation methods, fuzzy programming methods, among others. These methods can be investigated further and applied to the HEN maintenance scheduling problem with uncertainty. Results from these alternative approaches can be compared to those produced from the proposed multiple scenario based MIOCP feasible path approach in this thesis. This can be performed to determine the robustness and efficiency of each investigated method.

References

[1] Adloor, S. D., Al Ismaili, R., Vassiliadis, V. S., 2018. Errata: Heat exchanger network cleaning scheduling: From optimal control to mixed-integer decision making. Computers and Chemical Engineering 115, 243–245.

[2] Almquist, J., Leander, J., Jirstrand, M., 2015. Using sensitivity equations for computing gradients of the FOCE and FOCEI approximations to the population likelihood. Journal of Pharmacokinetics and Pharmacodynamics 42 (3), 191–209.

[3] Babuška, I., Silva, R. S., 2014. Dealing with uncertainties in engineering problems using only available data. Computer Methods in Applied Mechanics and Engineering 270, 57–75.

[4] Balasubramanian, J., Grossmann, I., 2003. Scheduling optimization under uncertainty—an alternative approach. Computers and Chemical Engineering 27 (4), 469–490.

[5] Bansal, B., 1994. Crystallisation fouling in plate heat exchangers. Ph.D. thesis, The University of Auckland.

[6] Bansal, B., Gill, W. N., 1974. Theoretical and experimental study of radial flow hollow fibre reverse osmosis. AIChE Symposium Series 70 (144), 136–149.

[7] Beale, E. . M. . L. ., 1955. On minimizing a convex function subject to linear inequalities. Journal of the Royal Statistical Society. Series B 17 (2), 173–184.

[8] Belghith, S. F., Lamnabhi-Lagarrigue, F., Rosset, M. M., 1986. Algebraic and geometric methods in nonlinear control theory. Vol. 29. Springer Netherlands, Dordrecht.

[9] Bellman, R., Glicksberg, I., Gross, O., 1956. On the bang-bang control problem. Quaterly of Applied Mathematics 14 (1), 11–18.

[10] Bemporad, A., Bozinis, N. A., Dua, V., Morari, M., Pistikopoulos, E. N., 2000. Model predictive control: A multi-parametric programming approach. In: Pierucci, S. (Ed.), European Symposium on Computer Aided Process Engineering-10. Vol. 8 of Computer Aided Chemical Engineering. Elsevier, pp. 301–306.

[11] Benders, J. F., 1962. Partitioning procedures for solving mixed-variables programming problems. Numerische Mathematik 4 (1), 238–252.

[12] Bhatia, T. K., Biegler, L. T., 1999. Multiperiod design and planning with interior point methods. Computers & Chemical Engineering 23, 919–932.

[13] Birge, J. R., Louveaux, F., 2011. Introduction to stochastic programming.

[14] Blakemore, N., Aris, R., 1962. Studies in optimization—V. The bang-bang control of a batch reactor. Chemical Engineering Science 17, 591–598.

[15] Bonami, P., Biegler, L. T., Conn, A. R., Cornuéjols, G., Grossmann, I. E., Laird, C. D., Lee, J., Lodi, A., Margot, F., Sawaya, N., Wächter, A., 2008. An algorithmic framework for convex mixed integer nonlinear programs. Discrete Optimization 5 (2), 186–204.

[16] Bott, T. R., Gudmundsson, J. S., 1978. Rippled silica deposits in heat exchanger tubes. In: 6th International Heat Transfer Conference. Hemisphere Publishing Corporation, Washington, pp. 373–378.

[17] Bryson, A. E., Ho, Y.-C., 1975. Applied optimal control: Optimization, estimation and control. Hemisphere Publishing Corporation, New York-Washington-Philadelphia-London.

[18] Casado, E., 1990. Model optimizes exchanger cleaning. Hydrocarbon Processing 69 (8), 71–76.

[19] Characklis, W. G., Bryers, J. D., 2009. Fouling biofilm development: A process analysis. Biotechnology and Bioengineering 102 (2), 309–347.

[20] Chen, C., Qi, M., Kong, X., Huang, G., Li, Y., 2018. Air pollutant and CO_2 emissions mitigation in urban energy systems through a fuzzy possibilistic programming method under uncertainty. Journal of Cleaner Production 192, 115–137.

[21] Chen, Y., Yuan, Z., Chen, B., 2017. Process optimization with consideration of uncertainties—an overview. Chinese Journal of Chemical Engineering.

[22] Chu, Y., Xia, Q., 2004. Generating Benders cuts for a general class of integer programming problems. In: Régin, J. C., Rueher, M. (Eds.), First International Conference, CPAIOR. Springer, Nice, pp. 127–141.

[23] Clausen, J., 1999. Branch and bound algorithms - principles and examples.

[24] Dantzig, G. B., apr 1955. Linear Programming under Uncertainty. Management Science 1 (3-4), 197–206.

[25] Dantzig, G. B., 1998. Linear programming and extensions. Princeton University Press, New Jersey.

[26] Dantzig, G. B., Folkman, J. O. N., Shapiro, N., 1967. On the continuity of the minimum set of a continuous function 17 (2), 519–548.

[27] Darby, M. L., Nikolaou, M., 2007. A parametric programming approach to moving-horizon state estimation. Automatica 43 (5), 885–891.

[28] Deshannavar, U. B., Rafeen, M. S., Ramasamy, M., Subbarao, D., 2010. Crude oil fouling: A review. Journal of Applied Sciences 10 (24), 3167–3174.

[29] Diangelakis, N. A., Manthanwar, A. M., Pistikopoulos, E. N., 2014. A framework for design and control optimisation: Application on a CHP system. In: Eden, M. R., Siirola, J. D., Towler, G. P. (Eds.), Proceedings of the 8th International Conference on Foundations of Computer-Aided Process Design. Vol. 34 of Computer Aided Chemical Engineering. Elsevier, pp. 765–770.

[30] Dias, L. S., Ierapetritou, M. G., 2016. Integration of scheduling and control under uncertainties: Review and challenges. Chemical Engineering Research and Design 116, 98–113.

[31] Domínguez, L. F., Pistikopoulos, E. N., 2010. Multiparametric programming based algorithms for pure integer and mixed-integer bilevel programming problems. Computers and Chemical Engineering 34 (12), 2097–2106.

[32] Dua, V., Bozinis, N. A., Pistikopoulos, E. N., 2002. A multiparametric programming approach for mixed-integer quadratic engineering problems. Computers and Chemical Engineering 26 (4-5), 715–733.

[33] Dueck, G., Scheuer, T., 1990. Threshold Accepting: A general purpose optimization algorithm superior to simulated annealing. Journal of Computational Physics 90, 161–175.

[34] Duran, M. A., Grossmann, I. E., 1986. Mixed-integer nonlinear programming algorithm for process systems synthesis. AIChE Journal 32, 592–606.

[35] El Amraoui, A., Mesghouni, K., 2014. Train scheduling networks under time duration uncertainty. Vol. 19. IFAC.

[36] Epstein, N., 1983. Thinking about heat transfer fouling: A 5 x 5 matrix. Heat Transfer Engineering 4 (1), 43–56.

[37] Evangelista, F., 1985. A short cut method for the design of reverse osmosis desalination plants. Industrial & Engineering Chemistry Process Design and Development 24, 211–223.

[38] Evangelista, F., 1986. Improved graphical-analytical method for the design of reverse osmosis plants. Industrial and Engineering Chemistry Process Design and Development 25 (2), 366–375.

[39] Faísca, N. P., Dua, V., Saraiva, P. M., Rustem, B., Pistikopoulos, E. N., 2006. A global parametric programming optimisation strategy for multilevel problems. In: Marquardt, W., Pantelides, C. (Eds.), 16th European Symposium on Computer Aided Process Engineering and 9th International Symposium on Process Systems Engineering. Vol. 21 of Computer Aided Chemical Engineering. Elsevier, pp. 215–220.

[40] Farrokh, M., Azar, A., Jandaghi, G., Ahmadi, E., 2018. A novel robust fuzzy stochastic programming for closed loop supply chain network design under hybrid uncertainty. Fuzzy Sets and Systems 341, 69–91.

[41] Fouskakis, D., Draper, D., 2002. Stochastic optimization: A review. International Statistical Review 70 (3), 315–349.

[42] Galetakis, M., Roumpos, C., Alevizos, G., Vamvuka, D., 2012. Production scheduling of a lignite mine under quality and reserves uncertainty. Reliability Engineering and System Safety 107 (12), 224–230.

[43] Gay, D. M., 2015. The AMPL modeling language: An aid to formulating and solving optimization problems. Springer Proceedings in Mathematics and Statistics 134, 95–116.

[44] Geoffrion, A. M., 1972. Generalized Benders decomposition. Journal of Optimization Theory and Applications 10 (4), 238–260.

[45] Georgiadis, M. C., Papageorgiou, L. G., 2000. Optimal energy and cleaning management in heat exchanger networks under fouling. Chemical Engineering Research and Design 78 (2), 168–179.

[46] Gonçalves, C. D. O., Queiroz, E. M., Pessoa, F. L. P., Liporace, F. S., Oliveira, S. G., Costa, A. L. H., 2014. Heuristic optimization of the cleaning schedule of crude preheat trains. Applied Thermal Engineering 73 (1), 1–12.

[47] Gorissen, B. L., Yanikoglu, I., den Hertog, D., 2015. A practical guide to robust optimization. Omega (United Kingdom) 53, 124–137.

[48] Grieder, P., Kvasnica, M., Baotić, M., Morari, M., 2005. Stabilizing low complexity feedback control of constrained piecewise affine systems. Automatica 41 (10), 1683–1694.

[49] Grossmann, I. E., Apap, R. M., Calfa, B. A., García-Herreros, P., Zhang, Q., 2016. Recent advances in mathematical programming techniques for the optimization of process systems under uncertainty. Computers and Chemical Engineering 91, 3–14.

[50] Grossmann, I. E., Kravanja, Z., 1995. Mixed-integer nonlinear programming techniques for process systems engineering. Computers & Chemical Engineering 19, 189–204.

[51] Guinand, F., Moukrim, A., Sanlaville, E., 2004. Sensitivity analysis of tree scheduling on two machines with communication delays. Parallel Computing 30 (1), 103–120.

[52] Hall, N. G., Posner, M. E., 2004. Sensitivity analysis for scheduling problems. Journal of Scheduling 7 (1), 49–83.

[53] Hart, W. E., Watson, J. P., Woodruff, D. L., 2011. Pyomo: Modeling and solving mathematical programs in Python. Mathematical Programming Computation 3 (3), 219–260.

[54] Hazır, Ö., Haouari, M., Erel, E., 2010. Robust scheduling and robustness measures for the discrete time/cost trade-off problem. European Journal of Operational Research 207 (2), 633–643.

[55] Hermans, J. J., 1978. Physical aspects governing the design of hollow fiber modules. Desalination 26, 45–62.

[56] Hewitt, G. F., Shires, G. L., Bott, T. R., 1994. Process heat transfer. CRC Press.

[57] Houze, M., Juhasz, N., Grossmann, I. E., 2003. Optimization model for production and scheduling of catalyst in a process with decaying performance. In: Proceedings Foundation of Computer-Aided Process Operations (FOCAPO). No. 1. pp. 311–314.

[58] Hu, Z., Hu, G., 2016. A two-stage stochastic programming model for lot-sizing and scheduling under uncertainty. International Journal of Production Economics 180, 198–207.

[59] Ishiyama, E. M., Falkeman, E. S., Wilson, D. I., Pugh, S. J., 2017. Quantifying implications of deposit aging from crude refinery preheat train data. In: Heat Exchanger Fouling and Cleaning XII. Aranjuez, pp. 5–13.

[60] Ishiyama, E. M., Heins, A. V., Paterson, W. R., Spinelli, L., Wilson, D. I., 2010. Scheduling cleaning in a crude oil preheat train subject to fouling: Incorporating desalter control. Applied Thermal Engineering 30 (13), 1852–1862.

[61] Ishiyama, E. M., Paterson, W. R., Ian Wilson, D., 2011. Exploration of alternative models for the aging of fouling deposits. AIChE Journal 57 (11), 3199–3209.

[62] Ishiyama, E. M., Paterson, W. R., Wilson, D. I., 2008. Thermo-hydraulic channelling in parallel heat exchangers subject to fouling. Chemical Engineering Science 63 (13), 3400–3410.

[63] Ishiyama, E. M., Paterson, W. R., Wilson, D. I., 2009. Platform for techno-economic analysis of fouling mitigation options in refinery preheat trains. Energy and Fuels 23 (3), 1323–1337.

[64] Ishiyama, E. M., Paterson, W. R., Wilson, D. I., 2009. The effect of fouling on heat transfer, pressure drop, and throughput in refinery preheat trains: optimization of cleaning schedules. Heat Transfer Engineering 30 (10-11), 805–814.

[65] Jia, Z., Ierapetritou, M. G., 2004. Short-term scheduling under uncertainty using MILP sensitivity analysis. Industrial & Engineering Chemistry Research 43 (14), 3782–3791.

[66] Karabegov, V. K., 1963. A parametric problem in linear programming. USSR Computational Mathematics and Mathematical Physics 3 (3), 725–741.

[67] Karmarkar, N., 1984. A new polynomial-time algorithm for linear programming. Combinatorica 4 (4), 373–395.

[68] Kawajir, Y., Laird, C., Vigerske, S., Wächter, A., 2016. Introduction to IPOPT: A tutorial for downloading, installing and using IPOPT.
URL `https://www.coin-or.org/Ipopt/documentation/documentation.html`

[69] Kazi, S., 2012. Fouling and fouling mitigation on heat exchanger surfaces. In: Mitrovic, J. (Ed.), Heat Exchangers - Basic Design Applications. InTech, Ch. 19.

[70] Kenan, N., Jebali, A., Diabat, A., 2017. An integrated flight scheduling and fleet assignment problem under uncertainty. Computers & Operations Research, In Press.

[71] Khor, C. S., Elkamel, A., Ponnambalam, K., Douglas, P. L., 2008. Two-stage stochastic programming with fixed recourse via scenario planning with economic and operational risk management for petroleum refinery planning under uncertainty. Chemical Engineering and Processing: Process Intensification 47 (9-10), 1744–1764.

[72] Kirkpatrick, S., Gelatt, C. D., Vecchi, M. P., 1983. Optimization by simulated annealing. Science 220 (4598), 671 LP – 680.

[73] Kocis, G., Grossmann, I., 1989. Computational experience with DICOPT solving MINLP problems in process systems engineering. Computers & Chemical Engineering 13 (3), 307–315.

[74] Kocis, G. R., Grossmann, I. E., 1987. Relaxation strategy for the structural optimization of process flow sheets. Industry and Engineering Chemistry Research 26, 1869–1880.

[75] Kusiak, A., Xu, G., Zhang, Z., 2014. Minimization of energy consumption in HVAC systems with data-driven models and an interior-point method. Energy Conversion and Management 85, 146–153.

[76] Lavaja, J. H., Bagajewicz, M. J., 2004. Managing financial risk in the planning of heat exchanger cleaning. In: European Symposium on Computer-Aided Process Engineering-14. Vol. 18. Lisbon, pp. 235–240.

[77] Lavaja, J. H., Bagajewicz, M. J., 2004. On a new MILP model for the planning of heat-exchanger network cleaning. Industrial & Engineering Chemistry Research 43 (14), 3924–3938.

[78] Lavaja, J. H., Bagajewicz, M. J., 2005. On a new MILP model for the planning of heat-exchanger network cleaning. Part III: multiperiod cleaning under uncertainty with financial risk management. Industrial & Engineering Chemistry Research 44 (21), 8136–8146.

[79] Li, Z., Ierapetritou, M., 2008. Process scheduling under uncertainty: Review and challenges. Computers and Chemical Engineering 32 (4-5), 715–727.

[80] Lim, S., 2013. A joint optimal pricing and order quantity model under parameter uncertainty and its practical implementation. Omega (United Kingdom) 41 (6), 998–1007.

[81] Liu, J., Wang, L., Jia, L., Wang, X., 2018. Thermodynamic modeling and sensitivity analysis of ejector in refrigeration system. International Journal of Heat and Mass Transfer 126, 485–492.

[82] Loukakis, E., Muhlemann, A. P., 1984. Parameterisation algorithms for the integer linear programs in binary variables. European Journal of Operational Research 17 (1), 104–115.

[83] Lusa, A., Corominas, A., Muñoz, N., 2008. A multistage scenario optimisation procedure to plan annualised working hours under demand uncertainty. International Journal of Production Economics 113 (2), 957–968.

[84] Mahdi, Y., Mouheb, A., Oufer, L., 2009. A dynamic model for milk fouling in a plate heat exchanger. Applied Mathematical Modelling 33 (2), 648–662.

[85] Markowitz, H., 1952. Portfolio Selection. The Journal of Finance 7 (1), 77–91.

[86] Markowski, M., Urbaniec, K., 2005. Optimal cleaning schedule for heat exchangers in a heat exchanger network. Applied Thermal Engineering 25 (7), 1019–1032.

[87] Mavromatidis, G., Orehounig, K., Carmeliet, J., 2018. Design of distributed energy systems under uncertainty: A two-stage stochastic programming approach. Applied Energy 222 (April), 932–950.

[88] Mohan, V., Singh, J. G., Ongsakul, W., 2015. An efficient two stage stochastic optimal energy and reserve management in a microgrid. Applied Energy 160, 28–38.

[89] Mohler, R., 1973. Bilinear control processes: With applications to engineering, ecology and medicine. Academic Press, New York.

[90] Montemanni, R., Barta, J., Mastrolilli, M., Gambardella, L. M., aug 2007. The robust traveling salesman problem with interval data. Transportation Science 41 (3), 366–381.

[91] Moore, G. E., 1975. Progress In Digital Integrated Electronics. In: Proceedings of the International Electron Devices Meeting. Washington, pp. 11–13.

[92] Moreno, M. S., Blanco, A. M., 2018. A fuzzy programming approach for the multi-objective patient appointment scheduling problem under uncertainty in a large hospital. Computers and Industrial Engineering 123 (November 2017), 33–41.

[93] Moscato, P., Fontanari, J., 1990. Stochastic versus deterministic update in simulated annealing. Physics Letters A 146, 204–208.

[94] Muela, E., Schweickardt, G., Garcés, F., 2007. Fuzzy possibilistic model for medium-term power generation planning with environmental criteria. Energy Policy 35 (11), 5643–5655.

[95] Müller-Steinhagen, H., Malayeri, M. R., Watkinson, A. P., 2005. Fouling of heat exchangers-new approaches to solve an old problem. Heat Transfer Engineering 26 (1), 1–4.

[96] Mulvey, J. M., Vanderbei, R. J., Zenios, S. A., 1995. Robust optimization of large-scale systems. Operations Research 43 (2), 264–281.

[97] Nocedal, J., Wright, S. J., Robinson, S. M., 2006. Numerical optimization. Springer Series in Operations Research and Financial Engineering. Springer New York.

[98] Oberdieck, R., Diangelakis, N. A., Nascu, I., Papathanasiou, M. M., Sun, M., Avraamidou, S., Pistikopoulos, E. N., 2016. On multi-parametric programming and its applications in process systems engineering. Chemical Engineering Research and Design 116, 61–82.

[99] Ottesen, S. O., Tomasgard, A., 2015. A stochastic model for scheduling energy flexibility in buildings. Energy 88, 364–376.

[100] Penz, B., Rapine, C., Trystram, D., 2001. Sensitivity analysis of scheduling algorithms. European Journal of Operational Research 134 (3), 606–615.

[101] Petrovic, D., Duenas, A., 2006. A fuzzy logic based production scheduling/rescheduling in the presence of uncertain disruptions. Fuzzy Sets and Systems 157 (16), 2273–2285.

[102] Pistikopoulos, E. N., Diangelakis, N. A., 2016. Towards the integration of process design, control and scheduling: Are we getting closer? Computers and Chemical Engineering 91, 85–92.

[103] Pistikopoulos, E. N., Dua, V., Bozinis, N. A., Bemporad, A., Morari, M., 2002. On-line optimization via off-line parametric optimization tools. Computers and Chemical Engineering 26 (2), 175–185.

[104] Pogiatzis, T., 2012. Application of mixed-integer programming in chemical engineering. Ph.D. thesis, University of Cambridge.

[105] Pogiatzis, T., Ishiyama, E. M., Paterson, W. R., Vassiliadis, V. S., Wilson, D. I., 2012. Identifying optimal cleaning cycles for heat exchangers subject to fouling and ageing. Applied Energy 89 (1), 60–66.

[106] Pogiatzis, T., Vassiliadis, V. S., Wilson, D. I., 2011. An MINLP formulation for scheduling the cleaning of heat exchanger networks subject to fouling and ageing. In: Malayeri, M. R., Müller-Steinhagen, H., Watkinson, A. P. (Eds.), Preceedings of International Conference on Heat Exchanger Fouling and Cleaning. Vol. 2011. Crete Island, pp. 349–356.

[107] Pogiatzis, T., Wilson, D. I., Vassiliadis, V., 2012. Scheduling the cleaning actions for a fouled heat exchanger subject to ageing: MINLP formulation. Computers & Chemical Engineering 39, 179–185.

[108] Pontryagin, L. S., Boltyanskii, V. G., Gamkrelidze, R. V., Mishchenko, E. F., 1962. The mathematical theory of optimal processes. Wiley-Interscience, New York.

[109] Prasad, R., Karmeshu, Bharadwaj, K., 2002. Stochastic modeling of heat exchanger response to data uncertainties. Applied Mathematical Modelling 26 (6), 715–726.

[110] Process Systems Enterprise, 2017. gPROMS.

[111] Pugh, S., Hewitt, G. F., Müller-Steinhagen, H., 2002. Heat exchanger fouling in the pre-heat train of a crude oil distillation unit - the development of a 'user guide'. In: Proceedings of the 4th International Conference on Heat Exchanger Fouling, Fundamental Approaches & Technical Solutions. Davos.

[112] Rao, C. V., Rawlings, J. B., Lee, J. H., 2001. Constrained linear state estimation—a moving horizon approach. Automatica 37 (10), 1619–1628.

[113] Restrepo, M. I., Gendron, B., Rousseau, L. M., 2017. A two-stage stochastic programming approach for multi-activity tour scheduling. European Journal of Operational Research 262 (2), 620–635.

[114] Rodriguez, C., Smith, R., 2007. Optimization of operating conditions for mitigating fouling in heat exchanger networks. Chemical Engineering Research and Design 85 (6), 839–851.

[115] Rosenthal, R. E., 2017. GAMS—a user's guide. Washington.

[116] Rountree, S. L., Gillett, B. E., 1982. Parametric integer linear programming: A synthesis of branch and bound with cutting planes. European Journal of Operational Research 10 (2), 183–189.

[117] Ryu, J. H., Dua, V., Pistikopoulos, E. N., 2004. A bilevel programming framework for enterprise-wide process networks under uncertainty. Computers and Chemical Engineering 28 (6-7), 1121–1129.

[118] Sager, S., 2009. Reformulations and algorithms for the optimization of switching decisions in nonlinear optimal control. Journal of Process Control 19 (8), 1238–1247.

[119] Sahinidis, N. V., 2004. Optimization under uncertainty: State-of-the-art and opportunities. Computers and Chemical Engineering 28 (6-7), 971–983.

[120] Sakizlis, V., Perkins, J. D., Pistikopoulos, E. N., 2004. Recent advances in optimization-based simultaneous process and control design. Computers and Chemical Engineering 28 (10), 2069–2086.

[121] Samikoglu, Ö., Honkomp, S., Pekny, J., Reklaitis, G., 1998. Sensitivity analysis for project planning and scheduling under uncertain completions. Computers & Chemical Engineering 22 (98), S871–S874.

[122] Schlünz, E., van Vuuren, J., 2013. An investigation into the effectiveness of simulated annealing as a solution approach for the generator maintenance scheduling problem. International Journal of Electrical Power & Energy Systems 53, 166–174.

[123] Schmitt, L. M., 2001. Theory of genetic algorithms. Theoretical Computer Science 259 (1-2), 1–61.

[124] See, H. J., 2002. Optimization of water and wastewater treatment processes. Ph.D. thesis, University of Cambridge.

[125] Sel, Ç., Bilgen, B., Bloemhof-Ruwaard, J., 2017. Planning and scheduling of the make-and-pack dairy production under lifetime uncertainty. Applied Mathematical Modelling 51, 129–144.

[126] Sharqawy, M. H., Zubair, S. M., 2010. Heat exchangers design under variable overall heat transfer coefficient: Improved analytical and numerical approaches. Heat Transfer Engineering 31 (13), 1051–1056.

[127] Smaïli, F., Angadi, D. K., Hatch, C. M., Herbert, O., Vassiliadis, V. S., Wilson, D. I., 1999. Optimization of scheduling of cleaning in heat exchanger networks subject to fouling. Food and Bioproducts Processing 77 (2), 159–164.

[128] Smaïli, F., Vassiliadis, V. S., Wilson, D. I., 2001. Mitigation of fouling in refinery heat exchanger networks by optimal management of cleaning. Energy & Fuels 15 (5), 1038–1056.

[129] Smaïli, F., Vassiliadis, V. S., Wilson, D. I., 2002. Long-term scheduling of cleaning of heat exchanger networks. Chemical Engineering Research and Design 80 (6), 561–578.

[130] Smaïli, F., Vassiliadis, V. S., Wilson, D. I., 2002. Optimization of cleaning schedules in heat exchanger networks subject to fouling. Chemical Engineering Communications 189 (11), 1517–1549.

[131] Spall, J., 2003. Introduction to stochastic search and optimization: Estimation, simulation and control. Wiley-Interscience, New Jersey.

[132] Sungur, I., Ordóñez, F., Dessouky, M., 2008. A robust optimization approach for the capacitated vehicle routing problem with demand uncertainty. IIE Transactions 40 (5), 509–523.

[133] Taborek, J., Aoki, T., Ritter, R. B., Palen, J. W., 1972. Fouling: The major unresolved problem in heat transfer.

[134] The MathWorks Inc., 2016. MATLAB and optimisation toolbox.

[135] Tragårdh, G., 1989. Membrane cleaning. Desalination 71, 325–335.

[136] UNESCO, 2018. The United Nations world water development report 2018: Nature-based solutions for water. Tech. rep., Paris.

[137] United Nations, 2017. Desalinization. In: United Nations (Ed.), The first global integrated marine assessment: World ocean assessment I. Cambridge University Press, Cambridge, Ch. 28, pp. 441–450.

[138] Vassiliadis, V. S., 1993. Computational solution of dynamic optimization problems with general differential-algebraic constraints. Ph.D. thesis, Imperial College London.

[139] Viswanathan, V., Sen, A. K., Chakraborty, S., 2011. Stochastic greedy algorithms. International Journal of Advances in Software 4 (1), 1–11.

[140] Wächter, A., Biegler, L. T., 2006. On the implementation of a primal-dual interior point filter line search algorithm for large-scale nonlinear programming. Mathematical Programming 106 (1), 25–57.

[141] Wang, Y., Smith, R., 2013. Retrofit of a heat-exchanger network by considering heat-transfer enhancement and fouling. Industrial and Engineering Chemistry Research 52 (25), 8527–8537.

[142] Watkinson, A. P., 1988. Critical review of organic fluid fouling. Argonne National Laboratory report No. ANL/CNSV-TM-208. Tech. rep.

[143] Wilson, D. I., Ishiyama, E. M., Polley, G. T., 2017. Twenty years of Ebert and Panchal—what next? Heat Transfer Engineering 38 (7-8), 669–680.

[144] Woodruff, S., Miller, R. L., 2015. Cost sensitivity analysis for a 100 MWe modular power plant and fusion neutron source. Fusion Engineering and Design 90, 7–16.

[145] Yan, S., Tang, C. H., 2009. Inter-city bus scheduling under variable market share and uncertain market demands. Omega 37 (1), 178–192.

[146] Yang, Y., Zhang, S., Xiao, Y., 2017. Optimal design of distributed energy resource systems based on two-stage stochastic programming. Applied Thermal Engineering 110, 1358–1370.

[147] Yeap, B., Wilson, D., Polley, G., Pugh, S., 2004. Mitigation of crude oil refinery heat exchanger fouling through retrofits based on thermo-hydraulic fouling models. Chemical Engineering Research and Design 82 (1), 53–71.

[148] Yousefi, S., Soltani, R., Farzipoor Saen, R., Pishvaee, M. S., 2017. A robust fuzzy possibilistic programming for a new network GP-DEA model to evaluate sustainable supply chains. Journal of Cleaner Production 166, 537–549.

[149] Zahiri, B., Torabi, S. A., Mohammadi, M., Aghabegloo, M., 2018. A multi-stage stochastic programming approach for blood supply chain planning. Computers and Industrial Engineering 122 (September 2017), 1–14.

[150] Zandvliet, M., Bosgra, O., Jansen, J., Van den Hof, P., Kraaijevanger, J., 2007. Bang-bang control and singular arcs in reservoir flooding. Journal of Petroleum Science and Engineering 58 (1-2), 186–200.

[151] Zhang, X., Huang, G. H., Nie, X., 2009. Robust stochastic fuzzy possibilistic programming for environmental decision making under uncertainty. Science of the Total Environment 408 (2), 192–201.

[152] Zhu, M., El-Halwagi, M. M., Al-Ahmad, M., 1997. Optimal design and scheduling of flexible reverse osmosis networks. Journal of Membrane Science 129, 161–174.